This document is downloaded from DR-NTU (https://dr.ntu.edu.sg)
Nanyang Technological University, Singapore.

Structural features that affect β2 integrin expression and regulation of adhesion

Guan, Siyu

2013

Guan, S. (2013). Structural features that affect β2 integrin expression and regulation of adhesion. Doctoral thesis, Nanyang Technological University, Singapore.

https://hdl.handle.net/10356/55003

https://doi.org/10.32657/10356/55003

Downloaded on 20 Mar 2024 19:57:48 SGT

NANYANG TECHNOLOGICAL UNIVERSITY

Structural Features That Affect β_2 Integrin Expression and Regulation of Adhesion

GUAN SIYU

SCHOOL OF BIOLOGICAL SCIENCES

2013

Structural Features That Affect β_2 Integrin Expression and Regulation of Adhesion

A Thesis for the Degree of Doctor of Philosophy (Ph.D)

Completed at

Nanyang Technological University

Guan Siyu

Supervised by Professor Alex Law

School of Biological Sciences

Nanyang Technological University

Acknowledgement

I owe my deepest gratitude to my supervisor Prof Alex Law for his guidance and support over the years. I learnt and benefited much from his knowledge, wisdom and personality. I am very appreciated for the patience and efforts that he spent, and insightful thoughts and valuable suggestions he shared during my research and thesis writing.

I also would like to express my gratitude to Dr. Tan Suet Mien for his kind permission of my using the fluorescent plate reader in his lab, as well as his generosity in providing me plasmid for the study in Chapter 3. I also want to thank all his lab members for the many helpful supports.

I am grateful to the previous lab member, Dr. Cheng Ming for she constructed two plasmids for the experiments in Chapter 4. And many thanks to Ms. Manisha Cooray, Mr. Rueben and Dr. Xiao Zhou for purifying the antibodies and iC3b used in my work. Thanks Dr. Sujit and Dr. Vararattanavech for the technique supports. And thanks to all the people in SBS who helped me.

I would like to give my sincere thank to my lovely friends Mr. Qiu Haodong, Ms. Shi Yu, Ms. Ju Peijun, and Ms. Wang Qi for their countless, supports, cares and encouragements.

Last but not least, I would like to thank my dear parents Ms. Zhao Hong and Mr. Guan Yijun. Their supports are always the source of my strength. Thanks my greatest supporters!

Abstract

A hallmark for the Leukocyte Adhesion Deficiency 1 (LAD-1) syndrome is the defect in the β_2 integrins due to mutations in the *ITGB2* gene. To establish the correlation between LAD-1 genotype and phenotype, as well as better understand integrin function and structure, 19 LAD-1 missense mutants that recently identified were introduced into the pcDNA3 plasmid containing the *ITGB2* cDNA. These plasmids were transfected into HEK293T cells together with that of either the αL, αM, αX subunits. These transfectants were subsequently examined for their ability in supporting the expression of the integrins and adhesion functions. Fourteen of these mutants do not support heterodimer expression of integrin LFA-1, Mac-1 and p150,95. Of the remaining 5, the integrins with the β_2-D77N, β_2-S453N and β_2-P648L mutations have normal ligand binding activities. These "mutations" are therefore rare polymorphisms of the β_2 subunit. In contrast, integrins with the β_2-G150D mutation have no binding activities. LFA-1 with the β_2-G716A mutation is constitutively active to bind ICAM-1 and requires only one activating agents to bind to ICAM-3. (It should be noted that wild-type LFA-1 requires one activating agent to bind ICAM-1 and two to bind ICAM-3.) Immunoprecipitation experiment with the reporter mAb KIM127 suggested that the LFA-1 bearing the β_2-G716A is in the bent configuration.

The epitope of the mAb H52 was mapped to the C-terminal half of the β_2 hybrid domain. However, the epitope was abolished by the β_2-L105P mutation, which is located in the N-terminal half. Based on this new information, it is concluded that the epitope is conformational.

It is established that integrin activation is regulated by the divalent cations. However, Mg^{2+}/EGTA (5 mM Mg^{2+} and 1.5 mM EGTA) had been shown to promote $\alpha L\beta_2$ adhesion to ICAM-1 but not $\alpha M\beta_2$ adhesion to denatured BSA. In order to determine the difference between αL and αM which contributes to Mg^{2+}/EGTA sensitivity, a series of αL/αM chimeric integrins were constructed. It was shown that LFA-1 with αM calf-1 domain is not responsive to the Mg^{2+}/EGTA activation. In the reverse experiment with Mac-1 bearing the αL calf-1 domain, the results were not clear cut due to the modified Mac-1 was constitutively active.

Contents

Abbreviations

ADMIDAS	Adjacent to Metal Ion-Dependent Adhesion Site
APC	Antigen Presenting Cells
BCECF	2',7'-bis-(2-carboxyethyl)-5(and -6) carboxy fluorescein, acetoxymethyl ester
COS-7 cells	African green monkey kidney cells
CR	Complement Receptor
CSK	Cytoskeleton Buffer
DEAE	Diethylaminoethyl
DMSO	Dimethyl sulfoxide
DTT	Dithiothreitol
EM	Electron Microscopy
FBS	Fetal Bovine Serum
GDP	Guanosine diphosphate
GP%	Percentage of Gated Positive
HEK293	Human Embroynic Kidney 293 cell line
iC3b	Inactive Complement 3b Fragment
ICAM	Intercellular Adhesion Molecule
I-EGF	Integrin-Epidermal Growth Factor
IMC	Inner Membrane Clasp
JAM	Junctional Adhesion Molecule 1
LAD	Leukocyte Adhesion Deficiency
LFA-1	Leukocyte Function-associated Antigen 1
Mac-1	Macrophage Antigen 1
ME	Mg^{2+}/EGTA
MIDAS	Metal Ion-Dependent Adhesion Site
MnE	Mn^{2+}/EGTA
N.A.R	No Activating Reagent
NK cells	Natural Killing cells
OMC	outer membrane clasp
PBS	Phosphate buffered saline
PDB	Protein Data Bank
PEI	Polyethylenimine
PMN	Polymorphonuclear Neutrophil
PSI	Plexin-Semaphorin-Integrin
$R_{Mi/Ki}$	Ration of increase brought by ME in that of KIM185
SD	Standard Deviation
SDS-PAGE	Sodium Dodecyl Sulfate Polyacrylamide Gel Electrophoresis
SyMBS	Synergistic Metal ion Binding Site
TD	Tail Domain
TM	Transmembrane
VCAM	Vascular cell adhesion protein
WT	Wild-type

Chapter 1: Introduction

1.1 Overview on the Integrins

Integrins are a group of cell adhesion molecules that bridge intracellular molecules with extracellular ligands. Each integrin molecule is formed by the non-covalent association of two subunits, namely the α and the β subunits. Both subunits are type-1 transmembrane glycoproteins **(Figure 1.1)**. In human, there are 18 α subunits and 8 β subunits that can combine to form 24 distinct integrin heterodimers.

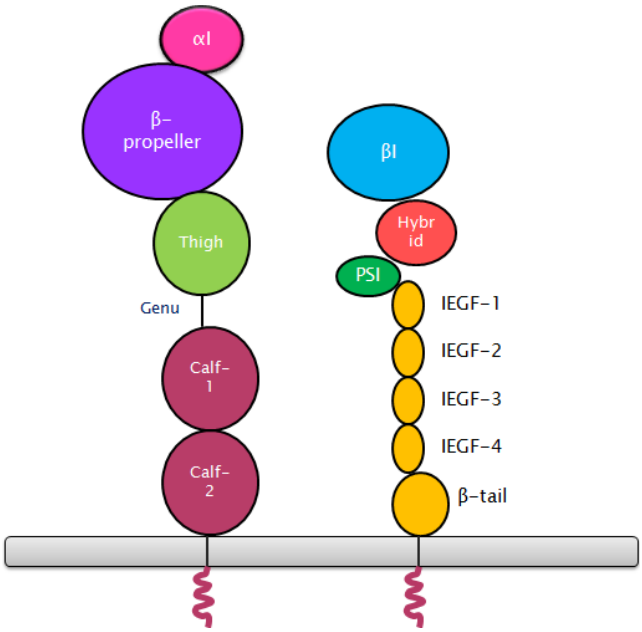

Figure 1.1. Domain organization of a typical integrin heterodimer.

1.1.1 The Structural Features of Integrin α Subunit

Integrin α subunits can be classified into two types depending whether it contains an I domain which is inserted in the β propeller head. Out of the 18

human α subunit, 9 contain an I domain. Generally, the α subunit consists of 7 domains: the β propeller (with or without I domain), the thigh domain, the genu region, the calf-1 domain, the calf-2 domain, the transmembrane and the cytoplasmic tail (Figure 1.2). Most integrin α subunits cannot associate with more than one β subunit. In contrast, β_1 can form dimer with 11 different α subunits and β_2 can form dimers with 4 different α subunits. It is considered that the α subunit has the greatest influence on ligand binding specificity (Springer and Dustin, 2012). To date, $\alpha IIb\beta_3$, $\alpha V\beta_3$ and $\alpha X\beta_2$ are the only three integrins that have their full ectodomain structures solved, in which αIIb and αV belong to the integrins without an αI domain while αX belongs to those with an αI domain (Xiong et al., 2001a; Zhu et al., 2008; Xie et al., 2010). In Figure 1.2, the linearized domain organization of the αL subunit, as a representative of α subunits, is shown.

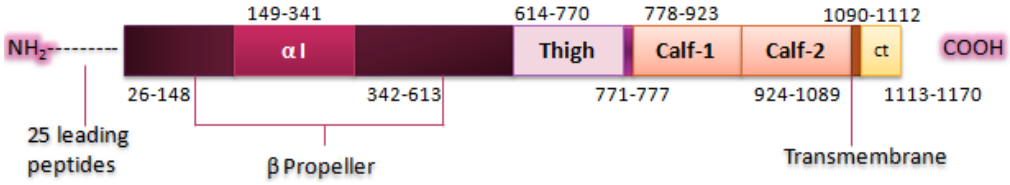

Figure 1.2. Domain arrangements of the integrin αL subunit. Amino acid counting starts from the first methionine of leading peptide. ct: cytoplasmic tail.

1.1.1.1 The Head Region

The β-propeller domain, which is located at the N-terminal of the integrin α subunit, has seven blades. Nine out of the 18 human integrin α subunits have an I domain inserted between blades 2 and 3 (Luo et al., 2007). When present,

the I domain in the α subunit is the major ligand binding domain. For the integrins that lack an I domain, the β-propeller, together with the βI domain, are responsible for αβ interaction and ligand binding (Springer and Dustin, 2012). There are 3 to 4 divalent cation binding sites on the β-propeller. Three divalent cation binding sites are found in blades 5-7 in all integrin α subunits. An additional one is found in blade 4 of the α5, α8, αIIb and αV subunits (Oxvig and Springer, 1998; Zhang and Chen, 2012). The alignment of the divalent cation binding sites is shown in Figure 1.3.

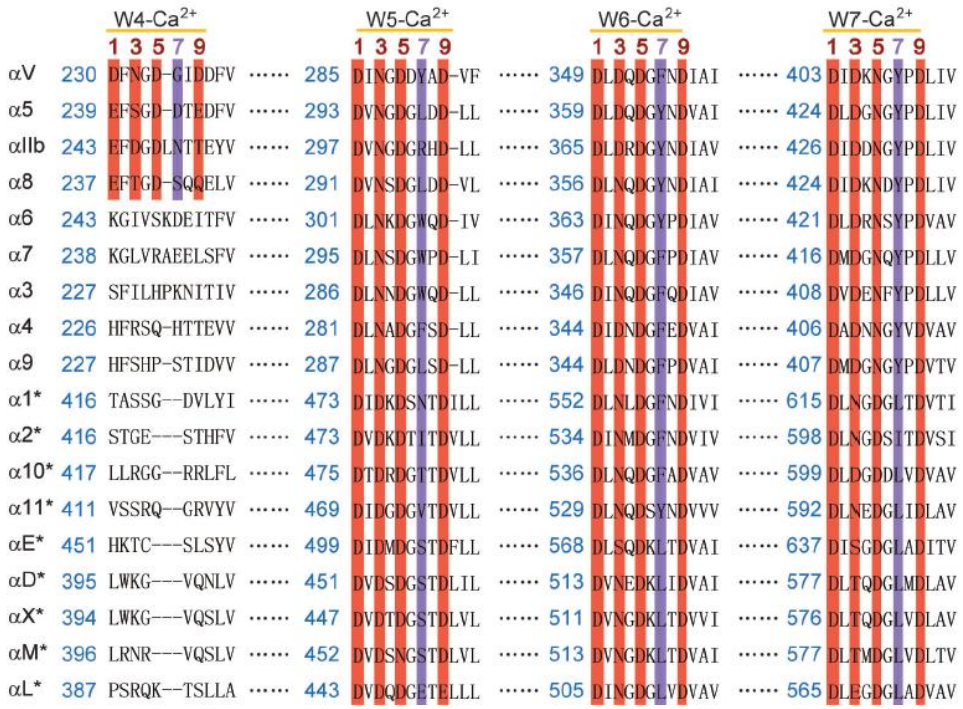

Figure 1.3. Sequence alignment of calcium binding sites on the β-propeller of the 18 human integrin α subunits (Zhang and Chen, 2012). Coordinating residues contributed by side chain atoms are highlighted in red and by backbone atoms are highlighted in purple. α subunits with * are those with an I domain.

The I domain has a Rossmann fold with a central β sheet flanked by several α helices. The I domain binds ligands via its Metal Ion-Dependent Adhesion Site (MIDAS). The motif can be identified by a six-residue signature sequence:

Asp-X-Ser-X-Ser (DxSxS), with an additional residue at a distal site (Chen et al., 2006; Xie et al., 2010; Zhang and Chen, 2012). MIDAS binds Mg^{2+} at physiological state. MIDAS exists in at least two conformations: open and closed. In the closed form, Mg^{2+} is coordinated by two serines and one aspartic acid from the DxSxS signature sequence. Depending on the individual I domain, such as αL I and αM I, the other coordinate residues come from three water molecules; the coordinate residues can also come from an aspartic acid and a threonine residue at distant sites such as in the case of αX I domain. The coordination of the open form MIDAS is similar to that of the close form except for one water molecule being replaced by a glutamic acid from the ligand (San Sebastian et al., 2006; Luo et al., 2007; Xie et al., 2009).

1.1.1.2 The Leg Region

The α subunit leg region consists of four sub-regions, including three β-sandwich structures: the thigh domain, the calf-1 and the calf-2 domain, and one loop structure, the genu, which locates between the thigh and the calf-1 domain.

The genu region is a small loop of 4-5 amino acids flanking by two cysteines which form a disulfide bond. The integrin α subunits are bent at this loop when inactive. Upon activation, structural rearrangement takes place at thigh/genu interface and leads the integrin to an extended structure (Xie et al., 2004). A well coordinated calcium binding site had been assigned to, the genu region of the resting $\alpha V\beta_3$ (Xiong et al., 2001b) and $\alpha IIb\beta_3$ (Zhu et al., 2008).

However, it is not seen in the ectodomain structure of $\alpha X\beta_2$ due to a different backbone conformation (Xie et al., 2010).

The two calf domains located at the C-terminal of α subunit ectodomain, they make contact with the I-EGF3, I-EGF4 and β tail domains of β subunit when the integrin is not activated (Xiong et al., 2003). It is reported that disruption of the α subunit calf-2 and β subunit I-EGF4 interface in the $\alpha IIb\beta_3$ integrin by introducing a glycosylation site resulted in an active integrin. Conversely, locking the two subunit interface by introducing a disulfide bond prohibits integrin activation induced by either inside-out or outside-in signaling (Wang et al., 2010). Kamata et al (2005) studied the divalent cation dependent adhesion of $\alpha IIb\beta_3$ and $\alpha V\beta_3$ suggested that the regulation site lie in the calf-2 region of the α subunits.

1.1.1.3 The Transmembrane and Cytoplasmic Segments

The transmembrane segment is a typical type-1 transmembrane protein. It has been shown that the interaction between the transmembrane domains of the α and β subunits can influence the activation state of the integrins. NMR studies have shown that the interface forms an outer-membrane association clasp (OMC) and an inner-membrane association clasp (IMC) (Lau et al., 2009). The OMC region is characterized by two interactions at the OMC N-terminal (detailed information see Section 1.1.2.6). The IMC is characterized by an electrostatic bond contributed by the arginine residue of the highly conserved membrane proximal motif GFFKR in the α subunit and the aspartic acid of the

HDR motif in the β subunit (Figure 1.4). Most interactions with the cytosolic proteins are via the β subunit. More detailed introduction on the transmembrane and cytoplasmic segments will be found under the β subunit Section 1.1.2.6.

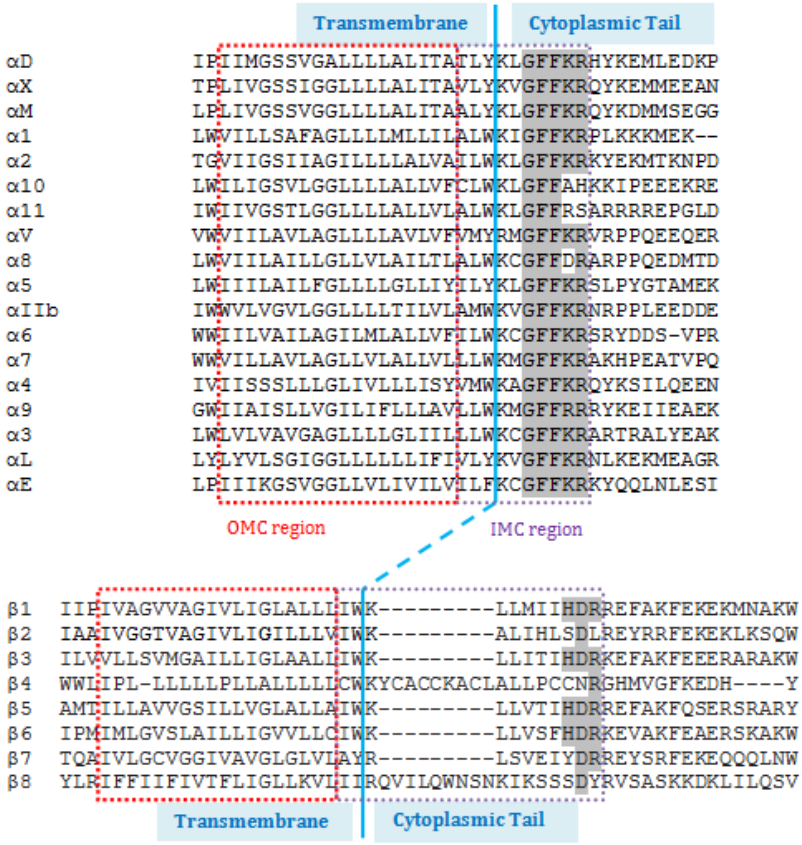

Figure1.4. Sequence alignment of α and β proximal transmembrane region. Boundary of TM and cytoplasmic tail is highlighted by blue line. Conserved residues in GFFKR and HDR motifs are highlighted in grey.

1.1.2 The Structural Features of Integrin β Subunit

The integrin β subunit is organized into seven major domains: the β I domain (βI), the plexin-semaphorin-integrin (PSI) domain, the hybrid domain, the I-EGF domain which consists four segments: I-EGF1 to I-EGF4, which

including a short link now has termed as the β ankle, the β tail domain, the transmembrane domain and the cytoplasmic tail domain (Figure 1.5). In 3D structure, βI is inserted into the hybrid domain, which is in turn inserted into PSI domain.

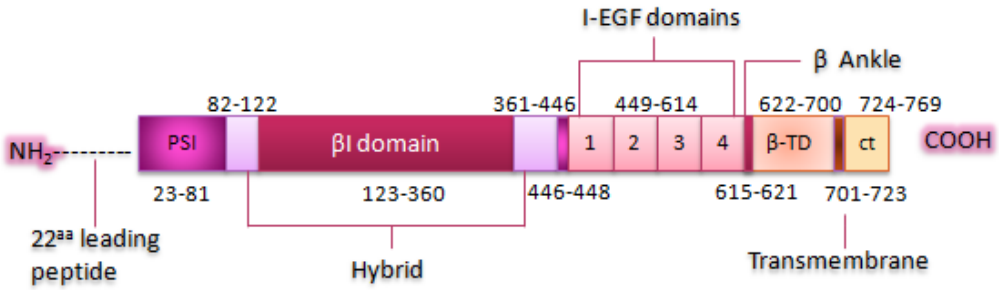

Figure 1.5. Structural schematics of the domain arrangement of a representative β subunit, the integrin β_2. Amino acid counting starts from the first methionine of leading peptide. Note that amino acid 446-448 belongs to PSI domain. Abbreviations: β-TD: β tail domain, ct: cytoplasmic tail.

1.1.2.1 The PSI Domain

The PSI domain is consisted of about 50 amino acids and is split into two segments by the hybrid and the βI domain in the linear sequence. The majority of the residues are in the N-terminal whereas the C-terminal consists of only three residues which located at the middle of the motif of CxCxC. There are 7 cysteines (numbered 1 - 7) in the N-terminal and the 8th cysteine (8) in the xCx motif in the C-terminal portion of PSI. They are engaged in four disulfide bonds with the arrangement of 1 - 4, 2 - 8, 3 - 6 and 5 - 7 (Xiao et al., 2004; Shi et al., 2005; Xie et al., 2010), such cysteine arrangement is commonly found in integrins, plexins and semaphorins (Figure 1.6). The disulfide bridges in PSI are considered to contribute to maintain the integrins in a resting state. Mutations in the PSI domain, such as C31A (disruption of cysteine pair 1 - 4

disulfide bond) in the β_3 subunit and the double substitutions of T26P and T44A in the β_2 subunit led to constitutively active integrins. (Arnaout, 2003; Xiao et al., 2004; Xiong et al., 2004).

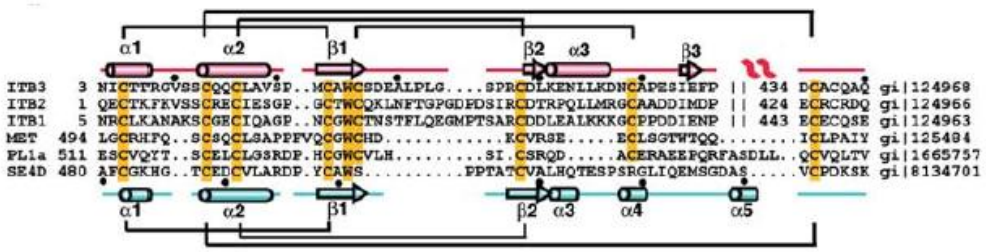

Figure 1.6. Sequence alignment of integrin β2, β3, β1, growth factor receptor MET, plexin a1 (PL1a) and semaphorins 4D (SE4D) PSI domains. Disulfide bridges are showed at top and bottom, secondary structures were denoted above and below the sequences, conserved residues are highlighted (Xiao et al., 2004).

1.1.2.2 The Hybrid Domain

The hybrid domain is separated into two fragments by the βI domain. The N-terminal segment is about 40 amino acids in length while the C-terminal is of approximately 85 residues. This hybrid domain is widely accepted to be involved in integrin activation signal propagation. The epitopes of two reporter mAb 15/7 and HUTS-4 have been mapped into the β_1 hybrid domain. They are only exposed when the integrin is in an active state, suggesting that there is an allosteric change in hybrid domain upon integrin extension (Mould et al., 2003). Another study examined the effect of the integrin function blocking mAb 7E4 on integrin LFA-1, whose epitope was mapped to the C-terminal segment of the hybrid domain. It showed that 7E4 blocked integrin adhesion by obstructing the activation signal propagated from the tailpiece to the headpiece (Tng et al., 2004).

The structure of $\alpha IIb\beta_3$ headpiece liganded with a therapeutic antagonist was published at 2004 (Xiao et al., 2004). By comparing this structure to the $\alpha V\beta_3$ structure with a closed headpiece (Xiong et al., 2002; Xiong et al., 2004) , it was confirmed that the "swing-out" movement (~70Å) of the hybrid domain is involved in integrin activation (Figure 1.7). This finding was in agreement with EM studies (Takagi et al., 2002; Takagi and Springer, 2002; Takagi et al., 2003; Iwasaki et al., 2005).

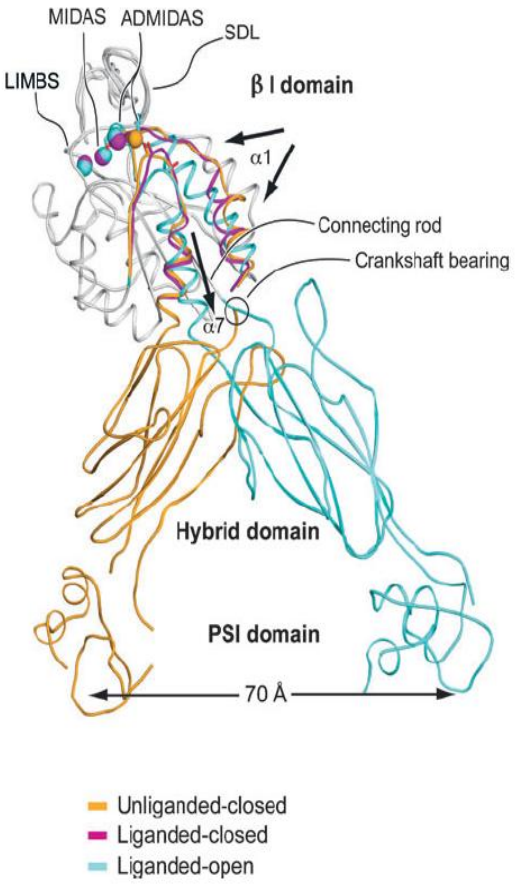

Figure1.7. Overlay structures of β_3 headpiece of liganded-open, liganded-close and unliganded-closed conformations (Xiao et al., 2004; Luo et al., 2007). Unliganded-closed $\alpha V\beta_3$ is showed in gold, liganded-closed $\alpha V\beta_3$ is showed in magenta and liganded-open $\alpha IIb\beta_3$ is showed in cyan. PDB IDs for these structures are 1U8C, 1L5G and 1TXV respectively.

1.1.2.3 The βI Domain

The βI domain assumes a Rossmann fold although it differs from the αI domains by having two additional inserted segments (Luo et al., 2007). It is responsible for αβ heterodimer formation and ligand binding for integrins without the αI domains (Luo et al., 2007). For integrins with αI domains, the βI domain is essential in the regulation of structure and function of the αI domain.

The βI domain has three cation binding pockets which are pivotal in mediating integrin activation and ligand association: the Metal Ion-Dependent Adhesion Site (MIDAS), the ADjacent to MIDAS (ADMIDAS) and the Synergistic Metal ion Binding Site (SyMBS). Mutations of the three cation binding sites severely affect integrin adhesion. Mutation of the MIDAS S136 and S138 of the β_2 subunit completely abolishes LFA-1 binding to ICAM-1 (Bajt et al., 1995; Hogg et al., 1999). In contrast, mutations of the ADMIDAS D141 and D142 enhance the binding of LFA-1 to ICAM-1. Mutations of the SyMBS coordinating residues N229 and D231 abolish LFA-1 adhesion (Chen et al., 2006). The structure and relative location of the three divalent cation binding sites of the β_2 subunit are shown in Figure 1.8 (Xie et al., 2010). It should be noted that some of the residues are shared among the three divalent cation binding sites. They act synergistically to regulate overall integrin structure and function. From many previous studies it is likely that the MIDAS is the major chelator for Mg^{2+} while ADMIDAS and SyMBS are for Ca^{2+}.

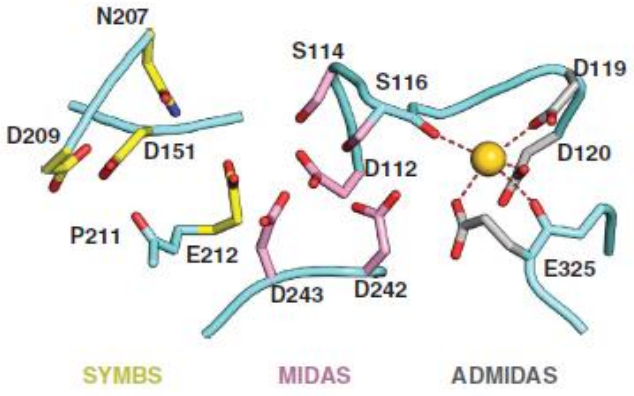

Figure 1.8. The MIDAS, ADMIDAS and SyMBS of the integrin β_2 I domain (Xie et al., 2010). The structure was extracted from the $\alpha X\beta_2$ crystal in an inactive and bent form. The Electron density shows the existence of a calcium ion at ADMIDAS, and possibly SyMBS, but not MIDAS. Sequence numbering starts with the 23rd amino acid glutamine which is the first amino acid in the mature protein.

1.1.2.4 The I-EGF Domain

Epidermal Growth Factor (EGF) repeats are evolutionary conserved domains that are found in the ectodomain of many membrane proteins (Kulkarni et al., 2005). In the integrin β subunits, there are four EGF-like repeats, which referred to as I-EGF repeats. These repeats are short and rich in cysteines, each repeat contains 8 cysteines (labeled 1 to 8). The disulfide bonds in these repeats are generally formed in a pattern of 1 - 5, 2 - 4, 3 - 6 and 7 - 8. However it should be noted that in the I-EGF1, the cysteine pair 2 - 4 is absent, thus only has three disulfide bonds (Shi et al., 2005; Shi et al., 2007).

As a part of integrin stalk region, the I-EGF domain not only serves connecting the β headpiece and β tail, but also plays essential role in propagating activating signals which lead to drastic conformational changes. Antibodies against the I-EGF domain in β_1 and β_2 integrins have been shown

to activate integrin functions. For example, the epitopes of KIM127 and KIM185 that used extensively in this thesis had been mapped to the I-EGF2/3 (Lu et al., 2001) and I-EGF4 (Stephens et al., 1995) sub-domains respectively. Another example is the 9EG7 mAb which has the same effects on the β_1 integrins (Bazzoni et al., 1995).

In the resting structure of the $\alpha X\beta_2$ ectodomain, a sharp bend is clearly shown at the I-EGF1/I-EGF2 interface. Correspondingly, αX was found to be bent at thigh/calf-1 interface (Xie et al., 2010) (Figure 1.9).

Although I-EGF domain is important in signal propagation and conformation reporting, not all mutations in I-EGF domain lead to defective integrin expression or function. In a study involving the truncation of the β_2 subunit, the I-EGF domain and the rest of the C-terminal regions were shown to be not required for LFA-1 and Mac-1 expression and adhesion (Tan et al., 2000). However, it should be noted that 17 mutations in the β_2 subunit I-EGF region of various natures have been shown to cause LAD-1 syndromes (van de Vijver et al., 2012).

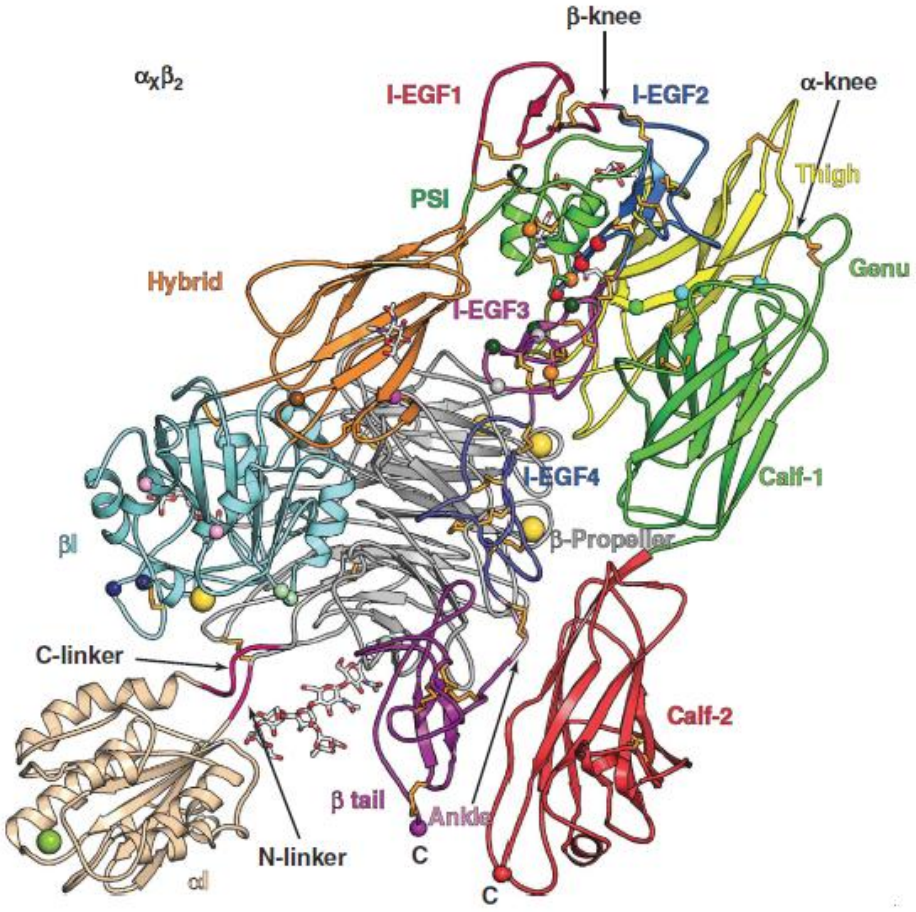

Figure 1.9. Structure of the αXβ$_2$ integrin heterodimer. The bend is located between the I-EGF1 and I-EGF2 in the β_2 subunit and the Genu between the Thigh and Calf-1 of the αX subunit (Xie et al., 2010).

1.1.2.5 The β Tail Domain (βTD)

This β tail domain (βTD) has four pairs of disulfide bonds (Xiong et al., 2001a). Disruption of the 4th disulfide bridges by cysteine mutation in the integrin β_2TD and β_3TD did not affect a normal surface expression but rendered constitutively active forms of the β_2 and β_3 integrins (Nolan et al., 2000; Butta et al., 2003). A loop, identified as the "CD loop", when mutated in the β_2 subunit, the resultant αMβ_2 was found to bind to its ligand iC3b constitutively (Gupta et al., 2007). However, similar results were not found in

experiments with $\alpha IIb\beta_3$ and $\alpha V\beta_3$ (Zhu et al., 2007). The CD loops in β_2 and β_3 appear not to superimpose to each other which may account for the difference in the functional studies (Figure 1.10).

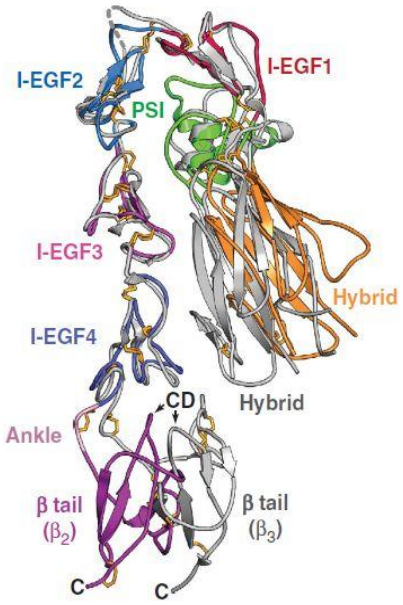

Figure 1.10. Superimposed structures of integrin β_2 and β_3. The βTD CD loops are shown by arrows. (Zhu et al., 2008; Xie et al., 2010) .

1.1.2.6 The Transmembrane Domain (TM) and Cytoplasmic Tail (CT)

The integrin TMs of the α and β subunits are typical as those of type-1 membrane glycoproteins. Recent studies have shown the direction that there are several interactions between the α and β TM, in the $\alpha IIb\beta_3$ and $\alpha L\beta_2$ integrins. Leucine and phenylalanine scan of the central region of TM suggested that these interactions are responsible for the regulation of integrin activities (Luo et al., 2005; Vararattanavech et al., 2008). The interaction sites are defined in two clusters in the TM domain, namely, the outer and inner

membrane association motifs or clasps (OMC, IMC respectively) (Lau et al., 2009) (Figure 1.11). The OMC is characterized in $\alpha L\beta_2$ with the interaction pairs of αL-S1096 and β_2-T708, and αL-G1100 and β_2-I712. Similarly it is characterized in $\alpha IIb\beta_3$ with the interaction pairs of αIIb-G1003 and β_3-V726, and αIIb-G1048 and β_3-I730. The IMC is characterized in $\alpha L\beta_2$ with the interaction of αL-F1117 and β_2-W723, and in the integrin $\alpha IIb\beta_3$ with the interaction of αIIb-F1024 and β_3-W741 (Lau et al., 2009; Chng and Tan, 2011) (Figure 1.11). In other structures, integrins became active when these key residues are substituted (Li et al., 2003; Luo et al., 2004; Li et al., 2005; Partridge et al., 2005; Vararattanavech et al., 2010).

Another possible electrostatic interaction pair lies in the cytoplasmic tail which proximal to the inner face of the membrane. It was first described in the integrin $\alpha IIb\beta_3$ with the interaction between αIIb-R1026 and β_3-D749 (Hughes et al., 1996). A disruption of the salt bridge resulted in the activation of the integrin. The putative electrostatic interaction was observed by NMR in one study (Vinogradova et al., 2002) but not in another (Ulmer et al., 2001) suggested the existence of a weak interaction. This electrostatic pair is conserved in all integrins except those with the β_4 and β_8 subunits.

Most integrin Cytoplasmic domains are very short in length (about 40-60 amino acids) comparing with their large ectodomains, with the only exception of β_4 which consists of more than 1000 residues (Hogervorst et al., 1990). The cytoplasmic tails play important roles in integrin inside-out signaling events. The integrin β cytoplasmic tails are the primary binding sites for many actin binding proteins, signaling proteins and other intracellular regulatory

molecules, the binding sites of these molecules are well described in recent review articles (Figure 1,12) (Kim et al., 2011; Tan, 2012). Few intracellular molecules are known to bind to integrin α subunit cytoplasmic tail (Liu et al., 2000), CD45 is the only one molecule that binds to the leukocyte specific integrin α subunit via αL (Geng et al., 2005).

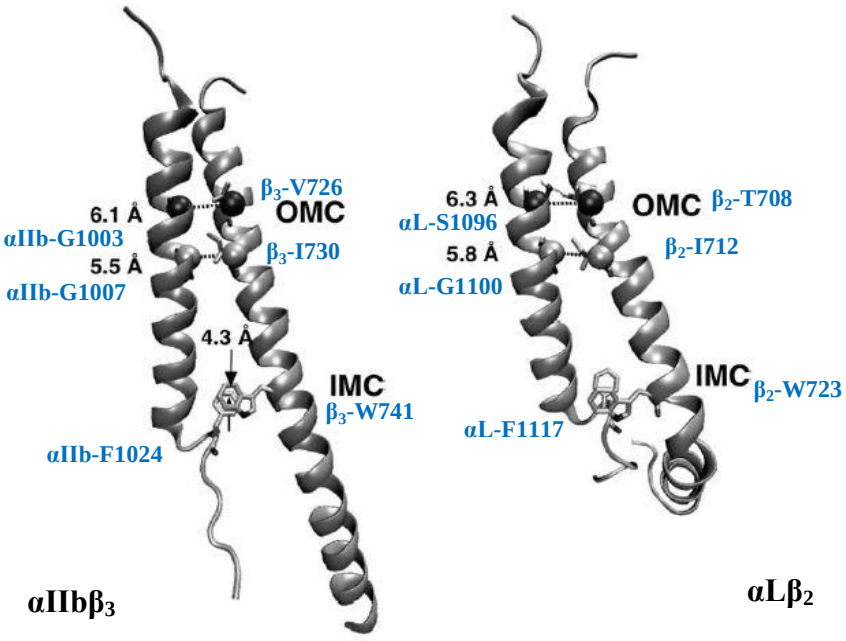

Figure1.11. Coarse-grained molecular dynamics simulations of αIIbβ$_3$ and αLβ$_2$ transmembrane dimerization. αIIbβ$_3$ is shown on left and αLβ$_2$ is shown on right, key residues in OMC and IMC are labeled by sphere or side chains (Chng and Tan, 2011).

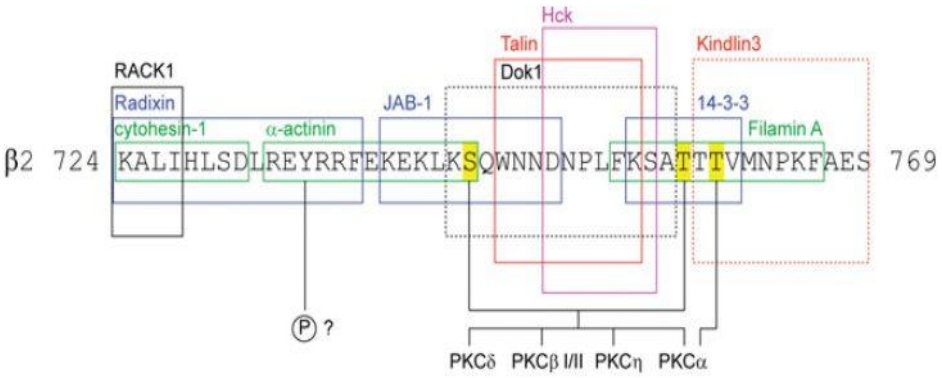

Figure1.12. Human integrin β$_2$ cytoplasmic tail protein sequences and intracellular regulatory stimuli binding sites. Residues labeled with yellow color represented the phosophorylation sites of PKCs (Tan, 2012).

1.1.3 Integrin Conformational States upon Activation

The integrin β subunits are important in contacting with the cytoskeleton and propagating the conformational change (Springer and Dustin, 2012). It is well established that integrins undergo drastic conformational changes from resting state to activating state upon receiving activating signals. Electron microscopy (Nishida et al., 2006) and structure studies (Xiong et al., 2001a; Xiong et al., 2002) revealed that integrin exists in three major conformations, distinguished by two critical changes. One is the leg extension and the other is the hybrid domain swing-out. The three conformation states, namely, (I) bent form, (II) extended form with a close headpiece, (III) extended form with an open headpiece (Figure 1.13) are generally accepted. Integrins in the three states have progressive increasing ligand binding affinity from state (I) to state (III). Recent study revealed that LFA-1 in the state (III) has 10^3-10^4 fold higher affinity to soluble ICAM-1 than in state (II) (Schurpf and Springer, 2011). Nonetheless, these conformations do not cover all cases. For example, a bent integrin $\alpha V\beta_3$ was shown to be able to bind ligand (Arnaout et al., 2007). As ligands can also induce integrin conformational change, the "defined" conformations may only be "snap-shots" of all possible conformations.

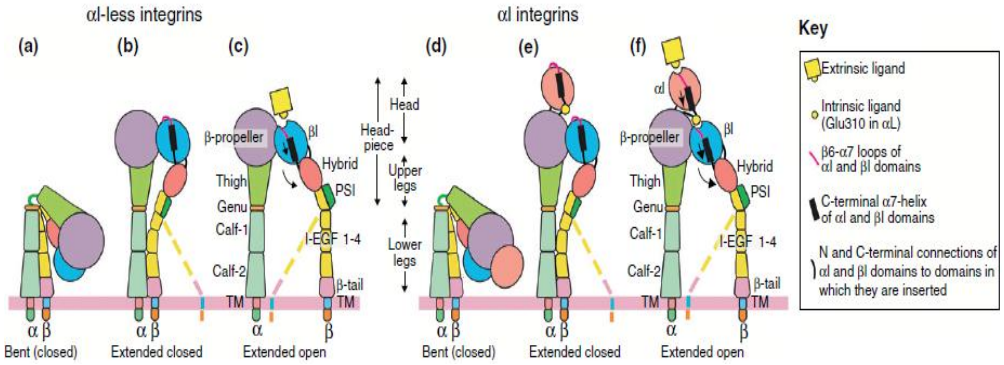

Figure1.13. Conformation transition of integrin with or without an αI domain from an inactive state to an activated state (Springer and Dustin, 2012).

1.1.4 The β_2 integrins

The work in this thesis is on the β_2 integrins. The integrin β_2 family has four members, $\alpha L\beta_2$ (LFA-1, CD11a/CD18), $\alpha M\beta_2$ (Mac-1, CD11b/CD18, CR3), $\alpha X\beta_2$ (p150,95, CD11c/CD18,CR4) and $\alpha D\beta_2$ (CD11d/CD18). Since the four integrins are exclusively expressed on leukocyte surface, therefore they are referred to as the leukocyte integrins (Hynes, 2002; Luo et al., 2007). The four α subunits do not combine with other β subunits, and the β_2 subunit is not known to combine with α subunits other than the four. The characteristics of the four β_2 integrin members are listed in Table 1.1

Table 1.1. β_2 integrin members overview.

Integrin	Distribution	Ligand	Function
Lymphocyte function associated antigen-1 (**LFA-1**)	Predominant on lymphocytes, also found in dendritic cells, NK cells, neutrophils, macrophage, monocytes	ICAM-1, ICAM-2, ICAM-3, ICAM-4, ICAM-5, JAM-1	Participate firm adhesion, facilitate T cell and APC adhesion[a], promote T cell activation and differentiation[b], involve in neutrophil rolling[c]
Macrophage antigen-1, (**Mac-1**) Complement receptor 3 (**CR3**)	Neutrophils, monocytes, macrophages, T cells, dendritic cells, NK cells	ICAM-1, ICAM-2, VCAM, iC3b, factor X, fibrinogen, denatured proteins. 30+ ligands for Mac-1 have been reported[d].	Phagocytosis, leukocyte extravasation and intraluminal crawling, PMN apoptosis and degranulation[e-g]
Complement receptor 4 (**CR4**, **p150,95**)	Monocytes, macrophages, lymphocytes, granulocytes	iC3b, fibrinogen, ICAM-1, lipopolysaccharide (LPS), heparin, and others	Phagocytosis in bacteria, fungi and apoptotic cells[h]
$\alpha D\beta_2$	Monocytes, neutrophils, eosinophils	VCAM-1, VCAM-3, fibronectin, vitronectin, fibrinogen, matricellular protein CCN1, and others	Macrophage migration[i,j]

a: (Bachmann et al., 1997)
b: (Perez et al., 2003)
c: (Henderson et al., 2001)
d: (Hyun et al., 2009)
e, f, g: (Schleiffenbaum et al., 1989; Fagerholm et al., 2006; Pluskota et al., 2008)
h: (Mevorach et al., 1998)
i, j: (Yakubenko et al., 2006; Yakubenko et al., 2008)

1.2 The Leukocyte Adhesion Deficiency (LAD)

Human LAD can be divided into three subtypes: LAD-I, LAD-II and LAD-III. LAD-I is caused by mutations found in the *ITGB2* gene encoding integrin β_2 (CD18) located in chromosome 21q22.3. Patients generally have a decreased or deficient expression of β_2 integrins on their leukocyte surfaces. In a few

cases, β_2 integrins can be expressed but with restricted adhesion properties. In LAD-II, mutations are found in Golgi GDP fucose transport protein encoded by *SLC35C1* gene at chromosome 11p11.2. The defects lie in the fucosylation of selectin ligands and therefore perturbs leukocyte rolling in the initial phase of adhesion. Fucose supplementation is one of current treatments that is showing encouraging results for LAD-II (Hidalgo et al., 2003). LAD-III is due to mutations in the *FERMT3* gene located at chromosome 11q13.1. *FERMT3* encodes fermitin family homolog 3, commonly known as Kindlin-3, which is a protein that interacts with integrin β cytoplasmic tails. Defects in Kindlin-3 cause impaired activation of β_1, β_2 and β_3 integrins (Becker and Lowe, 1999; Behmanesh and Nezhad, 2009; Moser et al., 2009). A recent study revealed that Kindlin-3 could induce integrin LFA-1 micro-clustering and was a requirement for integrin outside-in signaling (Feng et al., 2012). In this thesis, the focus is on LAD-1.

1.2.1 LAD-1, A Brief History

The clinical features of LAD-1 include recurrent, life-threatening bacterial infections with impaired pus formation at infection sites, impaired wound healing and strong leukocytosis. The first indication of an LAD-1 patient is possibly the delayed separation of umbilical cord. Antibiotic therapy is often used to treat LAD-1 patients, however many LAD-1 patients died at young age despite of intensive antibiotic therapy (Anderson and Springer, 1987; Behmanesh and Nezhad, 2009). Currently, the preferred treatments for LAD-1 patients are bone marrow transplantation (BMT) and allogeneic hematopoietic

stem cell transplant (HSCT) if a suitable donor can be found. Granulocyte transfusion is considered an optional treatment for LAD-1 patient. One successful case had been reported (Hamidieh et al., 2012). Gene therapy is still at the experimental phase (Fischer et al., 1994; Bauer and Hickstein, 2000; Qasim et al., 2009).

The first report of LAD-1 dates back to 1974 (Boxer et al., 1974) but the disease was not linked to any molecular defect. Crowley *et al* (1980) reported that a four-year boy with recurrent bacterial infections, abnormal neutrophil spreading and phagocytosis was due to an absence of a membrane glycoprotein of 110 kDa (Crowley et al., 1980). Other LAD-1 patients were found to have missing of 150 kDa or 180 kDa membrane glycoproteins in their leukocytes (Arnaout et al., 1982; Bowen et al., 1982). The deficient molecules were identified to be the CD11/CD18 antigens between the year 1984 and 1985, by specific monoclonal antibodies method and immunoprecipitation techniques (Arnaout et al., 1984; Beatty et al., 1984; Dana et al., 1984; Miedema et al., 1985; Ross et al., 1985). Note that the term "integrin" was not in use until 1986 (Tamkun et al., 1986)

A follow-up investigation on the first patient reported on 1974 (Boxer et al., 1974) by Southwick *et al*, confirmed that such disease was caused by deficiency of adhesion molecule which was recessively inherited (Southwick et al., 1986). In 1987, such disorder was officially termed as "Leukocyte Adhesion Deficiency" by Springer *et al* (1987). Since all the three β_2 integrins (CD11/CD18 antigens) were found missing in these patients, it was reasonable

to conclude that the defect lied in the common β_2 subunit (Tamkun et al., 1986; Anderson and Springer, 1987).

To date, 123 LAD-1 patients are reported worldwide (van de Vijver et al., 2012).

1.2.2 The Gene of Integrin β_2 Subunit: *ITGB2*

The human *ITGB2* gene is located between *PTTG1IP* (encoding pituitary tumor-transforming 1 interacting protein) and *FAM207A* (encoding family with sequence similarity 207, member A) genes at its chromosome. The primary structure of the β_2 subunit was first published at 1987 (Kishimoto et al., 1987; Law et al., 1987). The whole gene DNA has about 42 kb in length and is organized into16 exons (Weitzman et al., 1991).

1.2.3 Phenotypes of LAD-I

Clinically, LAD-1 (OMIM entry #116920) phenotype can be categorized into severe form and moderate form, which differ by the level of β_2 integrin expression on leukocytes. Severe form of LAD-1 is more acute and life threatening, sign of symptom appeared during infanthood. Whereas patients of moderate form of LAD-1 could survive into adulthood if given proper treatment (Anderson and Springer, 1987; Etzioni and Tonetti, 2001). β_2 integrin expression level less than 1% is usually recognized as severe

phenotype while moderate genotype has the β_2 integrin expression level at 1%-10% (Dimancheboitrel et al., 1989). The severity of the LAD-1 syndrome has been associated with particular mutations (Shaw et al., 2001).

1.2.4 Mutations in LAD-I

To date, genotypes of LAD-1 patients can be divided into four major categories including insertion/deletions, splice site mutations, nonsense mutation, and missense mutations, These genotypes have been summarized in a recent LAD-1 review article (van de Vijver et al., 2012) (Figure 1.14). The four major categories are further discussed.

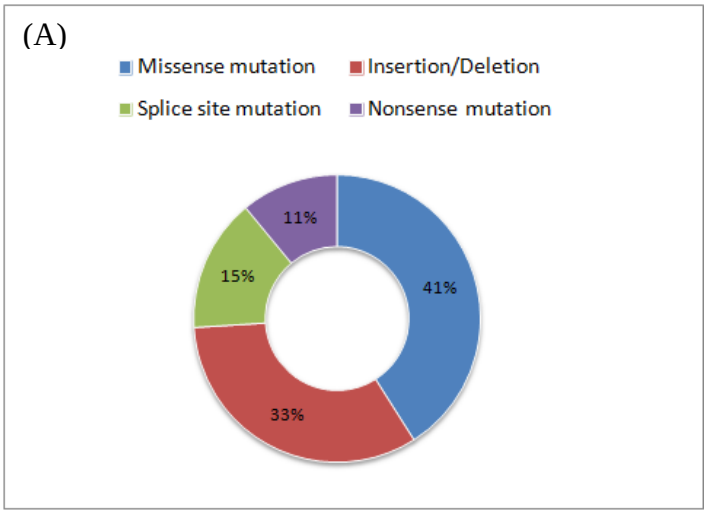

(B)

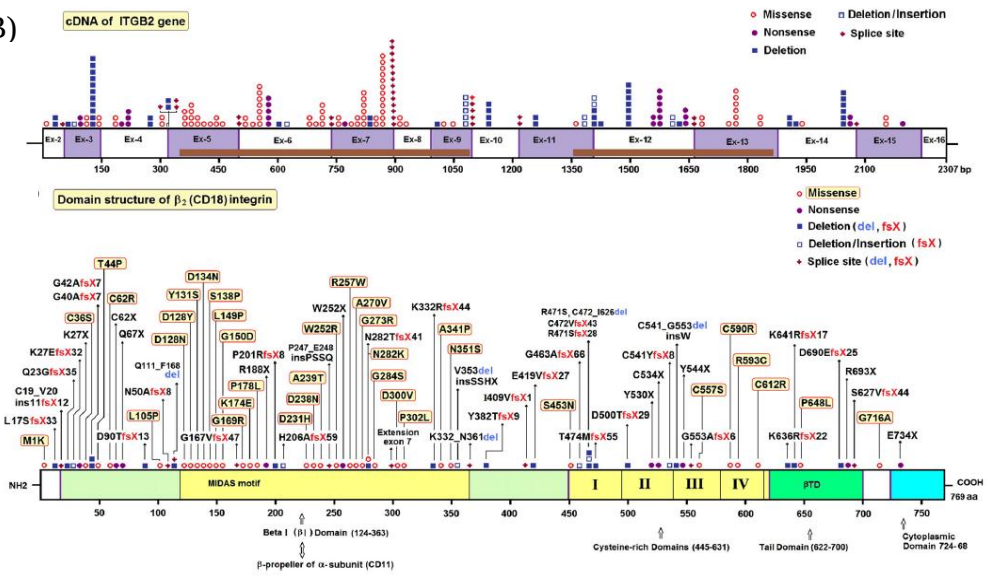

Figure1.14. LAD-1 genotypes distribution. (A): Pie chart statistics of 6 mutation types in LAD-1. (B): Schematic overview of mutations in *ITGB2* (van de Vijver et al., 2012).

1.2.4.1 Deletions

The deletions range from one nucleotide to the entire gene of the coding sequence of β_2 integrin (Riveramatos et al., 1995; Roos and Law, 2001; Hixson et al., 2004; Fiorini et al., 2009). Most deletions result in a reading frame shift and lead to a premature stop codon. The features of several deletion genotypes are highlighted below. The two most frequent found alleles are c.1498delG (deletion of G at position 1498 in the coding sequence, position 1 being the A in the initiation codon) (5 patients) and c.2070delT (5 patients). The 5 patients with the c.1498delG allele is from a highly inbred Tunisian family in North Africa (Fathallah, 2001). On the other hand, the 5 patients with the c.2070delT mutation are not known to be related. Therefore this mutation may have arisen independently multiple times (Sligh JE Jr, 1992; van de Vijver et al., 2012). A particular deletion

(g.43201_PTTG1IP:10890del27703) was found in Caucasian female patient. The deletion of 27,003 bp starts in intron 11 of *ITGB2* to intron 2 of the downstream gene Pituitary Tumor-Transforming Gene 1 Interacting Protein (*PTTP1IP*) (Cher et al., 2011).

1.2.4.2 Splice Site Mutations

Splice mutations are often occurred at proximal boundary of an intron, especially at the splice donor or acceptor sites which characterized by GU at 5' and AG at 3' ends respectively. A branch site at near splice acceptor site with consensus sequence YNYURAY (A: adenosine, N: any base, U: uracil, Y: pyrimidine, R: purine) is also perceived to be important in pre-mRNA splicing (Busslinger et al., 1981; Faustino and Cooper, 2003). All of the LAD-1 splice site mutations are found in one of these sites (Kishimoto et al., 1989; Matsuura et al., 1992; Nelson et al., 1992; Wright et al., 1995; Roos and Law, 2001; Roos et al., 2002; Tone et al., 2007; Uzel et al., 2008; Parvaneh et al., 2010; Cher et al., 2011).

1.2.4.3 Nonsense Mutation

Nonsense mutations are found throughout the coding region of the β_2 integrin (López Rodríguez C, 1993; Roos and Law, 2001; Shaw et al., 2001; Roos et al., 2002; Hixson et al., 2004; Castriconi et al., 2007; Fiorini et al., 2009; van de Vijver et al., 2012). However it should be noted that truncated β_2 subunit in

the leg region can support LFA-1 expression in transfection studies (Tan et al., 2000). Thus it is possible that nonsense mutations found in the leg regions may support some level of β_2 integrin expression. It remains to be determined why such expression is not found in the patients' leukocytes – but see Section 1.2.5.4 on Missense Mutations.

1.2.4.4 Missense Mutation

Missense mutation accounts for 41% among all LAD-1 alleles. A summary table adapted from van de Vijver et al (van de Vijver et al., 2012) that lists currently known 36 LAD-1 missense mutations is shown in Chapter 3 (Table 3.1). Several missense mutations were known to be important in the characterization of integrin features. Two LAD-1 missense mutations, β_2-S138P in the MIDAS and β_2-D231H in the SyMBS do not affect β_2 integrin expression, both in the patients' leukocytes and in laboratory transfections. However the expressed integrins have no adhesion activities (Hogg et al., 1999; Mathew et al., 2000).

Two other mutations in the I-EGF4 domain, β_2-C590R and β_2-R593C, support LFA-1 but not Mac-1 and p150,95 expressions on transfectants. The LFA-1 expressed is of intermediate active state: it is constitutively active in ICAM-1 binding but requires a single activating agent to bind ICAM-3 (Shaw et al., 2001).

The β_2-N351S (Arnaout et al., 1984; Nelson et al., 1992; Uzel et al., 2008), when transfected into fibroblasts with the αL subunit resulted in a fully active

LFA-1 that constitutively binds to ICAM-1 and ICAM-3 (Cheng et al., 2007). (It should be noted that wild-type LFA-1 requires one activating agent to bind ICAM-1 and two to bind ICAM-3) (Tang et al., 2005). Epitopes of activation reporter mAb KIM127, MEM148 and m24 are fully open in native state of integrins suggesting this mutant exists in a extended, open-headpiece form (Tang et al., 2008). Curiously, patients with the mutations, β_2-N351S, β_2-C590R and β_2-R593C showed limited expression of the β_2 integrins. This discrepancy is not understood, for details see Chapter 3.

1.3 Aim of the Study

To understand leukocyte integrin properties and functions, many methods are used to study the structures, conformational changes, activation mechanisms, ligand binding and inside-out/outside-in signaling.

LAD-1 is caused by defects in the gene *ITGB2* that lead to an absence or functional abnormal in β_2 integrin expression on leukocyte surface. Mutation studies are therefore important in providing insights in integrin function, expression and heterodimer formation. To this end, the work in the first part Chapter 3 of the thesis focuses on nineteen LAD-1 missense mutations that scattered in different parts of human integrin β_2 subunit: many of these mutations were identified but not characterized and others were reported for the first time (van de Vijver et al., 2012). These mutants are studied for their support in formation and expression of three β_2 integrin family members: LFA-1, Mac-1 and p150,95. For those that can support the surface expression

will be examined for their ligand binding ability. Characterization of these mutations would help in establishing the correlation between LAD-1 phenotypes and genotypes, as well as shading light on integrin structural and functional studies. In this study, all the experiments were performed in HEK293T (Human Embryonic Kidney) cells *in vitro*.

The integrin adhesion is regulated by divalent cations. It is indicated by many studies that Mg^{2+}/EGTA can induce the ligand binding between integrin LFA-1 and ICAM-1, the effect is minimal in the binding between integrin Mac-1 and BSA. We aim to find the region in LFA-1 that could respond to Mg^{2+}/EGTA mediated activation. Since LFA-1 and Mac-1 share a common β_2 subunit, it is reasonable to presume that some structural features that are located at αL but absent in the αM subunit. I constructed a series of αL/αM domain swopping chimeras with the aim to identify the region that is responsible for the divalent cation dependent activation on LFA-1 (Chapter 4).

Chapter 2: Materials and Methods

2.1 Materials

2.1.1 General Reagents

Most chemical reagents used in this work were purchased from Sigma-Aldrich, 1st Base Biochemicals, Biomed-Diagnostics Pte Ltd, Bio-Rad Laboratories Pte Ltd, Merck Pte Ltd, Research Instruments Pte Ltd, unless otherwise specified. DNA ladder and protein marker were obtained from Fermentas and Bio-Rad respectively. General enzymes, inhibitors, restriction enzymes, transfection reagents as well as PCR reagents were purchased from Stratagene, Clontec, Invitrogen, Fermentas, New England Biolabs, Promega and Roche. DNA/ RNA preparation and purification kits were brought from Qiagen, Promega, Zymo Research, Macherey-Nagel. Bradford assay dye solution and standard 2mg/ml BSA protein were purchased from Bio-Rad Laboratories. All media and supplements were obtained from Hyclone (Research Instruments Pte Ltd). BCECF was purchased from Invitrogen (Life Technologies Corporation).

2.1.2 Cells

HEK293T cells (human embryonic kidney cell with SV40 large T antigen), MOLT-4 cells (human T lymphoblast) and COS-7 cells (African green monkey kidney cells) were purchased from American Type Culture Collection (ATCC). Antibodies MHM23, MHM24, 1B4, KIM127, KIM185, H52, LPM19C and KB43 hybridoma cells origins were stated in Table 2.1.

2.1.3 cDNA Expression Plasmids

DNA sequences of human integrin αL, αM, αX and β_2 were amplified by PCR and introduced into expression vector pcDNA3.0 (Invitrogen BV, The Netherlands) as previously described (Al-Shamkhani and Law, 1998). The αL/αM chimera constructs αLMc-y and αMLc-y (both in pcDNA3.0) were made based on standard molecular biological method by previous lab members. All constructs were verified by DNA sequencing.

2.1.4 Antibodies

All antibodies that listed in Table 2 are mouse anti-human mAbs that were purified from hybridoma supernatant using Hi-Trap protein G columns (GE healthcare, formerly Amersham Biosciences) in our laboratory. All antibodies listed in Table 2.2 are obtained from commercial sources.

Table 2.1 mAbs against the β_2 integrins.

Antibody Name	Target	Function	Reference	Sources
MHM24	αL I Domain	Function Blocking	(Hildreth et al., 1983)	McMichael AJ (John Radcliff Hospital, Oxford, UK)
LMP19C	αM I Domain	Function Blocking	(Uciechowski and Schmidt, 1989)	Law SKA (SBS, NTU, Singapore)
KB43	αX I Domain	Function Blocking	(Watts and Lanzavecchia, 1993)	Pulford K. (LRF Diagnostic Unit, Oxford, UK)
H52	β_2 Hybrid	Function Blocking	(Al-Shamkhani and Law, 1998)	Law SKA (SBS, NTU, Singapore)
MHM23	β_2 Heterodimer	Function Blocking	(Hildreth and August, 1985)	McMichael (John Radcliff Hospital, Oxford, UK)
1B4	β_2 Heterodimer	Function Blocking	(Wright et al., 1983)	Law SKA (SBS, NTU, Singapore)
KIM185	β_2 I-EGF4	Activator	(Robinson et al., 1992)	Robinson MK(UCB, Celltech, UK)
KIM127	β_2 I-EGF2/3	Activator & Activation reporter	(Robinson et al., 1992)	Robinson MK (UCB, Celltech, UK)

Table 2.2 Commercial antibodies

Antibody Name	Application	Sources
FITC-conjugated sheep anti-mouse $F(ab')_2$	Secondary mAb	Sigma-Aldrich
Goat anti-human IgG (Fc specific)	Coating mAb	Sigma-Aldrich
Rabbit anti-mouse IgG (whole molecule)	Immunoprecipitation	Sigma-Aldrich
Sreptavidin-Horseradish Peroxidase conjugate	Secondary mAb	GE Healthcare

2.1.5 Ligands for Cell Binding Analysis

Human ICAM-1 (Domain 1-5)-Fc conjugate and ICAM-3 (Domain 1-5)-Fc conjugate were purified from supernatant of COS-7 transfected cells, using Hi-Trap protein A columns (GE Healthcare) in our laboratory. Bovine serum albumin (fraction V, BSA) was bought from Sigma-Aldrich.

2.1.6 Medium

All media and solutions in 2.1.7 prepared were sterilized by autoclaving or filtration.

LB broth	1% (w/v) Bacto-tryptone (BD), 0.5% (w/v) yeast extract (BD), 1% (w/v) NaCl
LB agar	LB broth plus 1.5% (w/v) Bacto-agar
LB-Amp	LB broth or LB agar with 100 μg/ml ampicillin (Merck)
TYM broth	2% (w/v) Bacto-tryptone, 0.5% (w/v) yeast extract, 0.59% (w/v) NaCl, 0.246% (w/v) $MgSO_4$, pH 7.5
TfBI	30mM KOAc, 100mM KCl, 10mM $CaCl_2$, 15% glycerol
TfBII	10mM MOPS, 75mM $CaCl_2$, 10mM KCl, 15%

	glycerol, pH 7.0
Solution C	50mM $MnCl_2$
HEK293T culture medium	Dulbecco's modified Eagle's medium (DMEM) (HyClone) containing 10 % (v/v) heat-inactivated fetal bovine Serum (Hi-FBS) (HyClone), 100 IU/ml penicillin (HyClone), 100 μg/ml streptomycin (HyClone)
MOLT-4 culture medium	Roswell Park Memorial Institute (RPMI)-1640 (HyClone) containing 10 % (v/v) Hi-FBS, 100 IU/ml penicillin, 100 μg/ml streptomycin
RPMI wash buffer	RPMI-1640 (HyClone, Logan, UT) containing 5 % (v/v) Hi-FBS and 10mM HEPES, pH 7.4
Cell freezing medium	10% (v/v) DMSO in Hi-FBS

2.1.7 Solutions

10x SDS-PAGE running buffer	25mM Tris, 192mM Glycine, 1% (v/v) SDS
10x transfer buffer	25mM Tris, 192mM Glycine
1x transfer buffer	10 times diluted 10x transfer buffer plus 10% (v/v) methanol
Lysis buffer	10mM Tris, 150mM NaCl, 0.5mM $MgCl_2$, 0.15mM $CaCl_2$, 1 % (v/v) Nonidet P (NP)-40, pH 8.0
Cytoskeleton (CSK) buffer	10mM PIPES, 300mM sucrose, 100mM NaCl, 3mM MgCl2, 1mM EGTA, pH 6.8
Cell permeabilize buffer	0.25% TritonX-100 in CSK buffer
SDS-PAGE resolving buffer	25% 1.5M Tris pH 8.8, 8% Acrylamide, 0.1% (v/v) SDS, 0.1% (w/v) NH_4 persulphate, 0.06% (v/v) TEMED (Bio-Rad)
SDS-PAGE stacking	25.3% 0.5M Tris pH 6.8, 5% Acrylamide, 0.1%

buffer	(v/v) SDS, 0.1% (w/v) NH_4 persulphate, 0.1% (v/v) TEMED (Bio-Rad)
Coomassie blue staining solution	50% (v/v) methanol, 10% (v/v) glacial acetic acid, 40% (v/v) ddH_2O, 0.05% (w/v) bromophenol blue
Coomassie blue de-stain solution	30% (v/v) methanol, 10% (v/v) glacial acetic acid, 60% (v/v) ddH_2O
Sodium bicarbonate buffer	0.136% (w/v) sodium carbonate, 0.735% (w/v) sodium bicarbonate, pH 9.2
PBS-T buffer	1x PBS pH 7.2 (Gibco) containing 0.05% (v/v) Tween-20
Quench buffer	100 mM glycine in PBS, pH 7.4
2x SDS sample buffer	50 mM Tris-HCl (pH 6.8), 2% SDS, 0.1% bromophenol blue, 10% glycerol
Blocking buffer	3% non-fat milk (Anlene) in PBS-T
DEAE transfection cocktail	10 ml of RPMI-1640, 100 µl of 10 mM chloroquin (Sigma-Aldrich) sterile, 40 µl of 100 mg/ml DEAE dextran pH 7.0 (sterile), 5 µg of plasmid per flask

2.2 Methods

2.2.1 Transformation of Plasmid DNA

Transformation was performed in 0.5 ml Eppendorf tube containing ~100µl DH5α competent cells. Competent cells were defrosted on ice. 1µl plasmid DNA which containing 0.1-10 µg DNA or 10 µl concentrated PCR products were added to the cells. The mixture was incubated on ice for 10-30 minute, followed by a 42 ℃ heat shock in a water bath or heating blocks for 1 minute and re-cool on ice for another 2 minutes. For plasmid selected by ampicillin

only, the mixture was directly plated onto LB-ampicillin agar plate using an L-shaped spreader. For other antibiotic selecting plasmid and mutagenesis, mixture was further incubated in 400 µl LB broth without any antibiotics at 37℃ orbital shaker with constant speed 200 rpm for 2-3 hours before plating.

2.2.2 Preparation of Plasmid DNA

Plasmid DNA was prepared from a single colony which inoculated from a freshly streaked selective plate and into LB broth containing appropriate antibiotics. The inoculated LB culture was incubated on 37℃ orbital shaker for 8-18 hours. For miniprep, 2 ml overnight bacterial culture was harvested by centrifugation at 16000 g for 10 minutes. DNA extraction was performed according to Promega Wizard® Plus SV MiniPreps manual. For midi and maxi prep, the 2 ml overnight bacterial culture was further expanded into 100 ml and 200 ml LB medium containing proper antibiotics respectively for reproduction and cultured on a orbital shaker at 37℃ for 12-18 hours. Cells were harvested by centrifugation at 4℃ 5500 g for 15 minutes. DNA extraction was followed by instructions provided by Nucleobond® Anion Exchange Column for Quick Purification of Nucleoacids (Macnerey-Nagel) or QIAFilter Plasmid Midi and Maxi Kits (Qiagen).

2.2.3 Quantitation of DNA

DNA concentration was determined by UV spectrophotometer (Nanodrop 1000) at the absorbance of 260 nm; the optical density (OD) of DNA = 1 at a concentration of 50 µg/ml. Quality of DNA is accessed by the ratio of OD 260 nm to OD 280 nm. A range between 1.6 and 2.0 is considered satisfactory.

2.2.4 DNA Electrophoresis

1.0 % (w/v) agarose in 0.5x TBE buffer (1st Base Biochemicals) was used to analyze DNA of the size ranging from 0.1 to 9 kb. For mini-gel electrophoresis apparatus, 50 ml agarose buffer was used for making one gel. 1-2 minutes heating by microwave was used to dissolve the agarose. The bottle containing the agarose solution was left uncapped at room temperature to cool down till no vapor coming out. Ethidium bromide was added to a final concentration of 1 μg/ml followed by casting in the gel apparatus. Electrophoresis was carried out in horizontal apparatus with the gel submerged in 0.5x TBE. DNA samples were mixed with 6X loading dye at the volume ratio of 5:1 and the mixtures were loaded onto the gel. Ethidium bromide stained DNA fragments were visualized by UV transilluminator (UVP).

2.2.5 Gel Purification of DNA and PCR Clean-up

For a direct downstream usage like transformation, PCR products were purified and concentrated to a total volume of 10 μl using the MinElute PCR purification kit (Qiagen). For other downstream usages, the PCR products were further separated by agarose gel electrophoresis. The DNA band was excised from gel using a clean gel cutter, and placed in a 2 ml microcentrifuge tube. The gel slice was weighed. Membrane binding solution was added to the tube at the ratio of 1 μl solution : 1 μg gel. The gel slice was incubated at 50-65 ℃ until gel slice is completely dissolved. DNA was extracted using a Wizard® SV Gel and PCR Clean-Up System Kit (Promega) according to manufacturer's instruction.

2.2.6 Preparation of E.coli Competent Cells

A fresh plate of cells was prepared by streaking out cells from frozen stocks and grown at 37 ℃ overnight. Single colony was picked up and cultured in 10 ml LB medium without any antibiotics at 37 ℃ overnight. 4 ml of the overnight culture was transferred in to 250 ml (two flasks, each 125 ml) TYM broth which has been warmed to 37 ℃. Cells were cultured at 37 ℃ in an orbital incubator until it reached an OD_{550} of 0.6, which usually takes 2 hours. The flasks were placed on ice to allow rapid cooling then the cells were transferred to five 50 ml falcon tubes and spun at 4200 rpm at 4 ℃ for 15 min. Pellets were gently re-suspended in a total of 50 ml (10 ml per tube) ice cold TfBIC buffer (Solution C added into 200ml TfBI, filtered). The cell suspension was centrifuged at 4200 rpm at 4 ℃ for 8 min. The pellet was then re-suspended in a total of 10 ml (2 ml per tube) ice cold TfBII buffer. Competent cells were distributed into convenient aliquots (0.1 ml) in pre-chilled microcentrifuge tubes. Cells were stored at -80 ℃. An aliquot of the cells was used to assay for viability and competence.

2.2.7 Site-Directed Mutagenesis and Domain Swapping

LAD-1 mutants were constructed by site-mutagenesis on CD18-pcDNA3 plasmid using a QuikChange™ Site-Directed Mutagenesis Kit (Stratagene), following the manufacturer's protocol. One 35 mer primer with the desired mutation in the center, 17 nucleotides of original sequences flanking at upstream and downstream respectively was designed, and synthesized by 1st base biochemicals Pte Ltd. PCR cycling was set as the following: initiation at

95 ℃ 2 minutes, followed by 30 cycles of denaturation (95 ℃, 30 seconds), annealing (T_m-5 ℃, 30 seconds) and elongating (72 ℃, 10 minutes), and completed by a final extension of 10 minutes at 72 ℃. The restriction enzyme Dpn I was used to digest the original template (37 ℃, 1 hour). The Dpn I treated PCR product was cleaned up and concentrated by using MinElute PCR purification kit (Qiagen) and was transformed into competent *E.coli* and plated onto LB agar plates with appropriate antibiotics.

αL/αM chimeras were made by two steps domain swapping PCR (Figure 2.1). Two 63-64bp chimera primers were designed with around 27 bp from the boundary of target domain (donor) in the 3' end of forward primer and reverse primer, around 37 bp from boundary sequences of being swapped into (receptor) was designed into the 5' end of the chimera primers. A maga primer that containing the donor domain in the middle and flanked with boundary sequences from the receptor was synthesized by PCR, thermo cycling parameters followed the manufacturer's instruction of Advantage® -GC cDNA Ploymerase Mix kit (ClonTech). This mega primer was obtained by gel purification from the first step PCR product. The final chimera was generated by Site-Directed Mutagenesis kit (Stratagene), the second step PCR was performed with the following parameters:

Cycles	Temperature	Time
1	95°C	5 minutes
18	95°C 76°C 75°C … 46°C 45°C 72°C	1 minute 30 seconds 30 seconds … 30 seconds 30 seconds 20 minutes
1	72°C	20 minutes
1	4°C	For ever

Note: The annealing temperature drops 1 ℃ every 30 seconds from 76 ℃ to 45 ℃, which represented by the ellipsis in the middle of table.

DpnI digestion, product elution, transformation and plating into LB agar plates as indicated in the manual of the kit. All PCR reactions were carried out in a volume of 50 µl. The authenticity of αL/αM chimeras and LAD-1 constructs were verified by sequencing (1st Base Biochemicals, Singapore or AIT Biolab, Singapore).

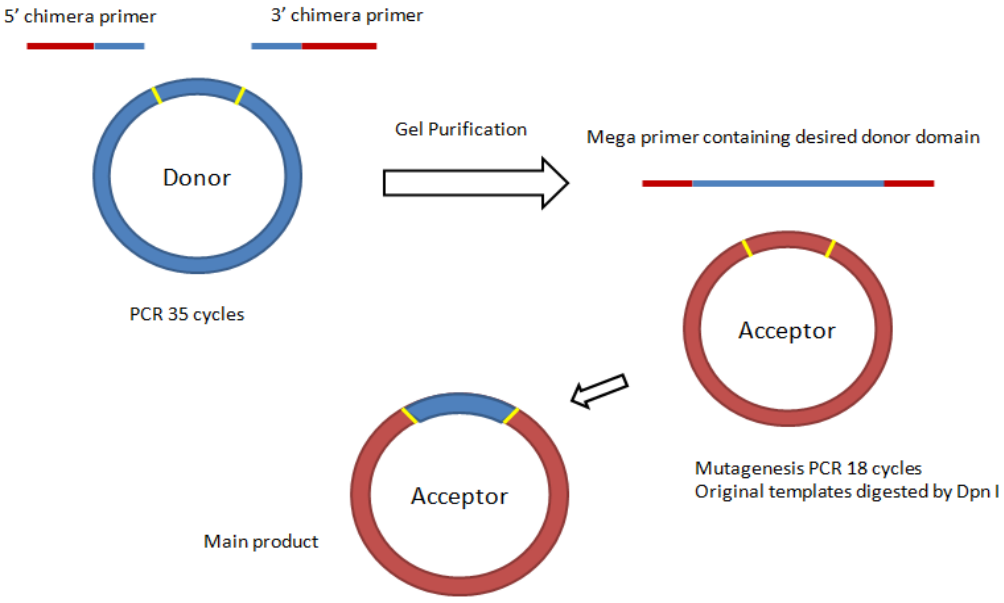

Figure 2.1. A schematic flow chart of domain swapping (2-step PCR). Mega primer was synthesized at ~500 bp.

2.2.8 Cryopreservation of Mammalian Cells

Cells culture was centrifuged at 400 g, 4 ℃ for 4 minutes. Supernatant was decanted. Cell pellets were resuspended in 2 ml freezing medium and dispensed into cryo vials (Greiner). Cryo vials were frozen in an isopropanol containing NALGENE^{TM} Cryobox (Thermo Fisher Scientific) at -80 ℃ for 1-2 days before transferring into liquid nitrogen tank for storage.

2.2.9 Recovery Cells From Liquid Nitrogen

Cryo vials that containing cells were taken out from liquid nitrogen and quickly thawed in a 37 ℃ water bath. Cells were transferred into a 15 ml falcon tube which contained 9 ml complete culture medium and sedimented at 400 g for 4 minutes to remove the DMSO. The cell pellets were resuspended in complete medium at 37 ℃, and cultured in the 5% CO_2 incubator.

2.2.10 Cell Culture

All cell cultures were maintained in a CO_2 incubator (Sanyo, Japan) at 37 ℃ in humidified air containing 5% CO_2. For HEK293T cells, DMEM medium with proper serum and antibiotics were used. Cells passage was conducted every two days with 1/6 splitting ratio when cells reached confluency. Cells were washed once in 1x PBS before detaching with complete media.

COS-7 and MOLT-4 were cultured in RPMI-1640 medium with proper serum and antibiotics in the CO_2 incubator. COS-7 cells were washed once with PBS before incubation with 0.25% (w/v) 1x trypsin (Gibco) for ~6 minutes at 37 ℃, followed by tapping the flask to dislodge the adherent cells. Trypsin was

inactivated by adding complete medium and cells were directly seeded into fresh culture media in new flask at the desired cell density. Non-adherent cells passages were done by dilution with fresh complete medium when cells reached confluency (~1x 10^6 cells/ml).

2.2.11 Transfection of HEK293T Cells

2.2.11.1 Preparation of PEI

PEI powder (Sigma-Aldrich) was dissolved to a concentration of 2 mg/ml in water which had been heated to 80 ℃ followed by letting it cooling down naturally into room temperature. The pH was adjusted to 7.0 by 5M HCl. The solutions were sterilized by filtration, allocated into 2 ml tubes and stored at -20 ℃.

2.2.11.2 PEI Transfection Protocol

Cells were seeded into 6-well dish one day prior to transfection to give 70%-90% confluency on the day of transfection. Purified plasmid DNA was used at a total of 3 μg, diluted in ~100 μl DMEM medium without antibiotics or FBS in a 1.5 ml tube. 6.5 μl of PEI was added to the tube followed by mixing gently with pipetting up and down several times. After incubation at room temperature for 15 minutes, 600 μl complete DMEM medium were added into the tube to re-suspend the mixture, and the mixture was dispensed into cell plate which containing 1.5 ml fresh complete medium drop by drop. The cell plate was then incubated for 22-26 hours in cell incubator. Cells were harvested in 1 ml media/wash buffer/1x PBS after wash once with 1x PBS and

were sedimented by centrifugation at 400g, 4 min, 25 ℃ for subsequent analysis. For large amount of cells transfection on 60 mm dish or 10 cm dish, a scale-up dose of cells, PEI, medium and DNA amount that proportional to the surface area of the dish were applied.

2.2.12 Transfection of ICAM-1 or ICAM-3 Fusion Protein on COS-7 Cells

COS-7 cells were seeded into 75 cm^2 flask one day prior to the day of transfection to give 50%-80% confluency on the day of transfection. The cells were washed with 10 ml of complete RPMI-1640 medium without FBS and antibiotics, following by adding freshly made transfection cocktail (Section 2.1.7). The cells were incubated at 37 ℃ for 5 hours. After that, cells were washed with 10 ml PBS, followed by adding 10 ml of 10% DMSO in PBS and incubating for exactly 3 minutes. The "shocked" cells we washed two times with 10 ml PBS followed by addition of 15 ml complete RPMI-1640 medium and incubated for 24 hours. The medium was removed and the cells were washed twice with PBS followed by adding 1 ml of trypsin to the 75 cm^2 flask. Detached cells were transferred to a new 75 cm^2 flask followed by adding 20 ml of complete RPMI-1640 medium with low IgG FBS (USA Origin). The cells were then left in cell incubator until the 8^{th} day. Supernatant was collected by centrifuging at 4000 g for 15 minutes, followed by filtration using 0.45 μm filter unit (Pall). The filtered supernatant was passed through a 1ml protein A HP HiTrap column (GE Healthcare) at a flow rate about 1.0 ml/min in a peristaltic pump (EYELA MP-1000, Tokyo Rikakikai Co., Ltd) and re-circulated for 24 hours. The protein was eluted by 100 mM sodium citrate at

pH 3.0, followed by adding 1 M Tris at pH 9.0 into the collecting tube to neutralize the eluted protein.

2.2.13 Preparation of Monoclonal Antibodies

Hybridoma cells (listed in Table 2.1) were initially cultured at 75 cm^2 flask using RPMI medium with low IgG FBS and appropriate antibodies. The cells were expanded into two 150 cm^2 flasks when the hybridoma cells adapted the environment and grew well. When cells became confluent, the two flasks' cell cultures were further expanded into 10 x 150 cm^2 flaks and incubated for 8 days. Supernatant that contained the desired antibodies was collected by centrifuging at 4000 g for 15 minutes at 4 ℃ to remove the cells. The clear supernatant was filtered by 0.45 μm filter unit (Pall). The mAb was purified using a1ml protein G HP HiTrap column (GE Healthcare). The column was washed with 10 ml of 20 mM sodium phosphate at pH 7.0 (1^{st} Base Biochemicals), followed by passing the filtered supernatant through the column at a flow rate about 1.0 ml/min in a peristaltic pump (EYELA MP-1000, Tokyo Rikakikai Co., Ltd) and re-circulating for 24 hours. The next day, the column was washed with 10 ml 20 mM sodium phosphate at pH 7.0. For elution antibodies from protein G beads, 0.1 M glycine at pH 2-2.5 was used as eluent. 5-10 ml of eluted proteins were collected in 5-10 x1.5 microtubes containing appropriate amount of neutralization buffer. The beads after elution was neutralized by 20 mM sodium phosphate pH 7.0, washed and saturated with 20% ethanol, detached from peristaltic pump and stored at 4 ℃.

2.2.14 Determination of Protein Concentration by Bradford Assay

Bradford assay was done in a microtiter plate. Standard BSA (Bio-Rad) which diluted in PBS at 100 µg/ml was used as a standard base. Each protein sample of standard dilution was prepared in a total volume of 100 µl ranging from zero to 50 µg/ml at 10 µg/ml per increase. Proteins to be tested were prepared to a final volume of 100 µl in PBS. Bradford reagent (Bio-Rad) was diluted 1/3 by PBS, 150 µl was added to each well. Protein samples were then transferred to the plate using a multi-channel pipette. The plate was left in room temperature for 20-30 minutes before measuring the absorbance at 595 nm by Infinite® 200 PRO plate reader (Tecan).

2.2.15 Flow Cytometry Analysis

Cells were mixed with 10 µg/ml primary mAb in wash buffer and were incubated for 45-60 minutes in 4 ℃. Cells were washed once with wash buffer and were re-suspended in full media/wash buffer containing 1:400 diluted FITC-conjugated sheep anti-mouse IgG at room temperature for 30 minutes. Stained cells were collected on a FACS Calibur (BD Biosciences) using CellQuest Pro software (BD Biosciences) or Flowjo (Tree Star, Inc.).

2.2.16 Cell Permeabilization

Cells were spun down at 400 g, 4 minutes and washed once with 1x PBS. The pallets were re-suspended in 3.7% para-formaldehyde in PBS for 10 minutes at room temperature. Fixed cells were washed once with CSK buffer and then

permeabilized by CSK buffer containing 0.25% Triton-X 100 (made freshly per usage) at room temperature for 2 minutes. Permeabilized cells were washed with CSK buffer once again and incubated with primary antibody in CSK buffer, followed by routine FACS staining.

2.2.17 Surface Biotinylation of HEK293T Cells

HEK293T cells were washed three times with ice-cold PBS (pH 8.0) to remove amine-containing media and proteins from the cells. EZ-Link® Sulfo-NHS-LC-Biotin (pierce, Product# 21335) powder was dissolved in ddH_2O to a final concentration of 2 mM (prepared freshly per usage), 1 ml of biotin reagent solution was added gently to the cells surface drop by drop. Cell plate was left at room temperature for 30 minutes. Biotinylated cells were washed three times with quench buffer to remove excess biotin reagent and byproducts. Labeled cells were detached and collected in 1.5 ml tubes for further analysis.

2.2.18 Preparation of Protein A Sepharose with Rabbit Anti-Mouse IgG Conjugation

Protein A sepharose CL-4B (GE Healthcare) (PAS) was swelled in PBS and rotated at 4℃ overnight. The next day, the PAS beads which formed a bed volume of approximately 4 ml were sedimented by centrifugation at 3000 g, 4℃ for 5 minutes. The beads were washed twice in PBS and then re-suspended in 12 ml PBS to obtain a 25% (v/v) PAS slurry. Following that, 4 mg of rabbit anti-mouse IgG (RAM) was added to the bead slurry and the mixture was rotated at 4℃ for 1 hour. The coated beads were washed twice in PBS followed by centrifugation at 3000 g, 4℃ for 5 minutes. The PAS-RAM

beads were re-suspended with PBS to achieve a 25% (v/v) slurry again and were stored at 4 ℃ for immunoprecipitation analysis.

2.2.19 Immunoprecipitation

Biotinylated HEK293T cells were detached from the 60 mm dish and were collected in 1.5 ml mircotubes with DMEM complete medium. The cells were incubated with the primary mAbs at 37 ℃ for 30 minutes. Incubated cells were washed with wash buffer and lysed on ice for 20 minutes in lysis buffer with protease inhibitors (Roche Diagnostics, Basel, Switzerland). Cell debris was precipitated by centrifugation at 13000 g in 4 ℃ for 10 minutes. Cell lysate were transferred into another pre-chilled 1.5 ml mircotubes. 80 µl of PAS-RAM beads was added into every 200 µl cell lysate. The new mixture was rotated at cold room (4 ℃) for 3 hours followed by 3 x washing in lysis buffer at 10000 g, 4 ℃ for 2 mintues. Bound proteins were eluted with 2x SDS sample buffer containing 40 mM DTT by heating at 100 ℃ for 5 minutes. The protein samples were then subjected to SDS-PAGE.

2.2.20 SDS-PAGE

Of the work stated in this thesis, 8% SDS gels were used to resolve integrin-containing proteins. Protocol basically followed the original paper published by Laemmli in 1970 (Laemmli, 1970) with some modifications. Protein samples (10 µl for minigel system) were denatured by mixing with an equal amount of 2x SDS sample buffer and boiling at 100 ℃ for 5 minutes under non-reducing condition. For reducing condition, protein samples were reduced by mixing with 2x SDS sample buffer containing 40 mM DTT.

Electrophoresis was carried out at a constant voltage of ~167V for around 50 minutes in a Mini Electrophoresis Set (Bio-Rad) in SDS-PAGE running buffer.

2.2.21 Western Blotting

Proteins separated by SDS-PAGE were transferred onto a polyvinylidene fluoride (PVDF) membrane (Immobilon-P, Millipore). The PVDF membrane was cut to an appropriate size and then activated by soaking in 100% methanol for 1-2 minutes before incubation in ice cold transfer buffer for 5 minutes. The gel was equilibrated in ice cold transfer buffer for 3-5 minutes before casting the sandwich. Proteins were electro-transferred from the SDS-PAGE gel onto the PVDF membrane using a Mini Trans-Blot® Cell (Bio-Rad) at 400 mA for 1 hour. Thereafter, the PVDF membrane was transferred to blocking buffer and was incubated at room temperature for one hour under agitation.

For detection of biotinylated proteins on PVDF membrane, the membrane was briefly rinsed after blocking, followed by incubated in PBS-T containing HRP-conjugated streptavidin at 1:3000 dilution for one hour under agitation. The membrane was washed for three times for 10 minutes with PBS-T buffer. Following that, biotinylated proteins were detected by ECL.

Proteins that bond with Horseradish peroxidase (HRP)-streptavidin were detected by Enhanced chemiluminescence (ECL). The detection procedures followed the instruction of ECL Prime Western Blotting Detection Reagent Kit (GE healthcare). Thereafter, the protein blot was exposed to an X-ray film (Kodak, Japan) in dark room. X-ray film was developed using a Kodak X-OMAT ME-1processor (Kodak).

2.2.22 Coating Microtitre Plates with Integrin Ligands for Cell Adhesion Assay

Ligands for integrin LFA-1 (ICAM-1 and ICAM-3) are fusion proteins that conjugated to Fc fragment of human IgG with ICAM-1 or ICAM-3 domain 1-5. 96 microtitre plate (Polysorb, Nunc Immuno-Plate) was firstly coated with goat anti-human IgG (Fc specific) antibody which was diluted to 5 μg/ml by sodium bicarbonate buffer, pH 9.2-9.4. 100 μl was coated to each well. The microtitre plates were left at 4 ℃ overnight. On the next day, the solution was discarded and the plate was washed twice with 120 μl PBS per well. A solution of 0.5 % (w/v) denatured BSA in PBS was added to each well (150 μl per well) and the plates were incubated at 37 ℃ for 30 minutes. After that, the plate was washed with PBS once. 50 μl of ICAM-Fc at a concentration of 1 μg/ml (with 0.1 % BSA) was added to each microtitre well. After 2-3 hours' incubation at room temperature, the plate was washed twice in wash buffer before addition of cells.

For denatured BSA adhesion assay, BSA powder was dissolved in bicarbonate buffer to reach 100 μg/ml. 100 μl was added to each well of a microtitre plate, and the plate was left overnight at 4 ℃. On the next day, the solution was discarded and the wells were washed twice with 120 μl PBS per well. The wells were blocked by 0.2% (w/v) polyvinylpyrrolidone (PVP) (Sigma-Aldrich), 100 μl per well, incubated at 37 ℃ for 30 minutes. The plate was ready to use after washing twice in wash buffer.

2.2.23 Cell Adhesion Assay

HEK293T cells were collected and incubated with 2',7'-bis-(2-carboxyethyl)-5(and -6) carboxy fluorescein, acetoxymethyl ester (BCECF) dye (Invitrogen), to the concentration of 1 μg/ml for 20 minutes at 37 ℃ incubator. Labeled cells were distributed evenly for each condition (ideal cells number is 1.6×10^4 cells/well). If needed, mAbs were added to a final concentration of 10 μg/ml, for cation treatment, $MgCl_2$ and EGTA (ME) were made freshly each time and added to the cells at a concentration of Mg^{2+} at 5mM and EGTA at 1.5mM. 50 μl of cells were transferred to the ligand coated plate for each well, and were incubated for 30 minutes at 37 ℃, 5% CO_2 incubator. Non-adherent cells were removed by washing. The relative number of cells that adhered to the ligand coated plates was determined by fluorescence intensity using FL600 fluorescence plate reader (Bio-Tek).

The "% Binding" of the adhesion assay was calculated as such:

$$\left(\frac{\text{FI of cells adhered after wash} - \text{FI of background}}{\text{FI of cells added before wash} - \text{FI of background}} \text{ X } 100 \right) \%$$

Where FI refers to "Fluorescent Intensity (BECEF Ex485nm/Em530nm)", background measurements were obtained from empty wells.

In each experiment, data is collected in triplicates (3 wells). Variation is shown by standard deviations (SD).

Note: In this study, all the experiments were performed in HEK293T (Human Embryonic Kidney) cells *in vitro*.

Chapter 3: Characterization of 19 novel LAD-1 mutants

To date, 36 LAD-1 missense mutations have been reported. In 2012, van de Vijver et al (2012) updated the LAD-1 mutation database. In the paper, 29 novel LAD-1 mutations, including 10 missense mutations, 4 nonsense mutations and 15 mutations involving either deletion, insertion or splice site mutations were reported. Twenty-six LAD-1 missense mutations were reported in earlier studies including 17 that had been characterized and 9 not characterized. The summary of all 36 LAD-1 missense mutations is shown in Table 3.1.

In this chapter, 19 missense mutations were studied for their ability to support the expression of the $\alpha L\beta_2$, $\alpha M\beta_2$ and $\alpha X\beta_2$ integrins on transfected HEK293T cells. Cells with the expressed integrins were further studied for their ability to adhere to ligands.

The locations of the mutations, and their mutated amino acids are shown in Figure 3.1.

Table 3.1. Summary of LAD-1 missense mutations.

Amino-acid change	Genetic Code Change	Location	Reference	Accession Number
Novel, reported by van de Vijver *et al*, 2012 **(10)**				
p.T44P	ACC→CCC	PSI	(van de Vijver et al., 2012)	A0090 A0091
p.C62R	TGC→CGC	PSI	(van de Vijver et al., 2012)	A0092
p.K174E	AAG→GAG	βI	(van de Vijver et al., 2012)	A0125
p.D238N	GAC→AAC	βI	(van de Vijver et al., 2012)	A0113
p.R257W	CGG→TGG	βI	(van de Vijver et al., 2012)	A0131
p.N282K	AAC→AAA	βI	(van de Vijver et al., 2012)	A0124
p.P302L	CCA→CTA	βI	(van de Vijver et al., 2012)	A0079
p.S453N	AGC→AAC	I-EGF1	(van de Vijver et al., 2012)	A0112
p.C557S	TGC→TCC	I-EGF3	(van de Vijver et al., 2012)	A0129
p.P648L	CCG→CTG	β tail	(van de Vijver et al., 2012)	A0110
Uncharacterized, reported by early studies **(9)**				
p.D77N	GAC→AAC	PSI	(Moore et al., 2008)	A0069
p.L105P	CTT→CCT	Hybrid	(Hinze et al., 2010)	A0095
p.D128Y	GAC→TAC	βI	(Parvaneh et al., 2010)	A0056 A0059
p.D134N	GAC→AAC	βI	(Lorusso et al., 2006)	A0076
p.G150D	GGT→GAT	βI	(Uzel et al., 2010)	A0099
p.A239T	GCC→ACC	βI	(Parvaneh et al., 2010)	A0055 A0130
p.D300V	GAC→GTC	βI	(Li et al., 2010)	A0084
p.C612R	TGC→CGC	I-EGF4	(Roos and Law, 2001; Fiorini et al., 2002; Eyerich et al., 2009)	A0082
p.G716A	GGC→GCC	TM	(Parvaneh et al., 2010)	A0054
Had been studied **(17)**				
p.M1K	ATG→AAG	PSI	(Sligh JE Jr, 1992)	A0016
p.C36S	TGC→AGC	PSI	(Kijas et al., 1999; Tng et al., 2004)	A0079
p.D128N	GAC→AAC	βI	(Matsuura et al., 1992; Roos and Law, 2001)	A0002 A0117
p.Y131S	TAT→TCT	βI	(Matsuura et al., 1992; Uzel et al., 2008)	A0046

Table 3.1 (Continue)

Amino-acid change	Genetic Code Change	Location	Reference	Accession Number
p.S138P	TCC→CCC	βI	(Hogg et al., 1999)	A0003
p.L149P	CTA→CCA	βI	(Wardlaw et al., 1990; Wright et al., 1995)	A0017 A0078
p.G169R	GGG→AGG	βI	(Wardlaw et al., 1990; Corbi et al., 1992)	A0010 A0027
p.P178L	CCG→CTG	βI	(Back et al., 1992; Ohashi et al., 1993; Malawista et al., 2003)	A0020 A0031 A0073 A0074 A0080 A0099
p.D231H	GAT→CAT	βI	(Mathew et al., 2000)	A0013 A0075
p.W252R	TGG→CGG	βI	(Roos and Law, 2001)	A0004
p.A270V	GCG→GTG	βI	(Shaw et al., 2001)	A0007 A0111
p.G273R	GGG→AGG	βI	(Hogg et al., 1999)	A0003 A0093 A0113 A0118 A0123
p.G284S	GGC→AGC	βI	(Kishimoto et al., 1989; Uzel et al., 2008)	A0011 A0012 A0013 A0014 A0023 A0043 A0044 A0047 A0072 A0091 A0116
p.A341P	GCC→CCC	βI	(Shaw et al., 2001)	A0006
p.N351S	AAT→AGT	βI	(Nelson et al., 1992; Cheng et al., 2007)	A0030
p.C590R	TGT→CGT	I-EGF4	(Shaw et al., 2001)	A0007
p.R593C	CGT→TGT	I-EGF4	(Arnaout et al., 1990; Shaw et al., 2001)	A0008 A0009 A0012 A0045 A0066 A0067

Note that in this thesis, the translation initiator Methionine was counted as +1 in the amino acid sequence, unless other naming method is specified.

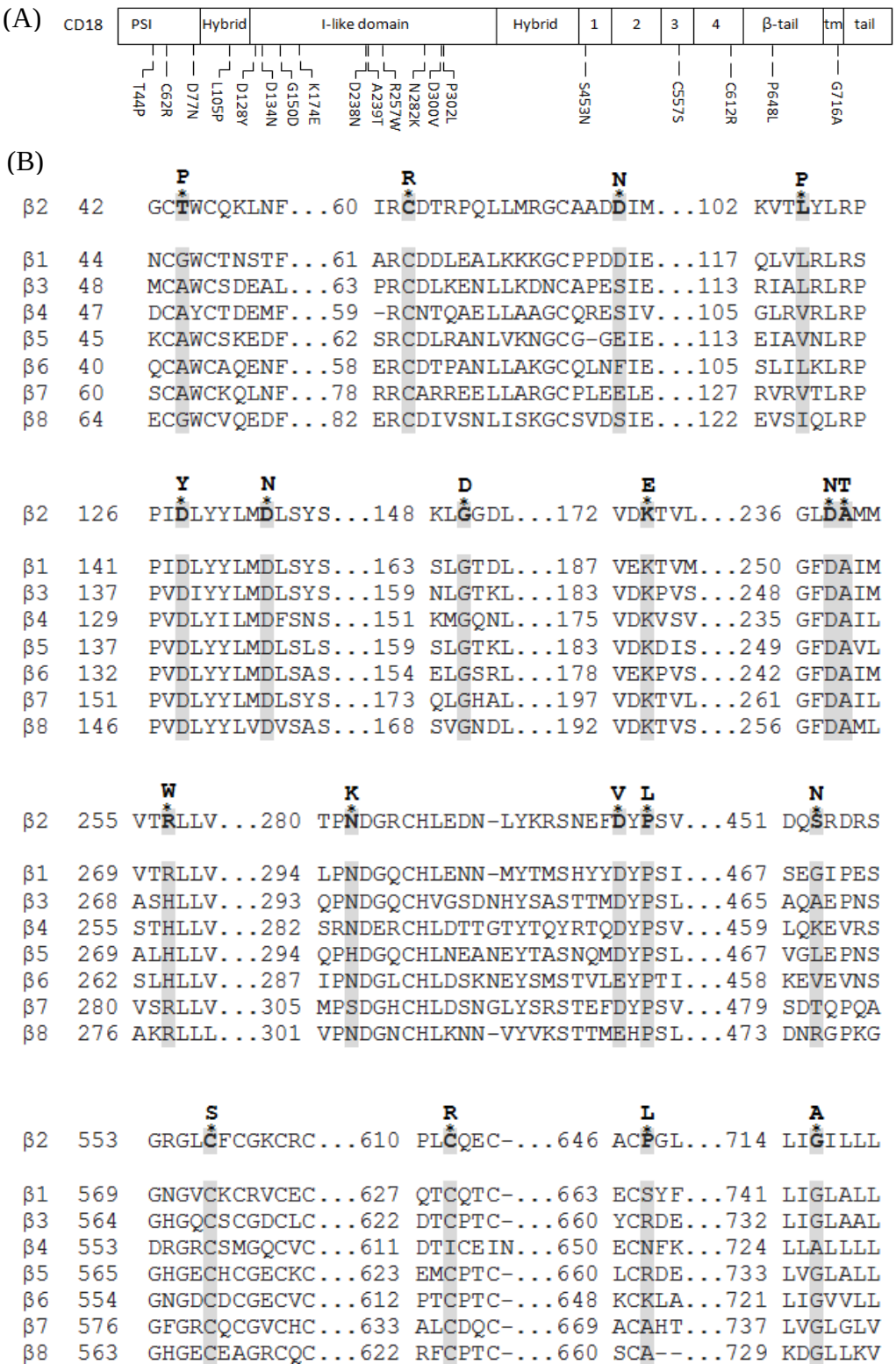

Figure 3.1 (A, B). 19 uncharacterized LAD-1 mutations in human integrin β2 subunit (CD18) shown in schematic map, alignment and structure. (A) The domain location of the mutations. (B) The β_2 sequence is aligned with the 7 other human integrin β subunits. The mutated amino acids are shown above the sequence alignment and in bold.

(C)

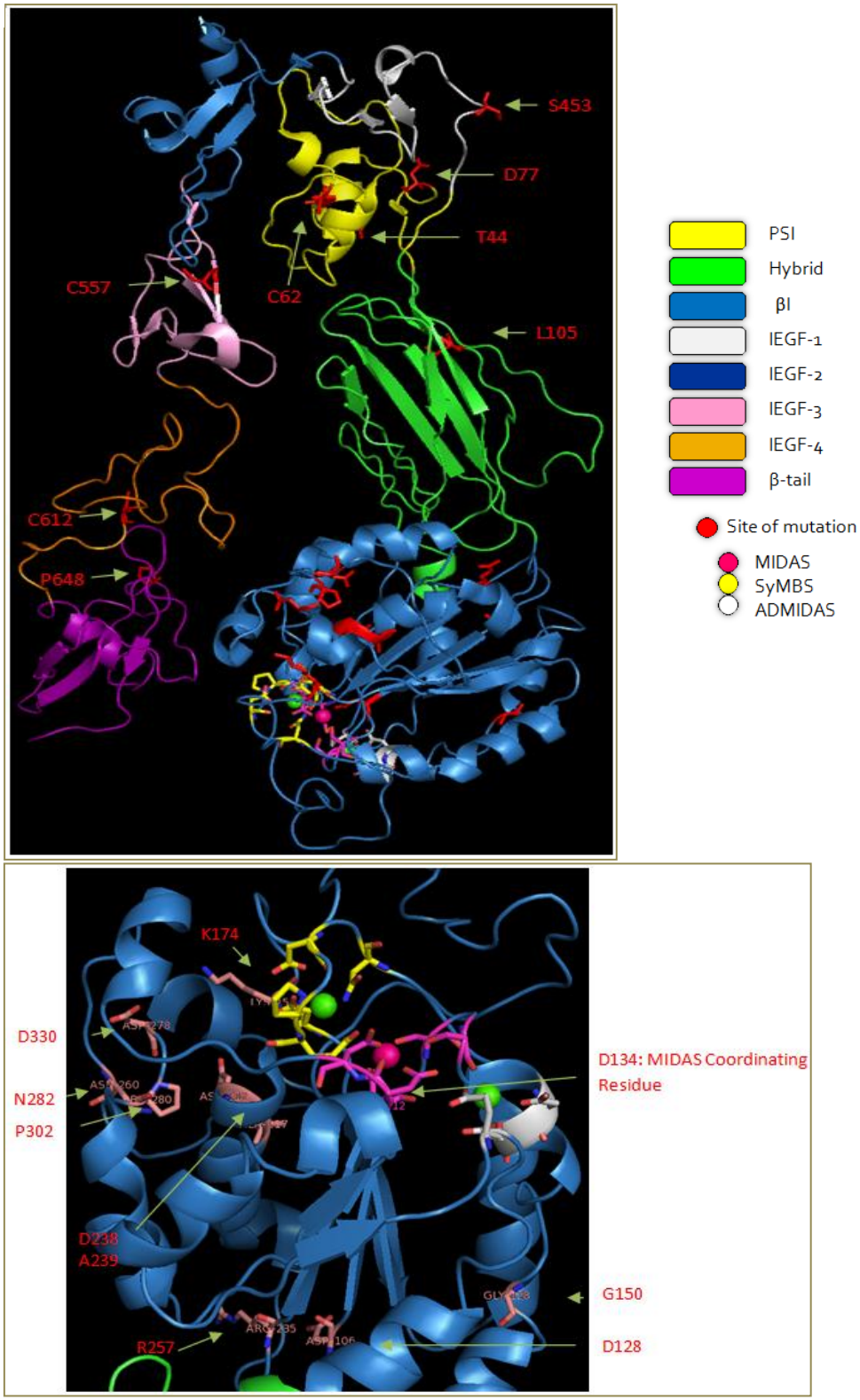

Figure 3.1 (C). Mutated sites are highlighted in red in β_2 whole ectodomain (upper panel), and in pink in the zoomed-in β_2 I domain (lower panel). Note that in this thesis, all β_2 3D structures are determined from the $\alpha X\beta_2$ structure (3K72).

3.1 Surface Expression of LAD-1 Mutants

LFA-1 surface expression was examined by flow cytometry using the β_2 integrin dimer-specific mAb MHM23 and 1B4, anti-αL mAb MHM24 and anti-β_2 mAb H52. Although the residues contributing to MHM23 epitope had been reported to locate in the β_2 I domain between residues 144-148 and 192-197 (Xiong and Zhang, 2001); 200-206 (Poloni et al., 2001), it had been well established that MHM23 can only detect the integrin in its heterodimeric form (Tan et al., 2000; Cheng et al., 2007; Shi et al., 2007; Tang et al., 2008). Similarly 1B4 is also a heterodimer specific reporter mAb whose epitope has been mapped to similar, but not identical regions of β_2 I domain (Wright et al., 1983; Xiong and Zhang, 2001; also SKA Law, personal communication). The epitope of MHM24 is located in the αL I domain, and H52 is in the C-terminal half of the hybrid domain (more updated information will be presented in Section 3.2). These epitopes should not be affected in the mutants as none of the mutations are located in the reported regions. As shown in Figure 3.2 A-C and Supplementary Figure 3A, 14 out of 19 β_2 mutants did not support integrin $\alpha L\beta_2$ surface expression. The mutations that support $\alpha L\beta_2$ expression are β_2-D77N, β_2-G150D, β_2-S453N, β_2-P648L and β_2-G716A. Three of these mutants, β_2-K174E, β_2-D238N and β_2-N282K, which failed to support surface expression of LFA-1, gave low expression of the H52 epitope (Figure 3.2 C).

A: MHM23

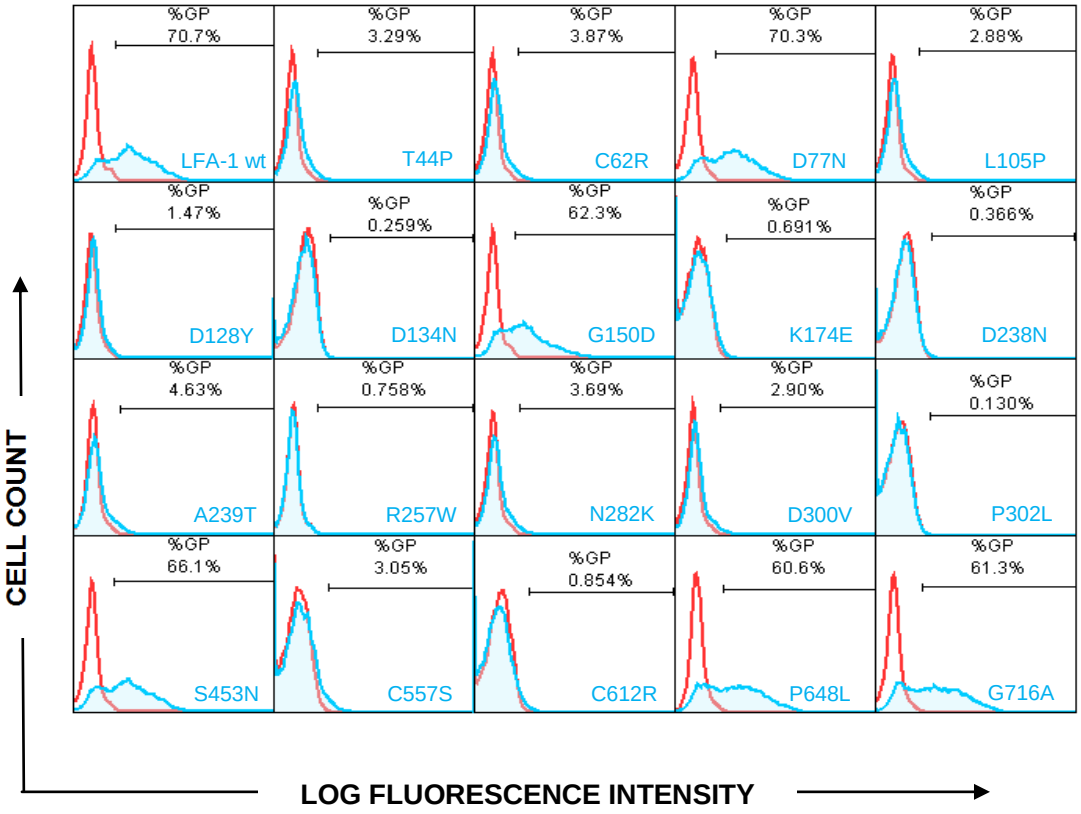

B: MHM24

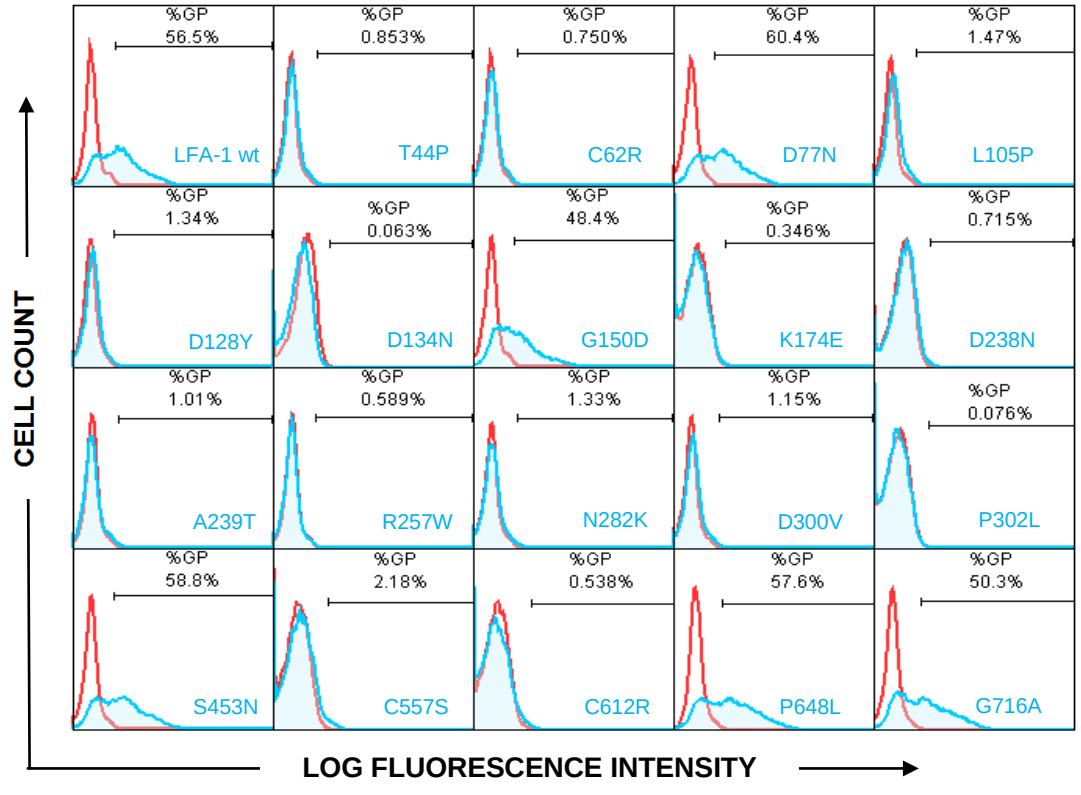

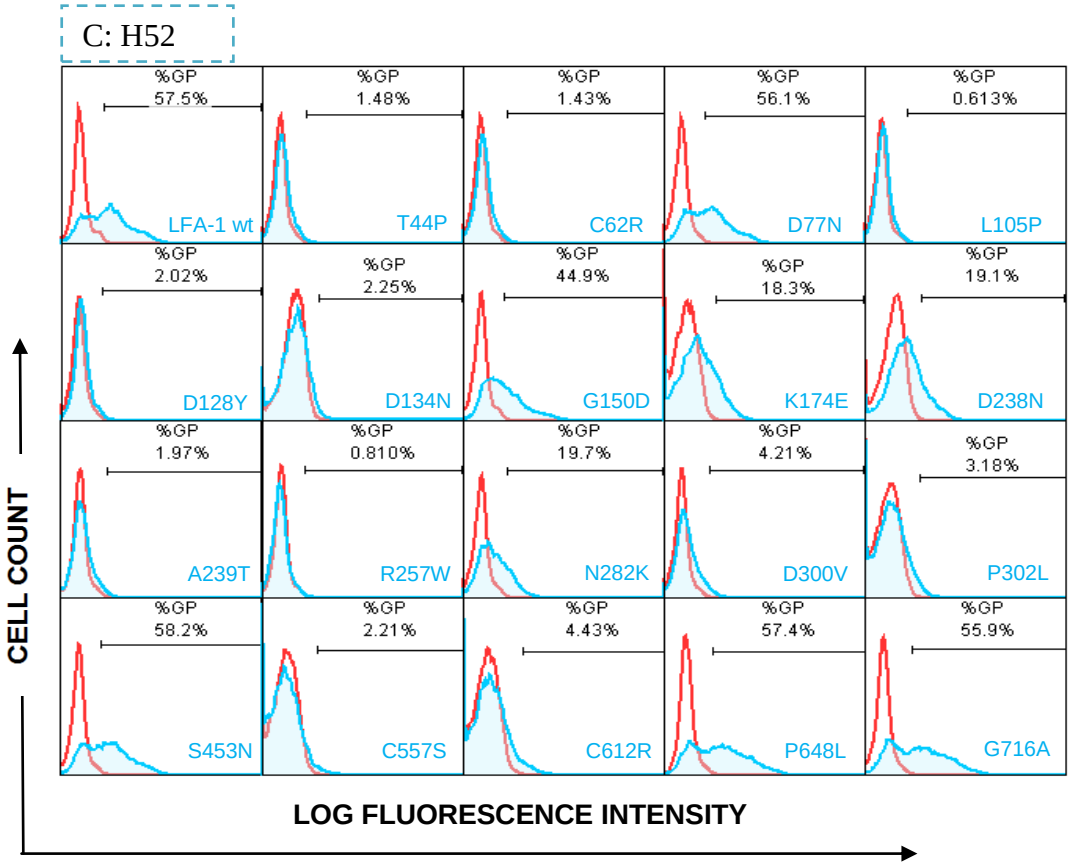

Figure 3.2. Surface expressions of 19 LAD-1 mutants in supporting integrin LFA-1. (A) Expression detected by the heterodimer specific mAb MHM23; (B) by the αL I domain specific mAb MHM24; (C) by the anti-β_2 subunit mAb H52. In all cases, anti αM I domain mAb LPM19C was used as background control, %GP stands for "percentage of gated positive". Background gating was controlled at a range from 0.1%-1.0%.

Similarly, these mutations were examined for their support of Mac-1 and p150,95 expression using the mAb MHM23 (Figure 3.3 and Supplementary Figure 3B, 3C). The same five β_2 mutations, β_2-D77N, β_2-G150D, β_2-S453N, β_2-P648L and β_2-G716A that were capable in supporting the surface heterodimer expression of LFA-1, supported the surface expression of Mac-1 and p150,95. No β_2 Integrin expression was detected for the other 14 mutations (Figure 3.2A, 3.3).

The summary of the expression data is shown in Table 3.2.

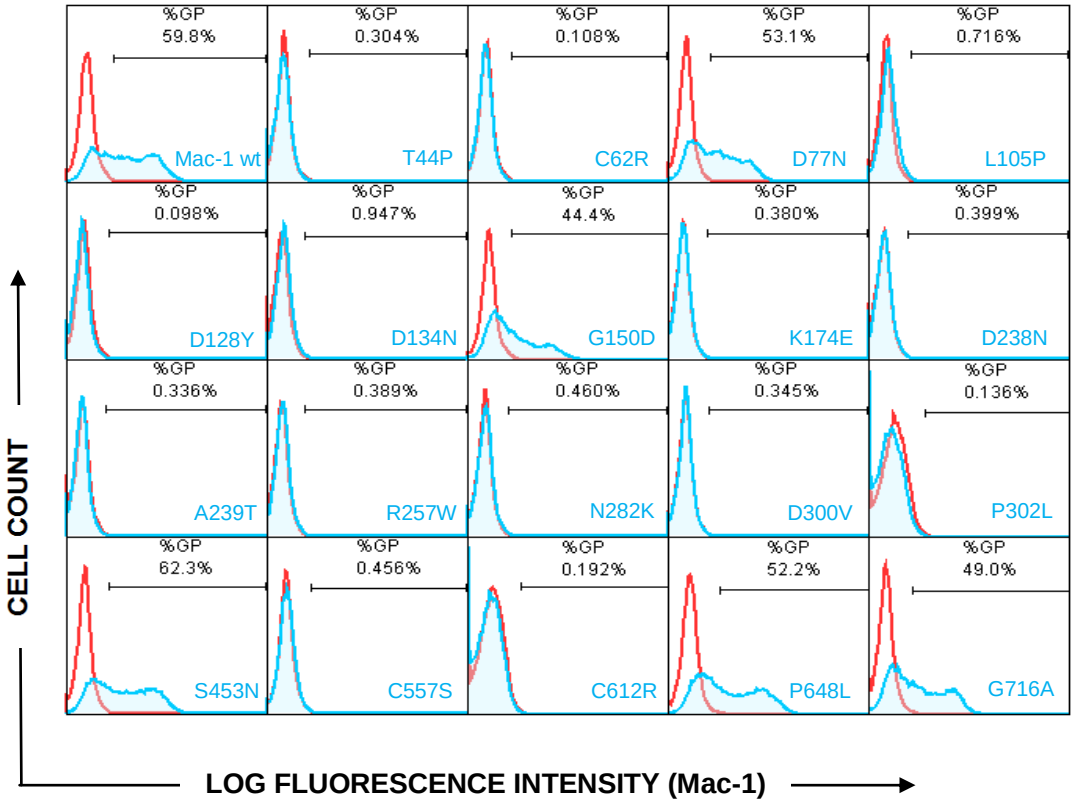

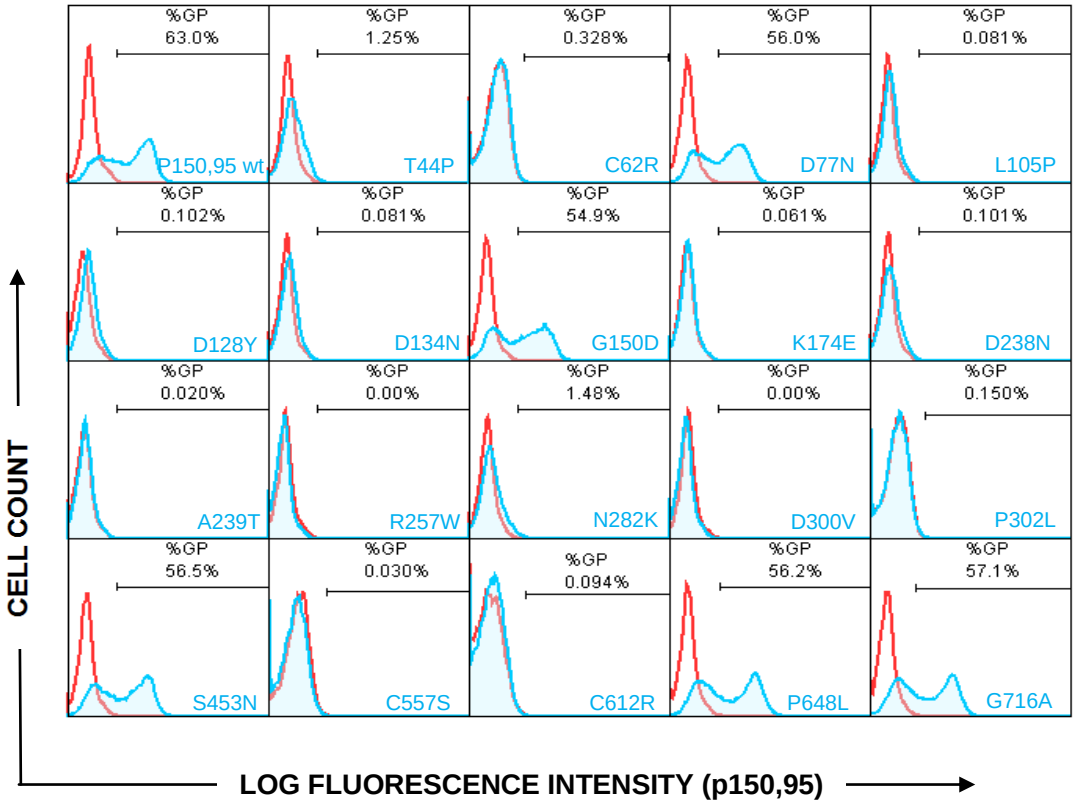

Figure 3.3. Surface expression of integrin Mac-1 and p150,95 bearing LAD-1 mutation (19) analyzed using mAb MHM23. In all cases, MHM24 (anti αL I domain) was used for background control.

Table 3.2. Summary of MHM23 stained LFA-1, Mac-1 and p150,95 transfectants bearing the LAD-1 mutations (19).

β_2 mutants	LFA-1	Mac-1	p150,95
Wildtype	70.7	59.8	63.0
T44P	3.3	0.3	1.3
C62R	3.9	0.1	0.3
D77N	70.3	53.1	56.0
L105P	2.9	0.7	0.1
D128Y	1.4	0.1	0.1
D134N	0.3	0.9	0.1
G150D	62.3	44.4	54.9
K174E	0.7	0.4	0.1
D238N	0.4	0.4	0.1
A239T	4.6	0.3	0.0
R257W	0.8	0.4	0.0
N282K	3.7	0.5	1.5
D300V	2.9	0.3	0.0
P302L	0.1	0.1	0.2
S453N	66.1	62.3	56.5
C557S	3.1	0.5	0.0
C612R	0.9	0.2	0.1
P648L	60.6	52.2	56.2
G716A	61.3	49.0	57.1

3.2 Biosynthesis of the Defective β_2 Subunits

To ascertain that the 14 mutants which do not support the heterodimer surface expression was not due to error in biosynthesis, the intracellular expression of the β_2 subunits bearing the mutations were examined. HEK293T transfectants were permeabilized before staining with the two β_2 specific mAbs: H52 and KIM185 (Figure 3.4).

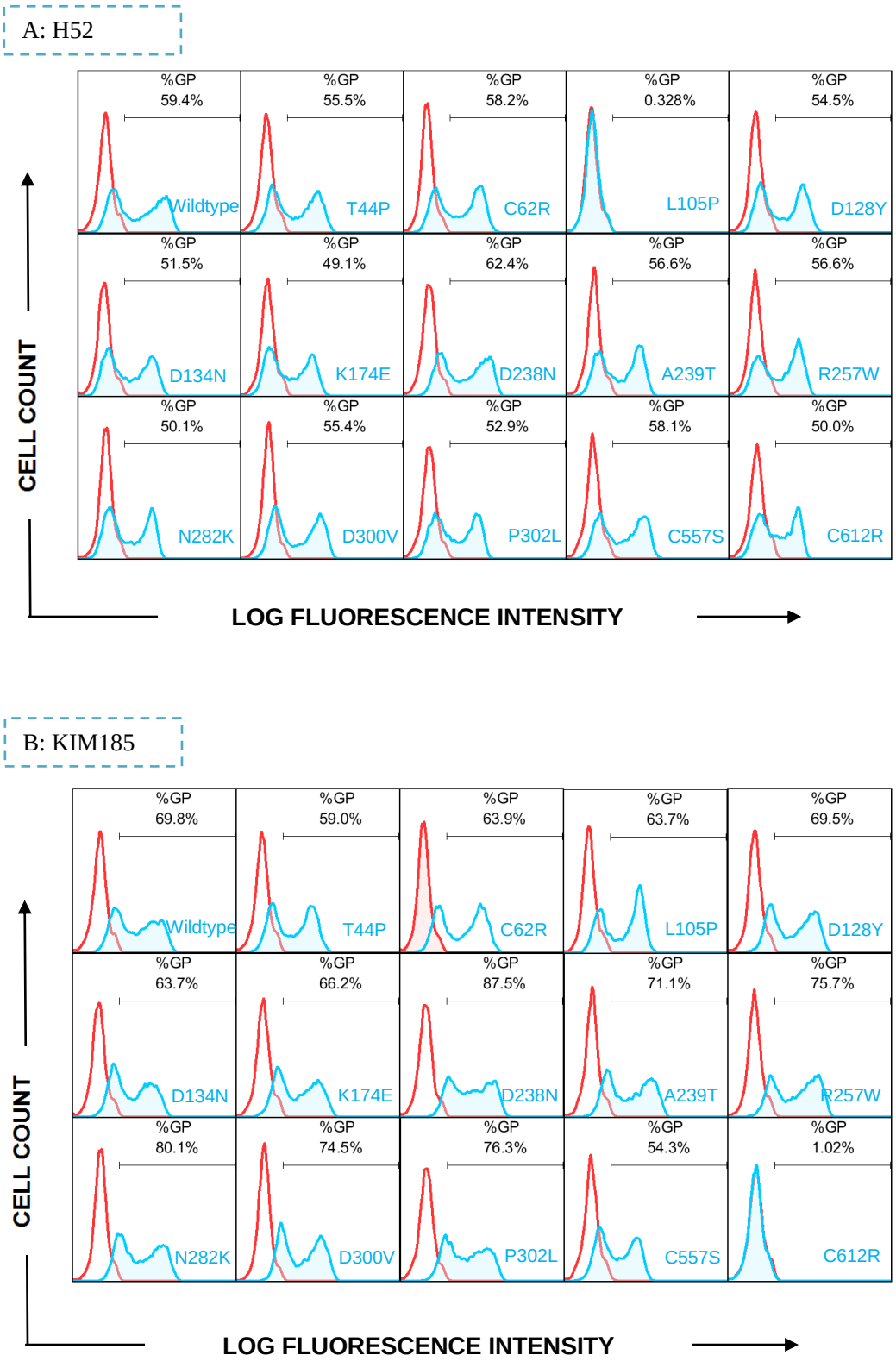

Figure 3.4. Flow Cytometry analysis of intracellular expression of β_2 variants (single subunit) on HEK293T transfectants. Transfected cells were permeabilized, followed by H52 or KIM185 staining. Mutants that support β_2 integrin heterodimer expression were not included in this experiment.

Twelve out of the 14 β_2 mutants could be detected by both H52 and KIM185. β_2-C612R could only be detected by H52, but not KIM185. The KIM185 epitope was mapped to the I-EGF4 domain (Lu et al; 2001) and it is therefore not unexpected that the epitope is not expressed in the β_2-C612R mutant.

Using chimeric β_2 and β_7 subunits, the H52 epitope was mapped to the C-terminal half of hybrid domain (β_2-K362 to β_2-H450) (Tan et al., 2001). The epitope was further narrowed down into 6 amino acids (β_2-T391 to β_2-P396) (Prof. Alex Law). Thus, it was a surprise that the β_2-L105P mutant, with the mutation located in the N-terminal half of the hybrid domain, failed to express the H52 epitope.

By aligning the β_2 and β_7 protein sequences, it was found that the amino acid corresponding to β_2-L105 in β_7 is valine (Figure 3.1). Since the structure and hydrophobicity of leucine and valine are similar, it is possible that substitution would not affect the H52 epitope. For this reason, a leucine to valine substitution at β_2-L105 was constructed. The intracellular expression of the H52 epitope was restored (Figure 3.5). Hence, our results indicated that the N-terminal half of the β_2 hybrid domain also contributes to the H52 epitope.

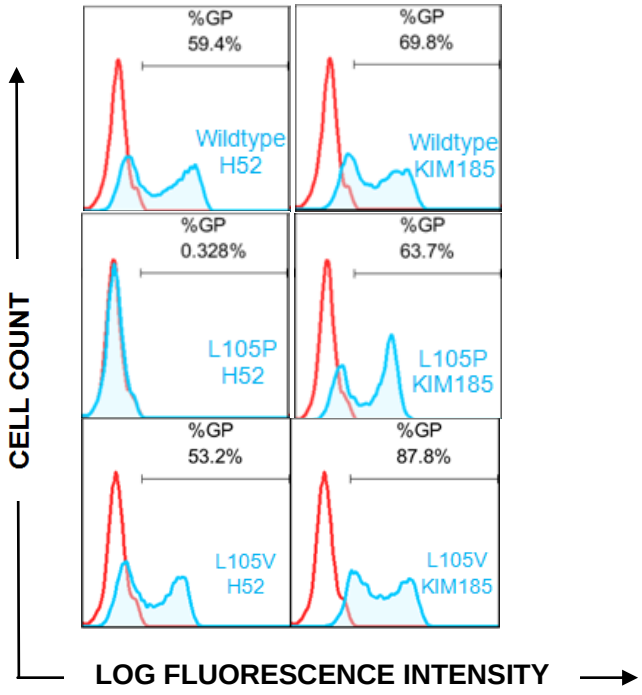

Figure 3.5. β_2-L105V restores the H52 epitope expression intracellularly. HEK293T transfected cells were permeabilized and stained with mAb H52 (left panel) and KIM185 (right panel).

3.3 Adhesion Analysis on LAD-1 β_2 Variants

The five mutants (β_2-D77N, β_2-G150D, β_2-S453N. β_2-P648L and β_2-G716A) that support surface expressions, are studied for the adhesion properties.

3.3.1 β_2-D77N, β_2-S453N and β_2-P648L were Potentially CD18 Polymorphism

The LFA-1 transfectants were tested for their adhesion properties to immobilized ligands ICAM-1 (Figure 3.6 A) and ICAM-3 (Figure 3.6 B). The Mac-1and p150,95 transfectants were tested for their adhesion properties to denatured BSA on coated surfaces (Figure 3.7A and B respectively).

(A)

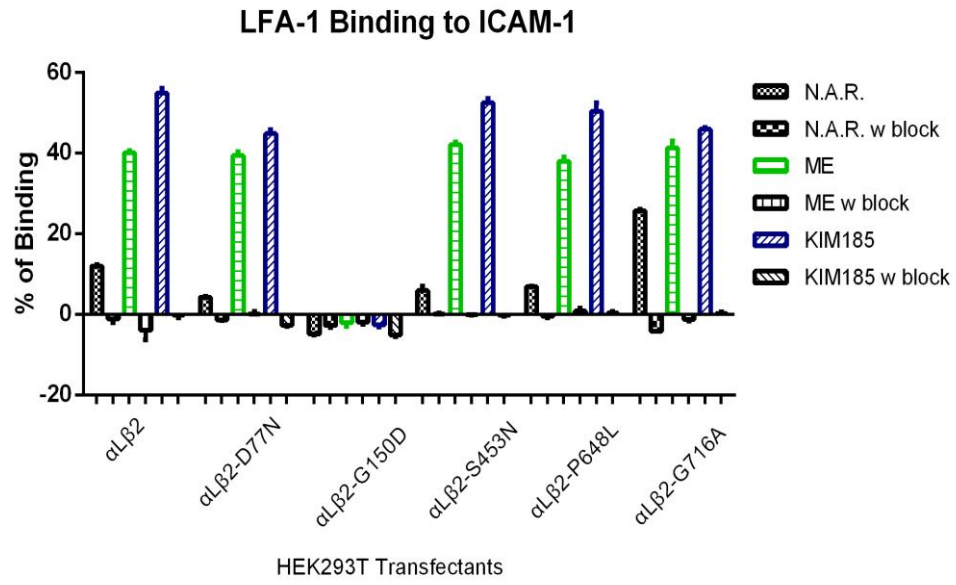

(B)

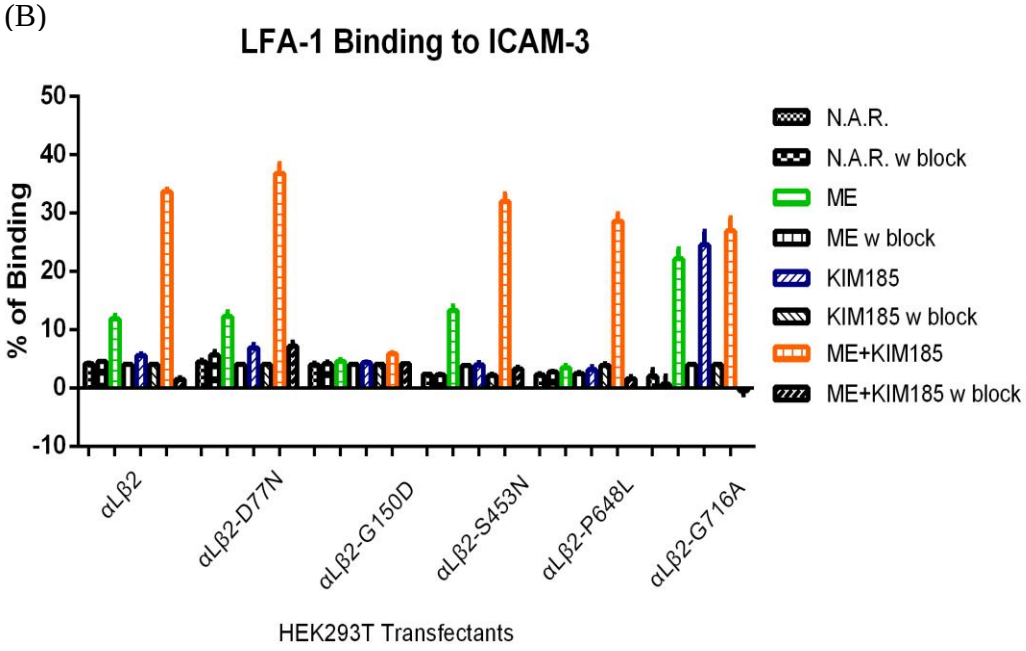

Figure 3.6. Adhesion assay of HEK293T transfectants binding to ICAM-1 (A) and ICAM-3 (B). In both assays, a combination of 5 mM $MgCl_2$ and 1.5 mM EGTA (ME) and 10 μg/ml mAb KIM185 were used to promote the activation of LFA-1. Adhesion specificity was shown by αL functional blocking mAb MHM24. N.A.R. is the abbreviation for "No activating reagents".

(A)

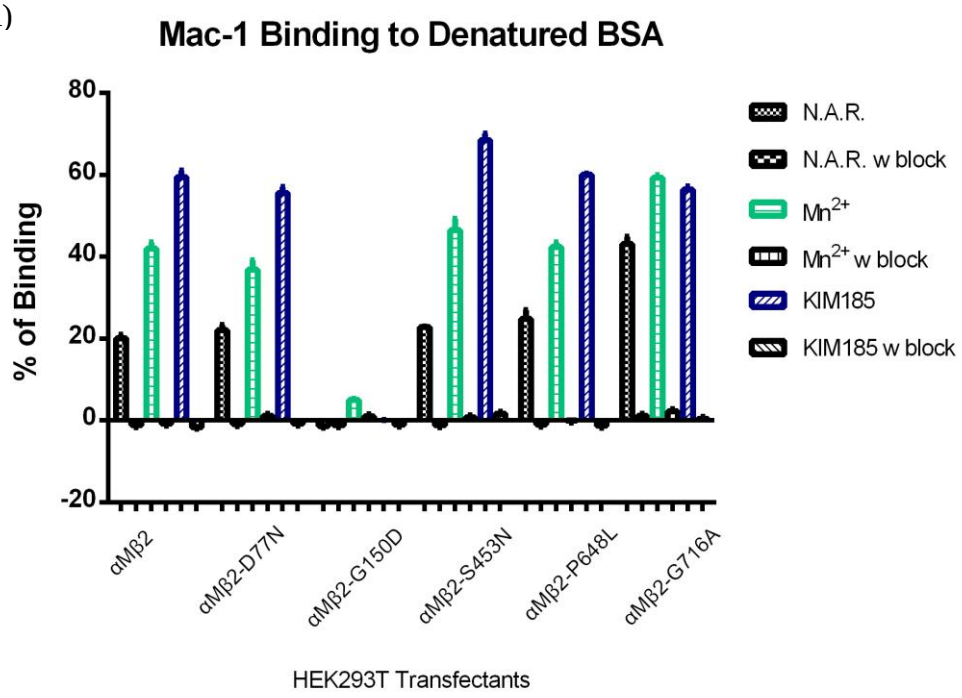

(B)

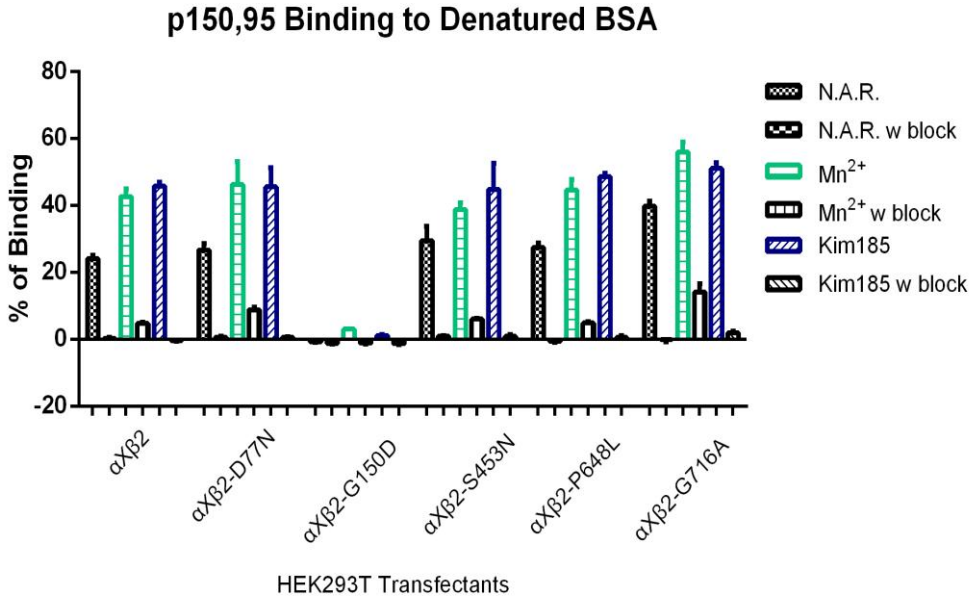

Figure 3.7. Adhesion assays of HEK293T transfectants binding to denatured Bovine Serum Albumin (BSA). (A) Mac-1 transfectants binding to BSA. 0.5 mM $MnCl_2$ was used to activate Mac-1, adhesion specificity was demonstrated by functional blocking antibody LPM19C. (B) p150,95 transfectants binding to BSA. Adhesion was specifically blocked by mAb 1B4. N.A.R. is the abbreviation for "No activating reagents".

The wild-type integrin LFA-1 has minimal adhesion to ICAM-1 but can be activated with either Mg^{2+}/EGTA or the activating mAb KIM185; and significant adhesion to ICAM-3 can only be observed in the presence of both Mg^{2+}/EGTA and KIM185. The integrin LFA-1 with the mutation of β_2-D77N, β_2-S453S and β_2-P648L exhibited similar binding behavior compared to the wild-type (Figure 3.6).

Similarly, the Mac-1 and p150,95 with these mutations have wild-type adhesion profiles to denatured BSA, i.e. adhesion can be promoted by either Mn^{2+} or KIM185 (Figure 3.7).

The integrin conformation was also studied by immunoprecipitation using the leg extension reporter mAb KIM127. The wild-type LFA-1 does not express the KIM127 epitope but does so under the activation of Mg^{2+}/EGTA. Similarly, the LFA-1 integrins with the three mutations do not express the KIM127 epitopes until being activated by Mg^{2+}/EGTA (Figure 3.8). Again, these mutations are wild type-like. Taken all these results together, these mutations should be classified as polymorphisms.

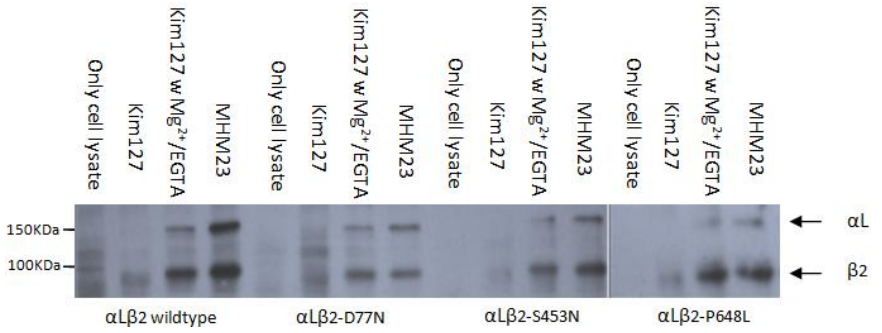

Figure 3.8. Immunoprecipitation of integrin subunits on $\alpha L\beta_2$ or $\alpha L\beta_2$ mutants transfected HEK293T cells. Transfectants were labelled with biotin, lysed and immunoprecipitated with KIM127 with or without ME. mAb MHM23 were included as control. Streptavidin conjugated HRP was used to detect the precipitated integrins via their biotin labels.

3.3.2 β_2-G150D Abolished the Ligand Binding Property

In contrast, the integrins with the β_2-G150D mutation showed no adhesion to their respective ligands under all conditions tested (Figure 3.6 and 3.7), although the integrins bearing the β_2-G150D mutation can be synthesized and expressed to the cell surface. Furthermore, $\alpha L\beta_2$-G150D failed to express the KIM127 epitope even in presence of Mg^{2+}/EGTA (Figure 3.9). In this experiment the constitutively active mutant β_2-N351S was included as a control, it can be pulled down by KIM127 in the absence of any activating agents. Thus we conclude that the β_2-G150D mutant is locked in the bent conformation, as opposed to the β_2-N351S mutant which is in the extended conformation with the open headpiece.

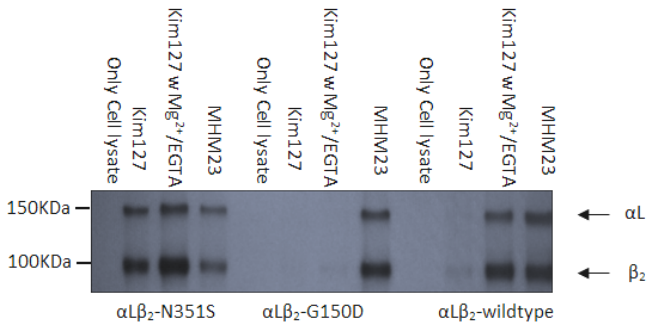

Figure 3.9. Immunoprecipitation of integrin subunits on $\alpha L\beta_2$ or $\alpha L\beta_2$–G150D transfected HEK293T cells using mAb KIM127.

3.3.3 β_2-G716A was Constitutively Active at Activation Stage I

The LFA-1 with the β_2-G716A mutation showed significant binding to ICAM-1 without the activating agents, and only required the presence of either

Mg^{2+}/EGTA or KIM185 for adhesion to ICAM-3 (Figure 3.6). The Mac-1 and p150,95 transfectants with the β_2-G716A mutation also showed significantly higher adhesion to denatured BSA in the absence of activating reagent (Figure 3.7). These results suggest that the integrins with the β_2-G716A is in the intermediate activation state.

Immunoprecipitation with integrin extension reporter mAb KIM127 was performed, and it was found that mAb KIM127 can only precipitated $\alpha L\beta_2$-G716A in the presence of Mg^{2+}/EGTA, similar to the wild-type $\alpha L\beta_2$. Thus, the $\alpha L\beta_2$ with the β_2-G716A mutation is in the bent configuration.

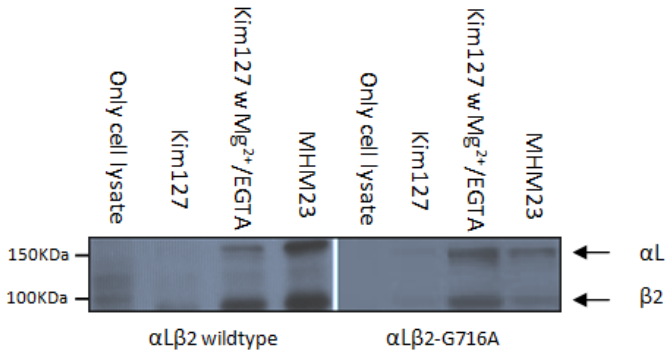

Figure 3.10. Immunoprecipitation of $\alpha L\beta_2$ or $\alpha L\beta_2$–G716A transfected HEK293T cells using mAb KIM127.

3.4 Discussion

To date 36 LAD-1 missense mutations were reported. Nineteen novel missense mutations which were presumed to be the cause of LAD-1 clinical symptoms were studied. Fourteen of these mutants did not support the expression of the dimeric integrin LFA-1, Mac-1 and p150,95. Of the remaining five, which support the surface expression of the leukocyte integrins, three of them, β_2-D77N, β_2-S453N, and β_2-P648L showed wild-type like adhesion activities. Integrins with the β_2-G150D mutation have no detectable adhesion activity whereas the LFA-1 with the β_2-G716A mutation is in the intermediate active state. The properties of the 19 mutants are listed in Table 3.3. Note that the presence of a broad peak or double peaks on FACS histogram profiles is due to approximately ~60% transfection efficiency. It was previously reported that some LAD-1 mutants support different levels of integrin expression and ligand binding among members of the β_2 integrin family (Shaw et al., 2001), such mutants are not identified here.

The local structure and orientation of the wild-types and mutated amino acids are shown in Figure 3.11.

Table 3.3. A summary table of 19 novel LAD-1 mutants' characteristics in expression and adhesion.

Mutant	Location	Surface Expression (Heterodimer)	Adhesion			
			LFA-1		Mac-1	p150,95
			ICAM-1	ICAM-3	BSA	BSA
T44P	PSI	No	/	/	/	/
C62R	PSI	No	/	/	/	/
D77N	PSI	Yes	wt-like	wt-like	wt-like	wt-like
L105P	Hybrid	No	/	/	/	/
D128Y	βI	No	/	/	/	/
D134N	βI	No	/	/	/	/
G150D	βI	Yes	Abolished	Abolished	Abolished	Abolished
K174E	βI	No	/	/	/	/
D238N	βI	No	/	/	/	/
A239T	βI	No	/	/	/	/
R257W	βI	No	/	/	/	/
N282K	βI	No	/	/	/	/
D300V	βI	No	/	/	/	/
P302L	βI	No	/	/	/	/
S453N	I-EGF1	Yes	wt-like	wt-like	wt-like	wt-like
C557S	I-EGF3	No	/	/	/	/
C612R	I-EGF4	No	/	/	/	/
P648L	β tail	Yes	wt-like	wt-like	wt-like	wt-like
G716A	TM	Yes	Adhesion State I		Self-Activated	

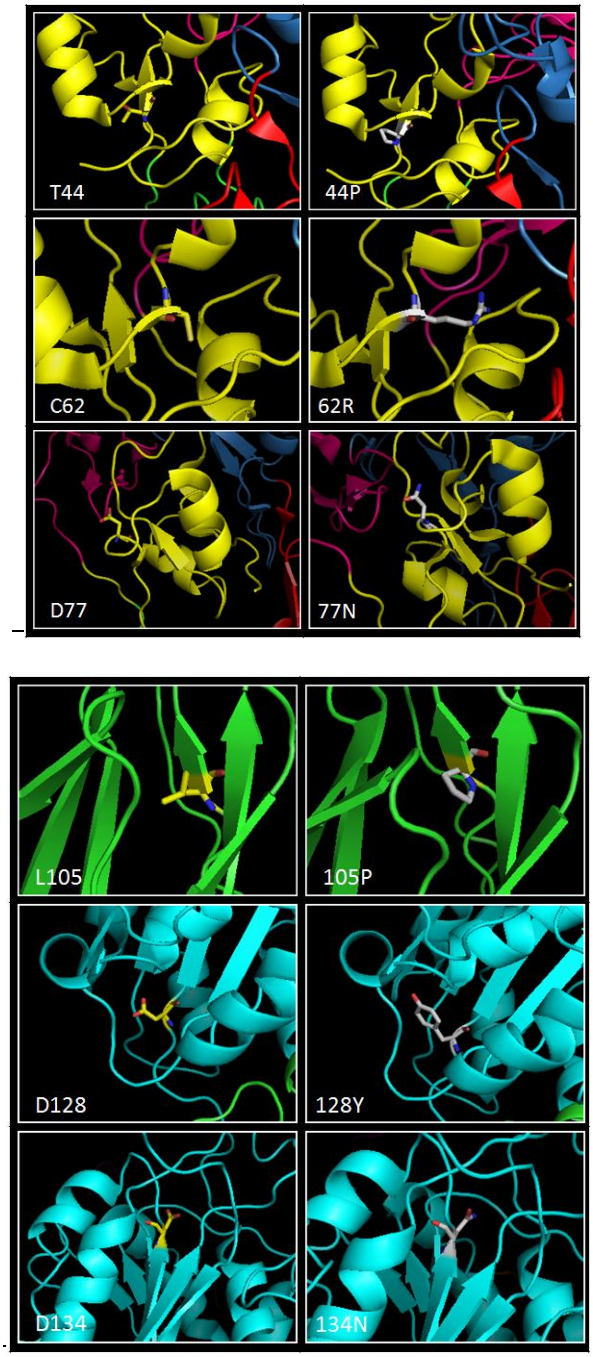

Figure 3.11. Closed up views of the 18 wild-types (Left column) and corresponding mutations (Right column) on the β_2 integrin structure. Mutated residues are generated by PyMol. Wild-type side chains are shown in yellow and the mutation side chains are shown in while. The secondary structures of each domain are coded by colors: PSI (yellow), Hybrid (green), I domain (cyan), I-EGF1 (hot pink) I-EGF2 (sky-blue), I-EGF3 (red), I-EGF4 (orange), β tail (purple). Noted that the β_2-G716 is located at the TM and therefore is absent in the structure views.

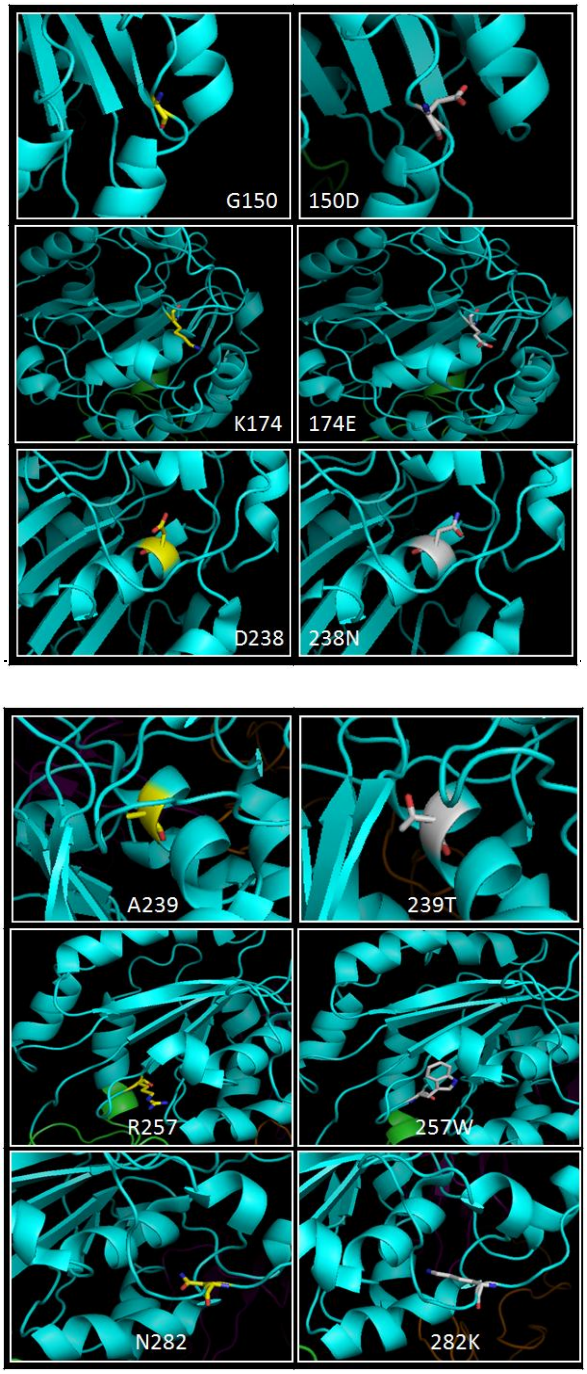

Figure 3.11 (Continue).

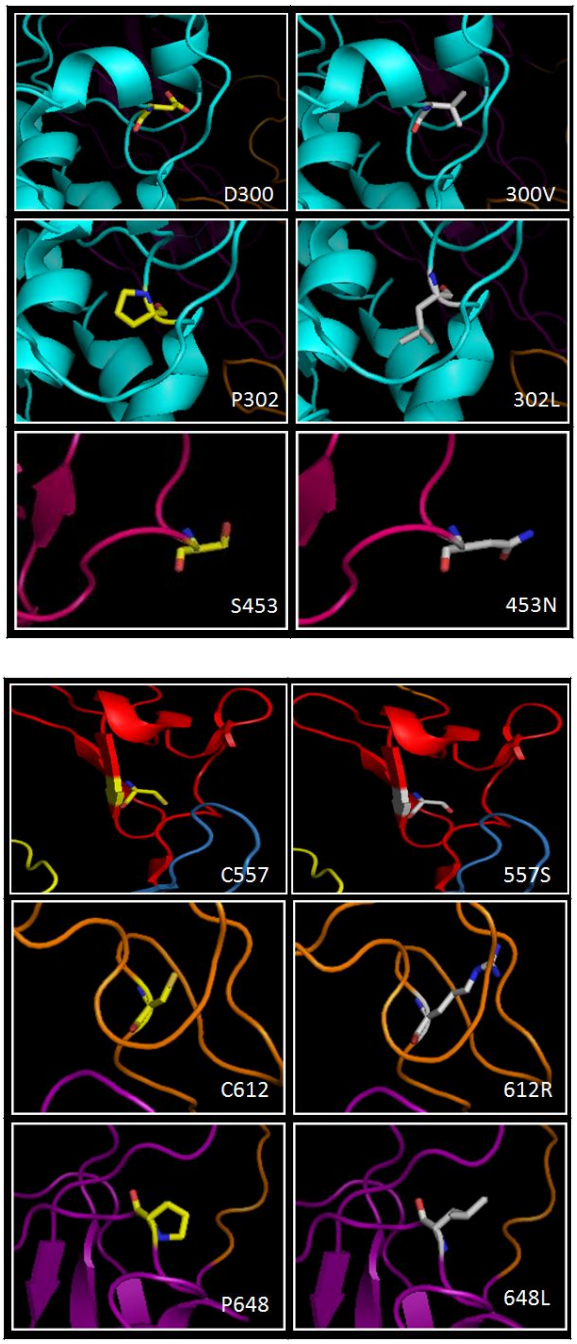

Figure 3.11 (Continue).

3.4.1 β_2-D77N, β_2-S453N and β_2-P648L

β_2-D77N was identified from a five-month old child who had been diagnosed with Hirschsprung's disease (HSCR)-associated enterocolitis (HAEC). The clinical features of HAEC include "repeated infections, pneumonia and failure to thrive" (Moore et al., 2008). The mutation was found in *ITGB2* by heteroduplex single-strand conformation polymorphism analysis. It was not reported explicitly if there was any β_2 integrins expressed on the patient's leukocytes. Our results showed that the human β_2 mutation D77N is not sufficient to cause defects in β_2 integrin expression or adhesion, hence it is not likely to be the responsible for LAD-1.

The mutations of β_2-S453N and β_2-P648L were found from two patients who were tentatively diagnosed as LAD-1. Their β_2 genes were investigated by genomic DNA sequencing and exon-level array comparative genomic hybridization (CGH) analysis. No other mutation was detected in their exons and in the intronic sequences flanking the exons. These two mutants both appear support to wild-type like in expression and adhesion according to our data. If the two patients are confirmed as LAD-1, the critical mutations leading to their LAD-1 status should lie elsewhere. More in-depth investigation may be required to determine the disease causing mutations. In a similar case, the polymorphism β_2-K196T was originally reported as a LAD-1 mutant in a compound heterozygote patient, the other allele was the β_2-R593C (Arnaout et al., 1990). From Law's lab unpublished work, the mutation β_2-K196T was not found to affect either expression or adhesion of the β_2 integrins. It has been reclassified as a polymorphism (van de Vijver et al., 2012).

3.4.2 β_2-G150D

The LAD-1 mutation β_2-G150D exhibited normal surface expression and dimer association of integrin β_2 members LFA-1, Mac-1 and p150,95. The integrin cannot adhesion to ligands. β_2-G150D belongs to a minority type of LAD-1 mutations that can support normal expression but not binding. These observations are in line with the diagnosis of the patient with LAD-1. Other such missense mutations are β_2-S138P (Hogg et al., 1999) and β_2-D231H (Mathew et al., 2000). β_2-S138 is the coordinating residue of βI divalent cation binding motifs MIDAS, whereas β_2-D231 is that of the synergistic metal ion binding site SyMBS (Xie et al., 2010). The β_2-G150 is a conserved residue across species, and also among the eight human β subunits (Figure 3.1B). By modeling, it appears that the extended side chain of the aspartic acid might interact with β_2-S214 and β_2-Q218 (Figure 3.12). However it is not clear how it would affect the binding properties, but not heterodimer formation and expression of the integrin.

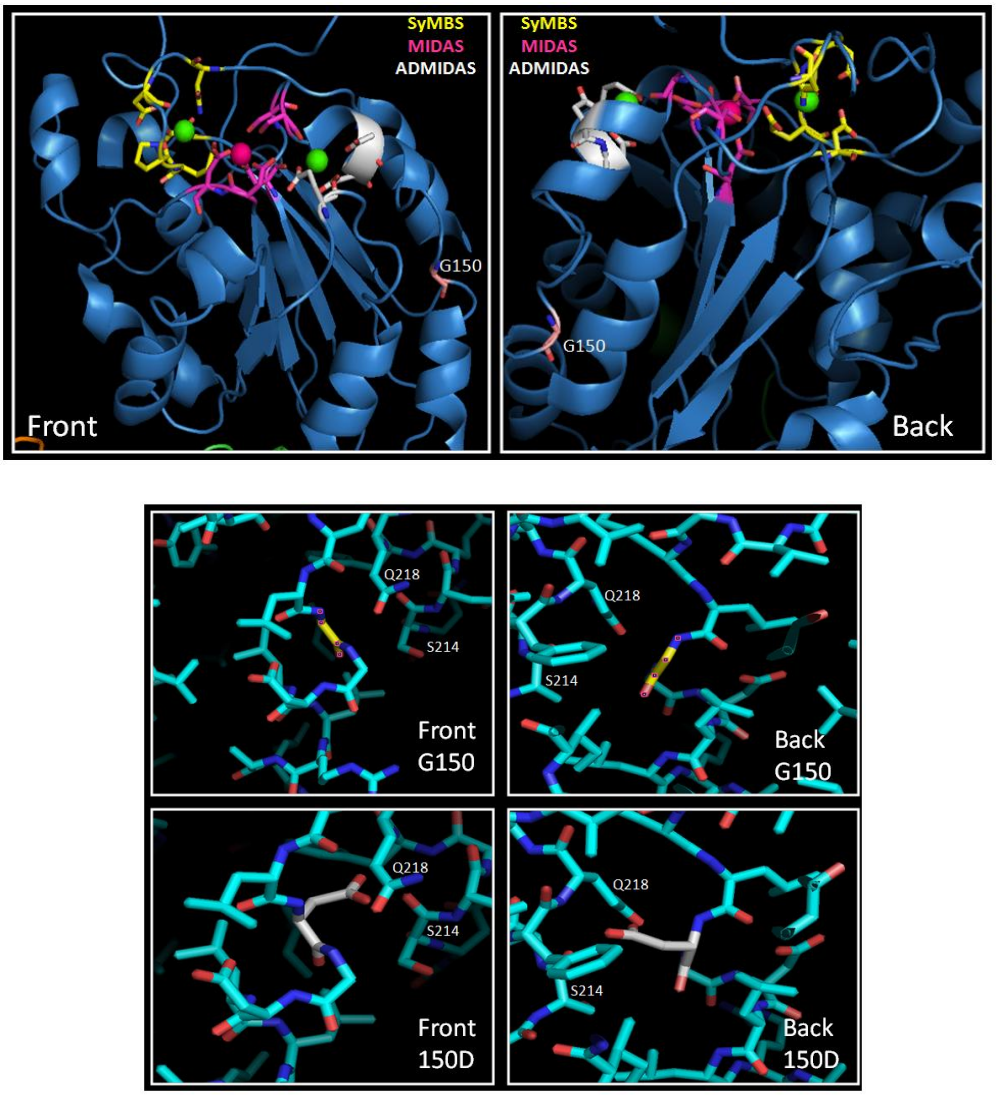

Figure 3.12. β_2 I domain close-up structure views. Upper: β_2-G150 was coloured in light pink and shown in residue. The distance from β_2-G150 to the most adjacent cation binding site ADMIDAS β_2-D142 is 14Å. Lower: β_2-G150 adjacent structures. Glycine 150 before mutation was showed in yellow, after mutation was showed in white.

3.4.3 β_2-G716A

The mutant β_2-G716A is the only missense mutation that is located in the transmembrane domain (TM) that caused LAD-1. The β_2-G716A mutation was found in an Iranian female patient who died at her 13th month, with the clinical symptoms of increased neutrophils counts and only 1% of β_2 integrin

expression (Parvaneh et al., 2010). However, β_2-G716A supports normal level of surface expression of LFA-1, Mac-1 and p150,95 on HEK293T transfectants. The LFA-1 expressed binds ICAM-1 constitutively and requires only one activating reagent: either Mg^{2+}/EGTA or KIM185 for adhesion to ICAM-3. Thus the LFA-1 is expressed in the intermediate activation state.

It should be noted that the mutated integrin expression level on transfectants contradicts the data of integrin expression on the patient's leukocytes. Similar finding had been reported for the LAD-1 mutations β_2-R593C, β_2-C590R and β_2-N351S. Although a very limited amount of β_2 integrins was detected in the patient's leukocytes, the COS-7 transfectants bearing the mutants β_2-R593C or β_2-C590R supported over 50% of LFA-1 expression. LFA-1 with the β_2-N351S mutation is extensively expressed in COS-7 and K562 cells. And in all cases, these mutants β_2-G716A, β_2-R593C, β_2-C590R and β_2-N351S are all constitutively active to ICAM-1 adhesion. β_2-N351S is fully active to both ICAM-1 and ICAM-3 adhesion. Therefore it is possible that some mechanism in the patients' leukocytes down regulated the expression of these "active" variants. It was shown that by culturing the T cells of the patient with the β_2-R593C mutation with phytohaemagglutinin, the LFA-1 expression can be restored to 50% (Miedema et al., 1985). It would be interesting to study the T cells of patients with the β_2-G716A and β_2-C590R mutation, in comparison with those with other β_2 mutations.

To investigate the role of β_2-G716, and its counterpart αL-L1104 in activation state, β_2-G716F and αL-L1104A were constructed. And their adhesion properties were examined (Figure 3.13 and 3.14).

(A)

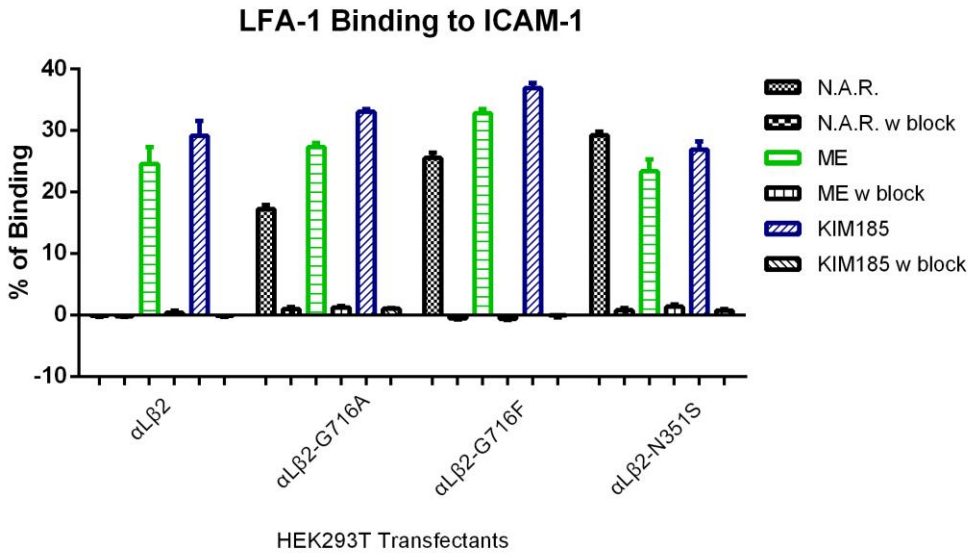

(B)

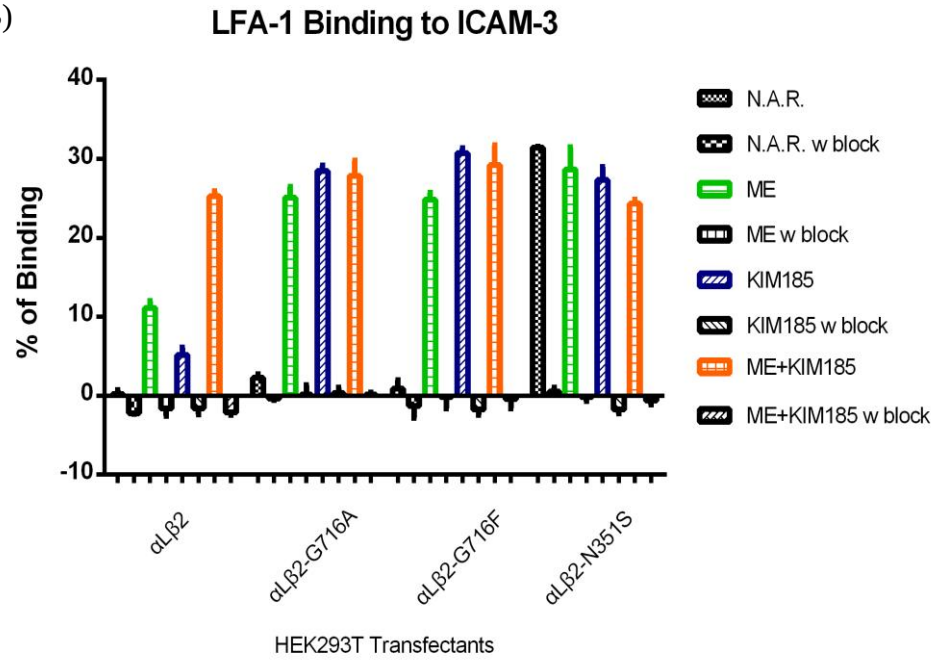

Figure 3.13. Adhesion assay of HEK293T transfectants binding to immobilized LFA-1 ligand ICAM-1 (A) and ICAM-3 (B).

(A)

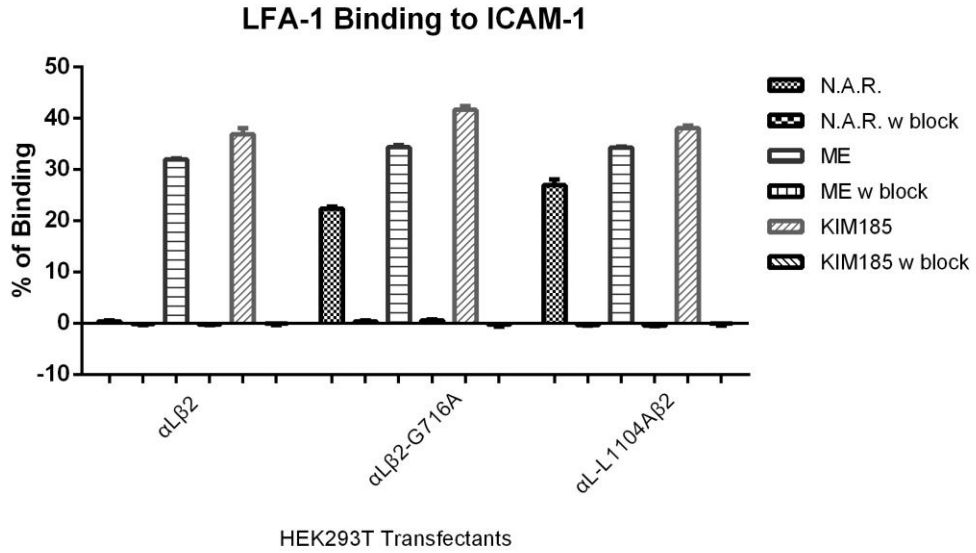

(B)

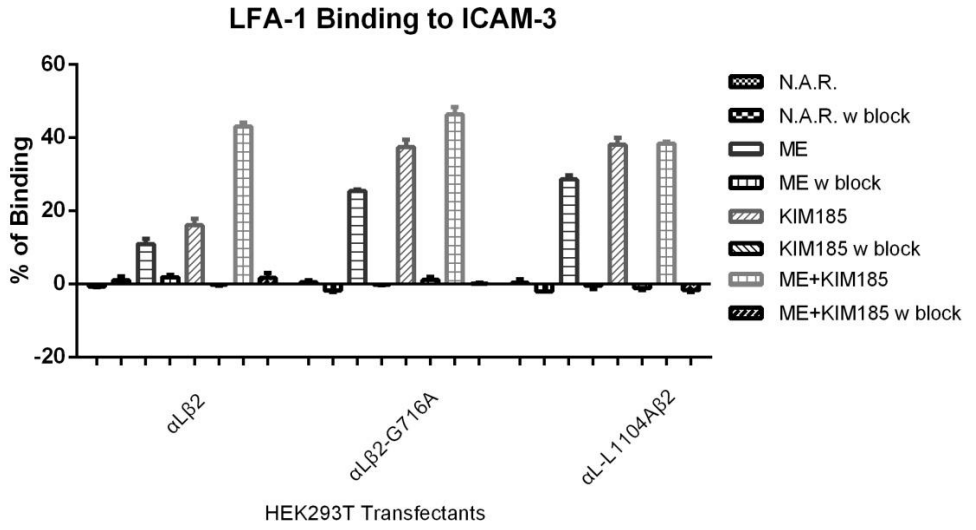

Figure 3.14. Adhesion assay of HEK293T transfectants binding to immobilized LFA-1 ligand ICAM-1 (A) and ICAM-3 (B).

We have confirmed that if the β_2–G716 was substituted with a phenylalanine, the resultant LFA-1 is active to bind ICAM-1 but not ICAM-3 (Figure 3.13). Similarly, the mutation of the L1104 to alanine on the αL subunit also resulted in an LFA-1 of intermediate activation state. Previous study which scanned the LFA-1 TM using phenylalanine suggested that it was the "bulkiness" of the introduced phenylalanine that perturbs the TM packing and lead to LFA-1 activation (Vararattanavech et al., 2010). The LAD-1 pathogenic mutation β_2–G716A suggested that it may not be the reason, as the alanine is only slightly larger than the wild type glycine. Another study which substituted the β_1–G743 (equivalent position to β_2–G716) with a leucine, found that the mutated $\alpha 2\beta_1$ was self active (Berger et al., 2010). We summarized the results from related studies in Table 3.4. Apparently, it requires a bulky residue on the α subunit and a glycine in the β subunit to maintain the integrin in an inactive form.

Table 3.4. A summary of mutagenesis study at the LFA-1 TM pair β_2–G716 / αL-L1104 and their equivalent sites on $\alpha 2\beta_1$.

	α	**β**	**Active ?**	**Reference**
Wt (for both $\alpha L\beta_2$ and $\alpha 2\beta_1$)	Leu	Gly	x	
$\alpha L\beta_2$	Leu	Ala	√	This study
$\alpha L\beta_2$	Leu	Phe	√	Vararattanavech et al., 2010
$\alpha L\beta_2$	Phe	Gly	x	Vararattanavech et al., 2010
$\alpha L\beta_2$	Ala	Gly	√	This study
$\alpha 2\beta_1$	Leu	Leu	√	Berger et al., 2010

Mutations were lighted in red.

3.4.4 β_2-L105P

The β_2-specific mAb H52 epitope is not expressed on mutant β_2-L105P. The H52 epitope was mapped into the C-terminal half of the hybrid domain of β_2 (K362 to H450) using β_2/β_7 chimeras (Tan et al., 2001)**,** and the epitope was subsequently narrowed down to T391 to P396 (Prof. Alex Law unpublished data). β_2-L105 is located in the N-terminal half of the hybrid domain, and by viewing the structure in the $\alpha X\beta_2$ model, it is at a distance site from the region T391 to P396 (Figure 3.15). The β_2-L105 is substituted with a valine which is its equivalent residue in β_7. The H52 epitope was restored in this construct. It is therefore the mutation to a proline that perturbs the local structure which is responsible for the abolition of the H52 epitope. We can conclude that the H52 epitope involves structure from both the N-terminal half and C-terminal half of the hybrid domain, and it is a conformational epitope. This also explains the finding that H52 cannot be used in Western blot of the denatured β_2 subunit in SDS polyacrylamide gels.

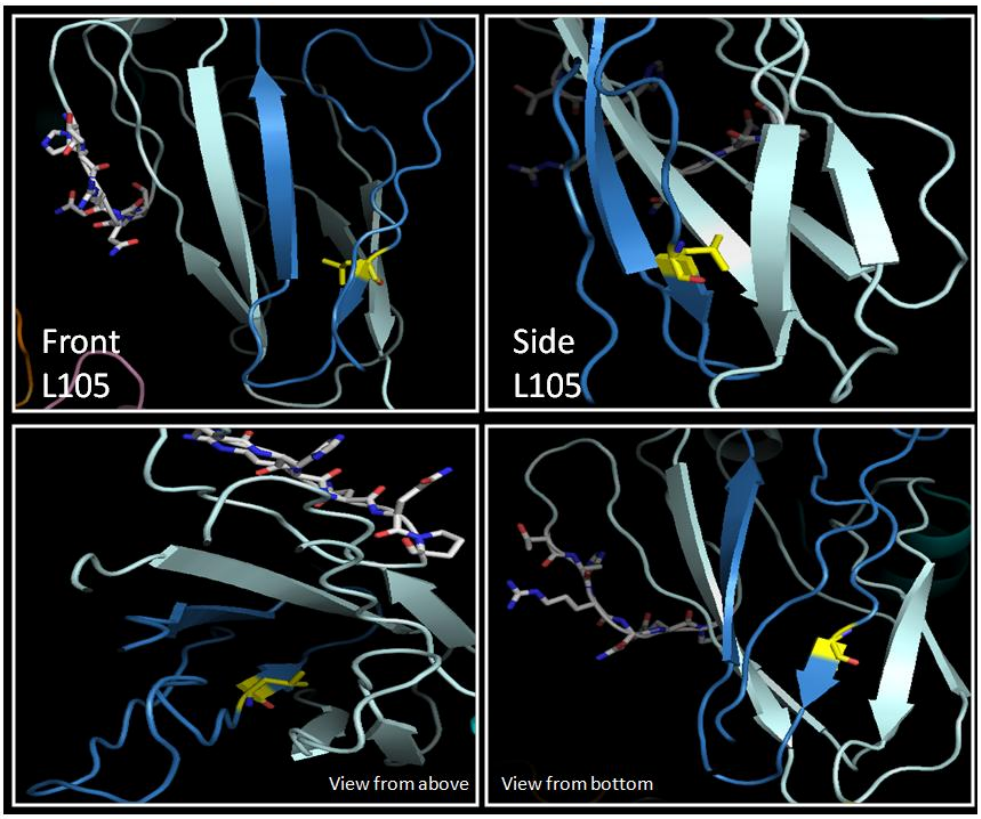

Figure 3.15. mAb H52 epitope in β_2 hybrid domain. Hybrid domain C-terminal half is shown in pale cyan, N-terminal half in blue. The β_2-K362 to β_2-H450 are showed with side chains and in white. β_2-L105 is shown in yellow. The figure is generated by Pymol using $\alpha X\beta_2$ (pdb: 3k6s) as template.

LAD-1 has been reported in more than 100 patients worldwide. More than 80 mutations have been identified. These 19 novel LAD-1 mutants characterized in this study may help in establishing the correlation between phenotypes and genotypes of LAD-1, and providing insights in integrin structure and function.

Chapter 4: Divalent Cation-Dependent Activation of Integrin

Integrins have multiple activation states. On a resting cell, the integrins have very low affinity to their ligands. Upon receiving signals, they can be activated to a high affinity state. The process is generally referred to an inside-out signaling. In the laboratory, the transition of integrin activity states can be studied by the manipulation of extracellular conditions: either by antibodies that promote the conformational change associated with activation, or by the alteration of the concentrations of divalent cations, namely Ca^{2+}, Mg^{2+} and Mn^{2+}.

4.1 Cation Selectivity between Leukocyte Integrin LFA-1 and Mac-1

Divalent cations Ca^{2+}, Mg^{2+} and Mn^{2+} are capable in regulating the adhesion between leukocyte integrins and ligands (Wright and Silverstein, 1982; Dransfield et al., 1992; Plow et al., 2000). In the laboratory, Mn^{2+} at micromolar level had been used to promote integrin activation (Altieri, 1991; Dransfield et al., 1992). Mg^{2+} and Ca^{2+}, at millimolar level, are also used, but their effects can be different for different integrins. For example, Mac-1 would require both Ca^{2+} and Mg^{2+} for its adhesion to iC3b (Wright and Silverstein, 1982), LFA-1 would require the suppression of Ca^{2+} with EGTA in the presence of Mg^{2+} for adhesion to ICAM-1 (Dransfield et al., 1992). Thus

Mg^{2+}/EGTA (5 mM Mg^{2+} and 1.5 mM EGTA, also referred to as Mg^{2+}/EGTA or ME) had been used as the standard condition to promote LFA-1 mediated adhesion to ICAM-1. Shown in Figure 4.1 are experiments on the adhesion of LFA-1 and Mac-1 transfectants (HEK293T) to their respective ligands ICAM-1 and denatured BSA under different divalent cation conditions. Specific attention should be paid to the different effects of Mg^{2+}/EGTA and KIM185 (Robinson et al., 1992), highlighted in green in Figure 4.1, on the activation of the integrins. For LFA-1 adhesion to ICAM-1, Mg^{2+}/EGTA and KIM185 have similar effects. In contrast, activation of Mac-1 to adhere to BSA with Mg^{2+}/EGTA is only marginal in comparison with KIM185.

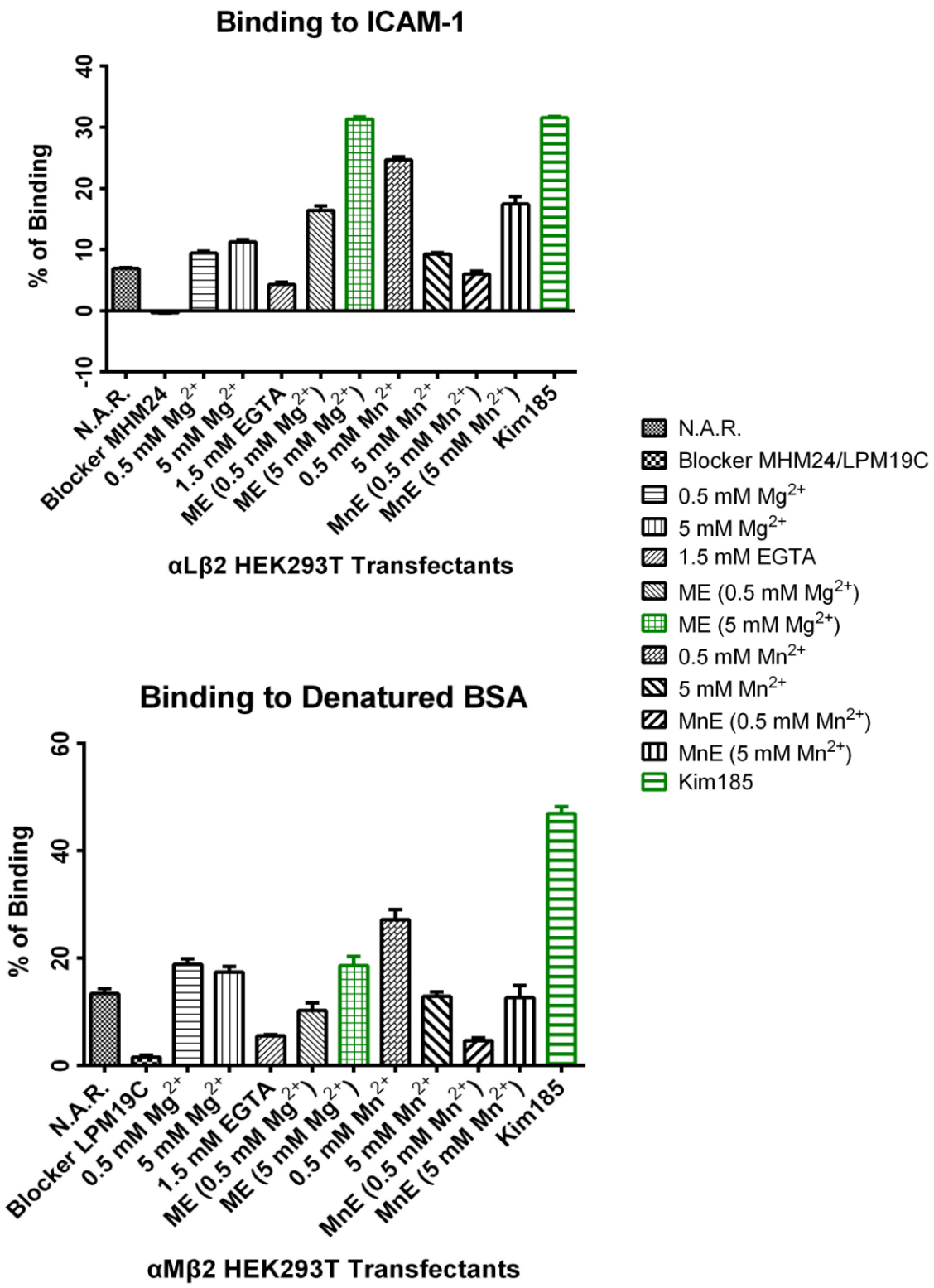

Figure 4.1. Adhesion of integrin $\alpha L\beta_2$ (upper) and $\alpha M\beta_2$ (lower) transfectants binding to their ligands ICAM-1 (upper) and denatured BSA (lower) promoted by varied divalent cation activators. Activating mAb KIM185 was used as positive control. Effective activators were highlighted in green color. N.A.R. is the abbreviation for "No activating reagents". ME and MnE represent "Mg^{2+}/EGTA" and "Mn^{2+}/EGTA" respectively, in both cases, EGTA was used at 1.5 mM.

Throughout the course of this work, many such adhesion assays had been conducted, essentially as controls in different experiments. Compilation of the data on the effects of Mg^{2+}/EGTA (ME) on LFA-1 and Mac-1 adhesions to ICAM-1 and denatured BSA are shown in Table 4.1 and Table 4.2 respectively.

In Table 4.1, a total of 16 independent experiments on LFA-1 adhesion to ICAM-1 were listed, the adhesion activated by ME was compared to the adhesion activated by mAb KIM185, as a ratio, which is defined as

$$R_{Mi/Ki} = \frac{\%\,\text{Adhesion(ME)} - \%\,\text{Adhesion(NAR)}}{\%\,\text{Adhesion(KIM185)} - \%\,\text{Adhesion(NAR)}}$$

"NAR" stands for "No activating reagent". The average $R_{Mi/Ki}$ of 16 adhesion assays is 1.009 with a standard deviation of 0.375. The propagated standard deviation of (%ME - %NAR) or (%KIM185 - %NAR) is obtained by the formula ①; and the propagated standard deviation of $R_{Mi/Ki}$ (expressed above) is obtained by formula ② (Bevington, 1969):

$$\text{For } x=u\pm v;\quad \sigma_x = \text{SQRT}(\sigma_u^2 + \sigma_v^2) \qquad \cdots\cdots\cdots\cdots\cdots\cdots ①$$

$$\text{For } x=u/v;\quad \sigma_x = \text{SQRT}\left[\, x^2 \left(\frac{\sigma_u^2}{u^2} + \frac{\sigma_v^2}{v^2} + \frac{2\sigma_{uv}^2}{uv} \right) \right] \qquad \cdots\cdots\cdots ②$$

$$\text{For no correlations of u and v, } \sigma_{uv}^2 = 0$$

Similarly, seven experiments on Mac-1 adhesion to BSA were analyzed (Table 4.2). The mean value of $R_{Mi/Ki}$ was found to be 0.229 with a standard deviation of 0.057. The two ratios, 1.009 ± 0.375, (N=16) for LFA-1 mediated adhesion and 0.229 ± 0.057, (N=7) for Mac-1 mediated adhesions, are clearly distinct. For subsequent adhesion experiments in this chapter, these two ratios will serve as the reference for the classification of ME promoted adhesion behavior of a specific chimera/mutant to be either LFA-1 like or Mac-1 like.

Table 4.1. Statistics of LFA-1 mediated adhesion to ICAM-1 (16).

I				Mean	Standard deviation
N.A.R	5.7	6.1	8.3	6.7	1.4
ME	16.8	20.2	19.6	18.9	1.8
KIM185	19.2	19.8	20.6	19.9	0.7
					Propagated SD
$ME_{Increase}$	11.1	14.1	11.3	12.2	2.28
$KIM185_{Increase}$	13.5	13.7	12.3	13.2	1.57
$R_{Mi/Ki}$				0.924	0.205

II				Mean	Standard deviation
N.A.R	-0.2	-0.2	0.1	-0.1	0.2
ME	22.4	24.9	27.6	25.0	2.6
KIM185	21.2	23.8	26.4	23.8	2.6
					Propagated SD
$ME_{Increase}$	22.6	25.1	27.4	25.1	2.56
$KIM185_{Increase}$	21.4	24.1	26.2	23.9	2.57
$R_{Mi/Ki}$				1.048	0.155

III				Mean	Standard deviation
N.A.R	0.1	0.4	0.1	0.2	0.2
ME	13.8	14.2	15.7	14.6	1.0
KIM185	14.2	14.7	16.3	15.1	1.1
					Propagated SD
$ME_{Increase}$	13.7	13.8	15.6	14.4	1.02
$KIM185_{Increase}$	14.1	14.3	16.2	14.9	1.12
$R_{Mi/Ki}$				0.966	0.100

IV				Mean	Standard deviation
N.A.R	2	1.6	2.7	2.1	0.6
ME	27.1	26.6	30	27.9	1.8
KIM185	36.2	33.6	34.4	34.7	1.4
					Propagated SD
$ME_{Increase}$	25.1	25.0	27.3	25.8	1.90
$KIM185_{Increase}$	34.2	32.0	31.7	32.6	1.52
$R_{Mi/Ki}$				0.791	0.069

Table 4.1 (Continue).

V				Mean	Standard deviation
N.A.R	0.1	-0.4	-0.1	**-0.1**	0.3
ME	19.2	26.3	28.2	**24.6**	4.7
KIM185	24.3	31.0	32.0	**29.1**	4.2
					Propagated SD
$ME_{Increase}$	19.1	26.8	28.2	24.7	4.76
$KIM185_{Increase}$	24.2	31.4	32.1	29.2	4.18
$R_{Mi/Ki}$				0.844	0.203

VI				Mean	Standard deviation
N.A.R	5.1	3.5	5.0	4.5	0.9
ME	43.9	46.0	47.0	45.6	1.6
KIM185	37.6	35.1	36.1	36.3	1.3
					Propagated SD
$ME_{Increase}$	38.8	42.5	42.0	41.1	1.84
$KIM185_{Increase}$	32.5	31.6	31.1	31.8	1.58
$R_{Mi/Ki}$				1.292	0.086

VII				Mean	Standard deviation
N.A.R	-0.2	-0.3	-0.8	-0.4	0.3
ME	22.1	21.9	21.9	21.9	0.1
KIM185	22.4	22.3	24.0	22.9	1.0
					Propagated SD
$ME_{Increase}$	22.2	22.2	22.7	22.4	0.34
$KIM185_{Increase}$	22.6	22.6	24.9	23.3	1.04
$R_{Mi/Ki}$				0.959	0.045

VIII				Mean	Standard deviation
N.A.R	6.6	1.8	4.8	4.4	2.4
ME	26.5	21.4	20.7	22.9	3.2
KIM185	31.3	29.9	27.8	29.7	1.8
					Propagated SD
$ME_{Increase}$	19.9	19.6	15.9	18.5	4.00
$KIM185_{Increase}$	24.7	28.1	23.0	25.3	3.00
$R_{Mi/Ki}$				0.731	0.180

Table 4.1 (Continue).

IX				Mean	Standard deviation
N.A.R	12.0	9.0	7.5	9.5	2.3
ME	45.6	44.9	44.8	45.1	0.4
KIM185	47.0	45.4	49.2	47.2	1.9
					Propagated SD
$ME_{Increase}$	33.6	35.9	37.3	35.6	2.33
$KIM185_{Increase}$	35.0	36.4	41.7	37.7	2.98
$R_{Mi/Ki}$				0.944	0.097

X				Mean	Standard deviation
N.A.R	0.0	1.5	6.3	2.6	3.3
ME	35.8	35.5	30.6	34.0	2.9
KIM185	44.7	45.6	45.7	45.3	0.5
					Propagated SD
$ME_{Increase}$	35.8	34.0	24.3	31.4	4.39
$KIM185_{Increase}$	44.7	44.1	39.4	42.7	3.34
$R_{Mi/Ki}$				0.735	0.118

XI				Mean	Standard deviation
N.A.R	13.3	14.2	19.6	15.7	3.4
ME	53.5	47.1	49.6	50.1	3.3
KIM185	58.0	51.8	49.7	53.2	4.3
					Propagated SD
$ME_{Increase}$	40.2	32.9	30.0	34.4	4.74
$KIM185_{Increase}$	44.7	37.6	30.1	37.5	5.48
$R_{Mi/Ki}$				0.917	0.184

XII				Mean	Standard deviation
N.A.R	6.0	3.8	5.0	4.9	1.1
ME	40.5	44.1	44.2	42.9	2.1
KIM185	47.6	47.0	43.2	45.9	2.4
					Propagated SD
$ME_{Increase}$	34.5	40.3	39.2	38.0	2.37
$KIM185_{Increase}$	41.6	43.2	38.2	41.0	2.64
$R_{Mi/Ki}$				0.927	0.083

Table 4.1 (Continue).

XIII				Mean	Standard deviation
N.A.R	-0.5	2.1	1.7	1.1	1.4
ME	34.6	37.9	37.9	36.8	1.9
KIM185	38.3	38.6	38.3	38.4	0.1
					Propagated SD
$ME_{Increase}$	35.1	35.8	36.2	35.7	2.36
$KIM185_{Increase}$	38.8	36.5	36.6	37.3	1.40
$R_{Mi/Ki}$				0.957	0.073

XIV				Mean	Standard deviation
N.A.R	2.9	2.2	2.0	2.3	0.5
ME	26.9	23.5	22.5	24.3	2.3
KIM185	30.2	28.5	28.9	29.2	0.9
					Propagated SD
$ME_{Increase}$	24.0	21.3	20.5	21.9	2.35
$KIM185_{Increase}$	27.4	26.4	27.0	26.9	1.00
$R_{Mi/Ki}$				0.815	0.092

XV				Mean	Standard deviation
N.A.R	2.6	1.1	1.3	1.7	0.8
ME	17.5	21.0	22.4	20.3	2.5
KIM185	9.9	12.5	13.5	11.9	1.8
					Propagated SD
$ME_{Increase}$	15.0	19.9	21.1	18.6	2.63
$KIM185_{Increase}$	7.3	11.3	12.2	10.3	2.00
$R_{Mi/Ki}$				1.817	0.436

XVI				Mean	Standard deviation
N.A.R	5.2	5.1	5.9	5.4	0.4
ME	43.0	46.5	46.2	45.2	1.9
KIM185	44.9	48.1	51.5	48.2	3.3
					Propagated SD
$ME_{Increase}$	37.8	41.4	40.3	39.8	1.94
$KIM185_{Increase}$	39.7	43.0	45.6	42.8	3.32
$R_{Mi/Ki}$				0.930	0.085

Summary statistics on $R_{Mi/Ki}$ values of LFA-1adhered to ICAM-1.

ICAM-1	$R_{Mi/Ki}$ [Ratio (**ME** increase/**K**im185 increase)]								Mean/SD(p)
	0.924	0.966	0.791	1.292	0.731	0.994	0.735	0.917	0.978
	0.927	0.957	0.930	1.048	0.959	0.815	0.844	1.817	
	Propagated Standard Deviation								
	0.205	0.100	0.069	0.086	0.180	0.097	0.118	0.184	0.171
	0.083	0.073	0.085	0.155	0.045	0.092	0.203	0.436	
									(mean 0.978, SD 0.171, N 16)

SD(p): Propagated standard deviation

Table 4.2. Statistics of Mac-1 mediated adhesion to denatured BSA (7).

I				Mean	Standard deviation
N.A.R	5.3	5.6	7.8	6.3	1.4
ME	16.0	15.6	19.0	16.9	1.8
KIM185	65.3	63.7	61.9	63.6	1.7
					Propagated SD
$ME_{Increase}$	10.7	10.0	11.1	10.6	2.29
$KIM185_{Increase}$	60.0	58.1	54.0	57.4	2.20
$R_{Mi/Ki}$				0.185	0.040

II				Mean	Standard deviation
N.A.R	2.2	5.0	4.6	4.0	1.5
ME	15.2	15.1	15.3	15.2	0.1
KIM185	59.0	59.8	56.5	58.4	1.7
					Propagated SD
$ME_{Increase}$	13	10.1	10.7	11.2	1.50
$KIM185_{Increase}$	56.8	54.8	51.9	54.4	2.27
$R_{Mi/Ki}$				0.206	0.029

III				Mean	Standard deviation
N.A.R	1.8	1.2	2.8	1.9	0.8
ME	9.8	8.2	10.7	9.6	1.3
KIM185	33.2	36.3	34.0	34.5	1.6
					Propagated SD
$ME_{Increase}$	8.0	7.0	7.9	7.7	1.53
$KIM185_{Increase}$	31.4	35.1	31.2	32.6	1.79
$R_{Mi/Ki}$				0.236	0.049

IV				Mean	Standard deviation
N.A.R	11.1	7.3	8.1	8.9	0.3
ME	23.8	17.9	21.0	20.9	0.5
KIM185	48.4	58.8	55.3	54.2	5.1
					Propagated SD
$ME_{Increase}$	12.7	10.6	12.9	12	0.58
$KIM185_{Increase}$	37.3	51.5	47.2	45.3	5.11
$R_{Mi/Ki}$				0.265	0.033

Table 4.2 (Continue).

V				Mean	Standard deviation
N.A.R	0.9	1.5	1.9	1.4	0.5
ME	3.4	3.9	3.1	3.5	0.4
KIM185	20.6	24.2	20.9	21.9	2.0
					Propagated SD
$ME_{Increase}$	2.5	2.4	1.2	2.1	0.64
$KIM185_{Increase}$	19.7	22.7	19.0	20.5	2.06
$R_{Mi/Ki}$				0.102	0.033

VI				Mean	Standard deviation
N.A.R	1.5	2.5	2.9	2.3	0.8
ME	13.7	12.1	13.3	13.0	0.8
KIM185	24.6	25.8	27.0	25.8	1.2
					Propagated SD
$ME_{Increase}$	12.2	9.6	10.4	10.7	1.13
$KIM185_{Increase}$	23.1	23.3	24.1	23.5	1.44
$R_{Mi/Ki}$				0.455	0.056

VII				Mean	Standard deviation
N.A.R	11.7	13.7	14.8	13.4	1.5
ME	15.7	21.6	18.6	18.6	2.9
KIM185	44.9	49.4	46.5	46.9	2.3
					Propagated SD
$ME_{Increase}$	4.0	7.9	3.8	5.2	3.26
$KIM185_{Increase}$	33.2	35.7	31.7	33.5	2.75
$R_{Mi/Ki}$				0.155	0.098

Summary statistics on $R_{Mi/Ki}$ values of Mac-1 mediated adhesion promoted by ME and KIM185.

BSA	$R_{Mi/Ki}$ [Ratio (ME increase/Kim185 increase)]							Mean/SD(p)
	0.185	0.206	0.236	0.265	0.102	0.155	0.455	0.229
	Propagated Standard Deviation							
	0.040	0.029	0.049	0.033	0.033	0.098	0.056	0.057
								(mean 0.229, SD 0.057, N 7)

4.2 Mg^{2+}/EGTA Effects on Chimeric Integrin LFA-1 Mediated Adhesion Studies

I have shown in previous section that ME can promote integrin $\alpha L\beta_2$ mediated adhesion to ICAM-1, but its effects on integrin $\alpha M\beta_2$ mediated adhesion to denatured BSA is minimal. It is therefore reasonable to hypothesize that some structural features in $\alpha L\beta_2$ are responsible for ME mediated activation of $\alpha L\beta_2$, and these features are absent in $\alpha M\beta_2$. Since $\alpha L\beta_2$ and $\alpha M\beta_2$ both share the β_2 subunit, the differences therefore lie in αL and αM subunits. To this end, a series of αL/αM chimeric subunits were constructed. The headpiece consisted of the β-propeller and the α I domain is treated as a single unit. These chimeras are schematically shown in Figure 4.2. The identities and similarities between αL and αM primary sequences of the various domains are shown in table under the figure. Note that the chimeras were constructed in different phases of the project.

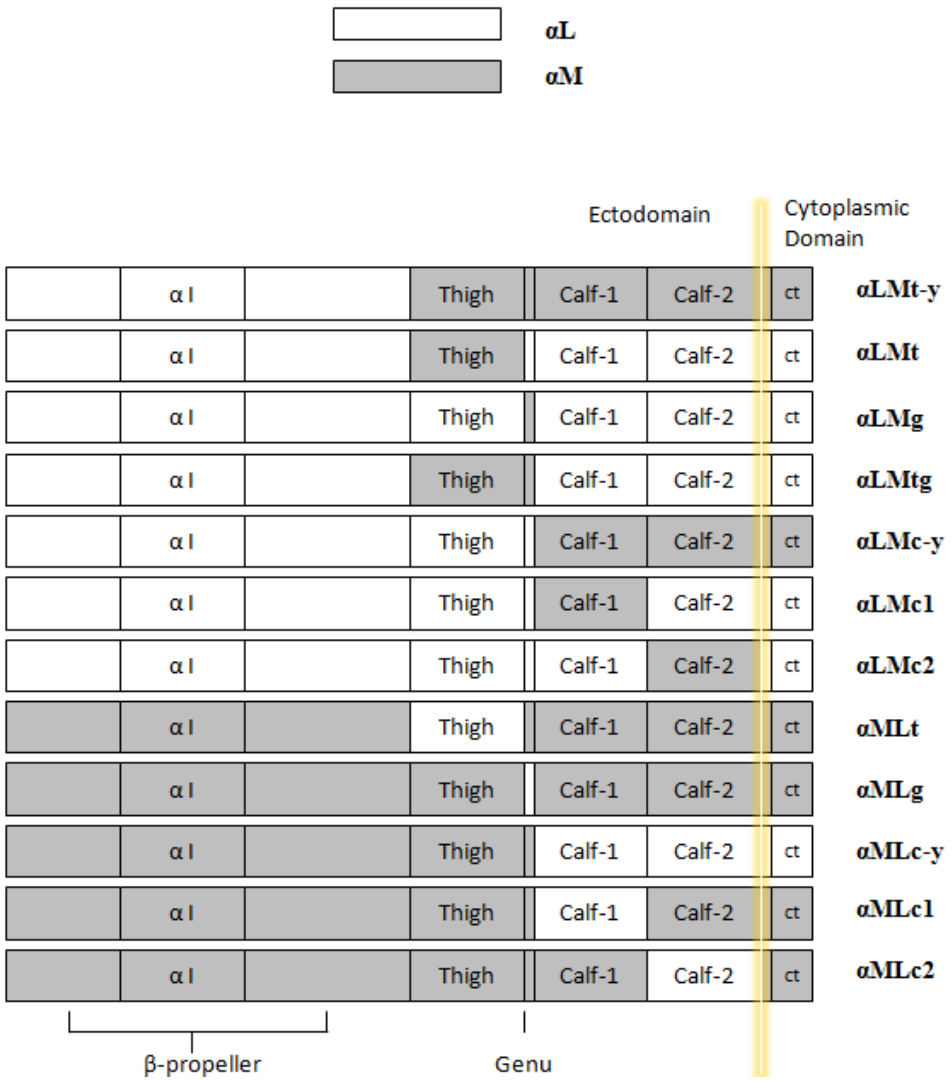

Domain	No. of Residues αL/αM	Identity (%)	Similarity (%)
Calf-1 to C-terminal (c-y)	394/377	24.5	35.4
Genu (g)	5/5	40.0	40.0
Thigh and genu (tg)	163/160	28.5	41.2
Thigh to C-terminal (t-y)	557/537	25.6	37.1
Thigh	158/155	28.1	41.3
Calf-1	147/150	25.8	40.4
Calf-2	166/180	19.4	28.9

Figure 4.2. Schematic maps of integrin α subunit chimeras (ectodomain), and amino acids sequence comparison between αL and αM. % Identity and % Similarity (taking into account of the properties of the residues) are obtained after alignment of the sequences.

4.2.1 Expression of αL/αM Chimeric Integrins

The αL/αM chimeras were individually transfected together with the wild-type β_2 subunit. The expressions of the integrins on transfectants were assessed by flow cytometry. Although the protein sequences of αL and αM shares low identity and similarity (Figure 4.2, Table), all recombinant αL/αM chimeras can support the integrin heterodimer formation and be detected on transfected HEK293T cell surfaces using the mAb MHM24 or MHM23 (Figure 4.3). It should be noted that although MHM24 only represents for expressed αL single unit, it has been established that αL cannot be transported to the cell surface without β_2. As shown in Figure 4.3, the α subunit chimeras supported heterodimer expressions to various levels. Since we are comparing the effects of ME v.s. KIM185 on the activation of the transfectants, the absolute level of the expressions would not affect our analysis.

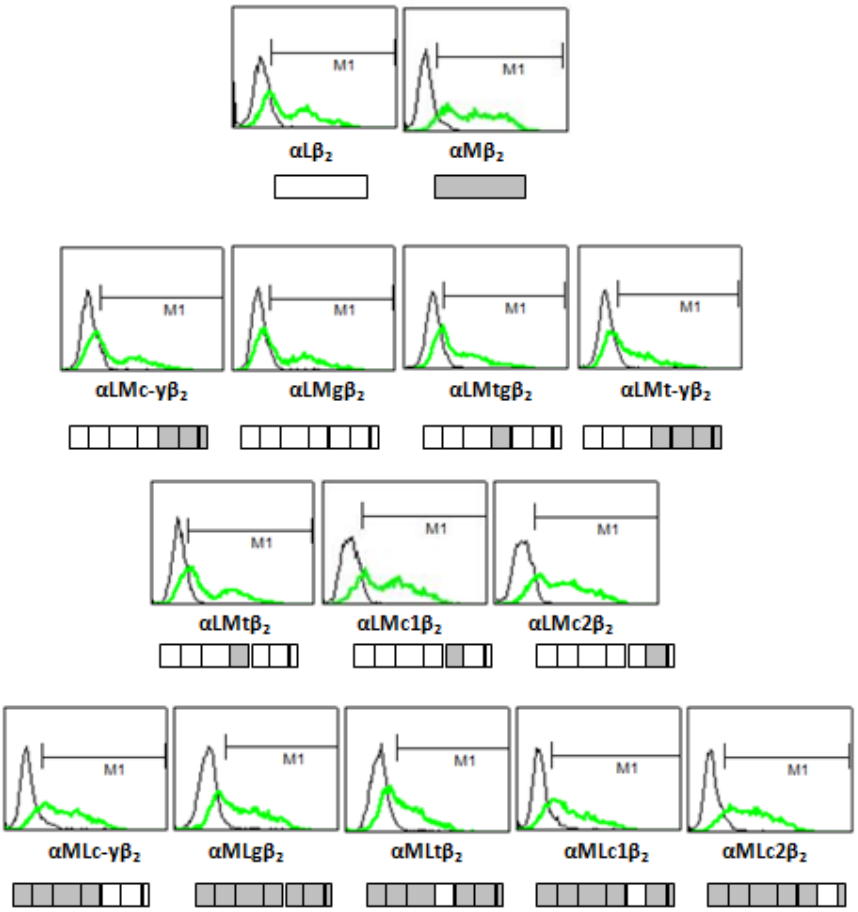

Figure 4.3. Surface expression detection of recombinant integrin LFA-1 with αL/αM chimeras by flow cytometry. Integrin heterodimer expression were assessed using the αL I domain specific mAb MHM24 at 10 μg/ml or heterodimer specific mAb MHM23 at 10 μg/ml. Note that αL cannot come to HEK293T cell surface without forming dimer with β_2.

4.2.2 Adhesion of Chimeric Integrin LFA-1and ICAM-1

The first five chimeric integrins (with αL I domain) were assessed by the adhesion to ICAM-1 in the presence of ME or KIM185. The binding histogram and $R_{Mi/Ki}$ value statistics are shown in Figure 4.4. All five recombinant integrins (containing αL I domain) were able to recognize and bind to the immobilized ligand ICAM-1 under the activation of the anti-β_2 activating mAb KIM185, indicating that αL leg regions being swapped to that

of αM did not affect integrin LFA-1 mediated adhesion. Moreover, in the presence of ME, the αLMgβ_2 (genu swapped), αLMtβ_2 (thigh swapped) and αLMtgβ_2 (genu & thigh swapped) transfectants can be activated to adhere to ICAM-1 coated surfaces. The $R_{Mi/Ki}$ values (0.783, 0.999, 1.162) were compared with the standard $R_{Mi/Ki}$ values (0.978) established from Table 4.1. Unpaired two-tailed student *t* test suggested that they are not statistically different from the wild-type. In contrast the other two variants, αLMt-yβ_2 (Thigh till C-terminal swapped) and αLMc-yβ_2 (Calf-1 till C-terminal swapped), their $R_{Mi/Ki}$ values are less than 0.1 and are significantly different from LFA-1 wild-type in statistics.

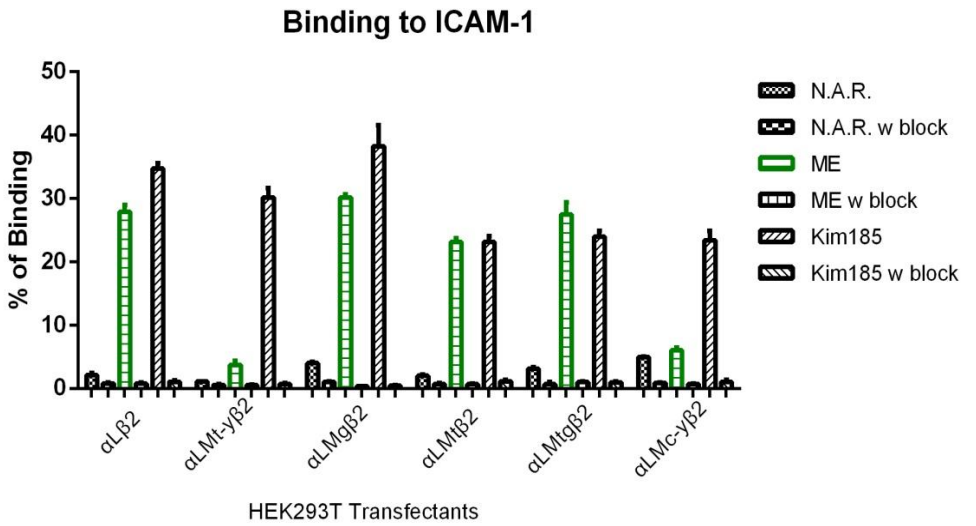

wt	aLMt-γβ2	aLMgβ2	aLMtβ2	aLMtgβ2	aLMc-γβ2	
0.792	0.062	0.783	0.999	1.162	0.089	$R_{Mi/Ki}$
0.068	0.036	0.134	0.091	0.187	0.039	SD(p)
						v.s. ICAM-1 ref.

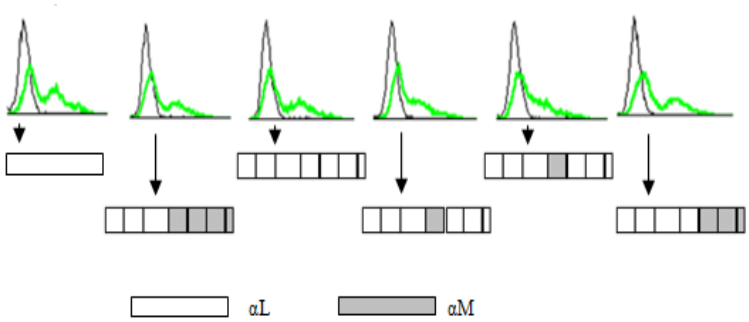

Figure 4.4. ME mediated activation tested by adhesion of recombinant αLβ$_2$ transfectants and ICAM-1. Surface expression of each transfectants and the schematic of each construct were shown under the binding plot. Ligand recognition and adhesion were established by β$_2$ activating mAb KIM185. ME effects were highlighted in green color. Statistics: Unpaired two-sample student *t* test (two-tailed), comparing with standard reference established from Table 4.1. In all cases, specificity was established by the functional blocking mAb MHM24.

Color code:

P>=0.05 Not statistically different	P<0.05 Statistically different

The above evidences suggested that the lack of ME response is due to the presence of the Mac-1 C-terminal to calf-1 domain, i.e. calf-1 domain, calf-2 domain, transmembrane domain and cytoplasmic tail, and is not due to the thigh domain or genu region. Since ME was added extracellularly, we can further argue that the domains responsible for ME activation is at the $\alpha L\beta_2$ calf-1 to calf-2 domains, and not due to the transmembrane domain and cytoplasmic tail.

Therefore, calf-1 and calf-2 domains were selected and the two chimeras, in which αL calf-1 and calf-2 domains were replaced by corresponding domains of αM respectively, were assessed by their ME sensitivity via ligand binding. Both constructs supported cell surface expression of the integrin heterodimer (Figure. 4.5). Except for the $\alpha LMc\text{-}y\beta_2$ that did not response to ME activation, $\alpha LMc1\beta_2$ (calf-1 swapped) totally abolished ICAM-1 binding induced by ME. The $R_{Mi/Ki}$ value obtained was 0.032, which is statistically significant from ICAM-1reference $R_{Mi/Ki}$ (0.978), and is even lower than BSA reference $R_{Mi/Ki}$ 0.229 ± 0.057. Changing αL calf-2 domain did not result a decrease in ME promoted ICAM-1 adhesion suggesting the αL calf-2 was not the determinant region for ME sensitivity. Notably, the adhesion to immobilized ICAM-1 were well observed in transfectants $\alpha LMc\text{-}y\beta_2$ and $\alpha LMc1\beta_2$ under mAb KIM185 activation, but the KIM185 stimulated adhesion was somehow affected by transfectants $\alpha LMc2\beta_2$, although the adhesion mediated by ME is not affected (Figure 4.5).

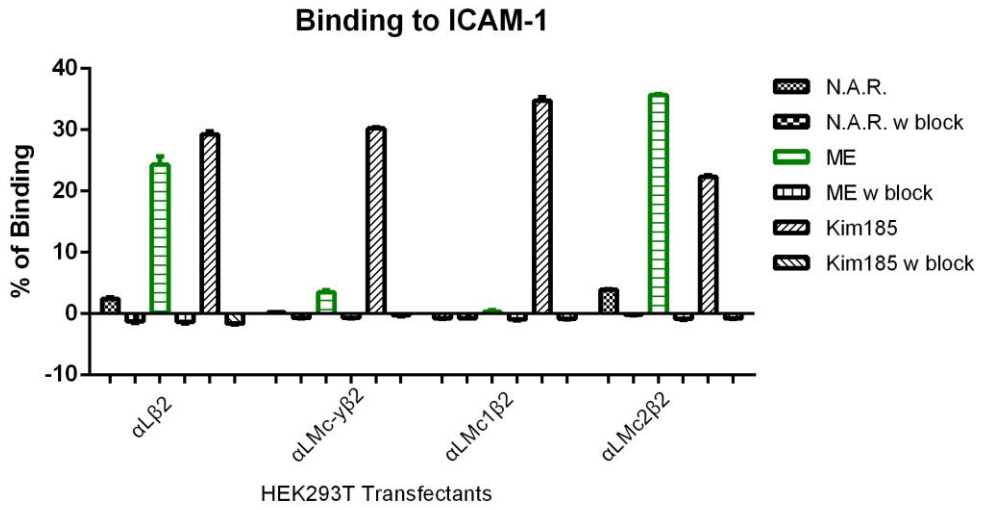

wt	αLMc-γβ2	αLMc1β2	αLMc2β2	
0.815	0.111	0.032	1.720	$R_{Mi/Ki}$
0.092	0.017	0.011	0.047	SD(p)
				v.s. ICAM-1 ref.

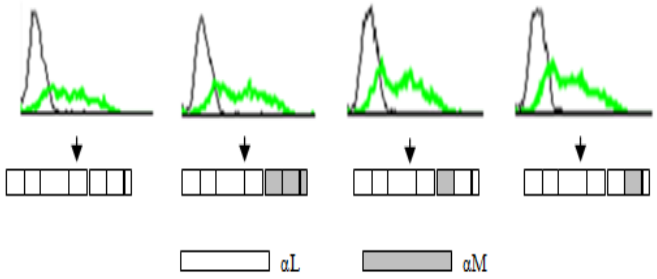

Figure 4.5. ME mediated activation on calf-1 or calf-2 swapped integrin $\alpha L\beta_2$. HEK293T transfected cells binding to immobilized ICAM-1. Adhesion specificity demonstrated by αL functional block mAb MHM24. Surface expression assessed by flow cytometry using mAb MHM23 (anti-αβ heterodimer).

4.3 αL Calf-1 and Calf-2 Domains Helped to Restore the ME Mediated Activation on Integrin Mac-1

We have established that the lack of ME sensitivity lies in the calf-1 domain of integrin Mac-1. We would like to explore if the converse is true, i.e. if the calf-1 domain of LFA-1 could confer ME sensitivity in Mac-1. The three regions: thigh, genu, and C-terminal to calf-1, of αL were introduced into the plasmid containing αM cDNA. Cell transfected with above mentioned chimeric Mac-1 were assessed by adhesion with denature BSA. Exchange of genu or thigh domain resulted in a low adhesion to Mac-1 stimulated by ME, whereas exchange of C-terminal to calf-1 region, showed a high binding to denatured BSA in the presence of ME. The $R_{Mi/Ki}$ of αMLc-yβ_2 had a value of 1.475, even higher than LFA-1/ICAM-1 reference $R_{Mi/Ki}$ 0.978 ± 0.171, and it is significantly different from Mac-1 like behavior in statistics, thus this variant is not Mac-1 like (Figure 4.6).

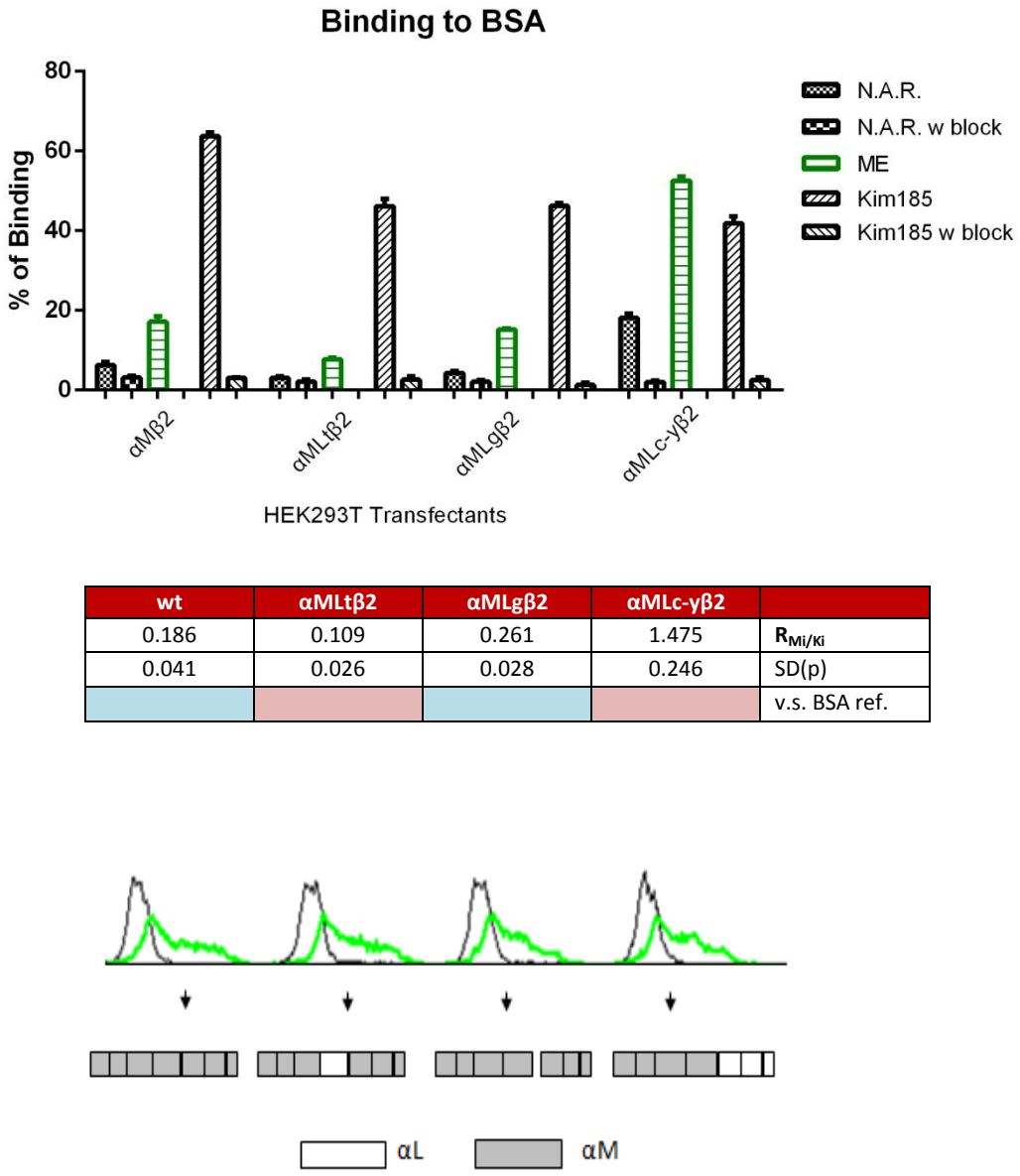

wt	αMLtβ2	αMLgβ2	αMLc-γβ2	
0.186	0.109	0.261	1.475	$R_{Mi/Ki}$
0.041	0.026	0.028	0.246	SD(p)
				v.s. BSA ref.

Figure 4.6. ME mediated activation assessed by recombinant αMβ$_2$ transfected cells binding to denatured BSA. HEK293T transfected cells binding to denatured BSA. Adhesion specificity demonstrated by αM functional block mAb LPM19C. Surface expressions examined by mAb MHM23. Statistics: unpaired two-sample student *t* test (two-tailed), taking Table 4.2 summary as reference.

Next, the αL calf-1 and αL calf-2 domains were introduced into αM respectively, yielding chimeras αMLc1 (calf-1 swapped) and αMLc2 (calf-2 swapped). Recombinant $\alpha M\beta_2$ integrins were transfected into HEK293T cells and the standard adhesion to BSA was performed (Figure 4.7). The introduction of the αL calf-1 domain into the αM construct resulted in an integrin that had high binding without either ME or KIM185. The addition of the two agents did not appear to enhance the binding further. Although the adhesion of $\alpha MLc2\beta_2$ to denatured BSA can be promoted by ME and KIM185, it also showed a high background adhesion to the ligand in the N.A.R condition. It is therefore difficult to confidently establish that the ME response element is functional in the construct.

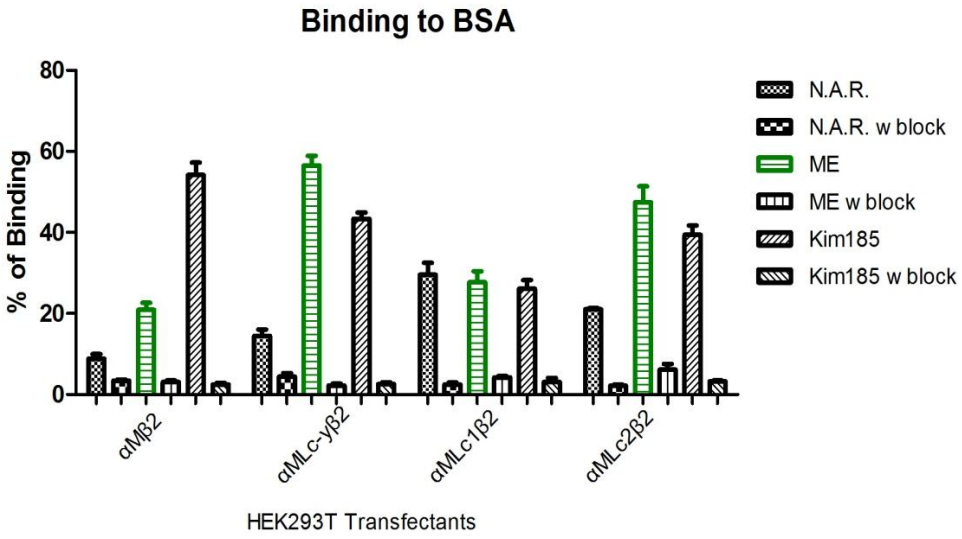

wt	αMLc-γβ2	αMLc1β2	αMLc2β2	
0.273	1.467	0.679	1.441	$R_{Mi/Ki}$
0.034	0.145	0.997	0.159	SD(p)
				v.s. BSA ref.

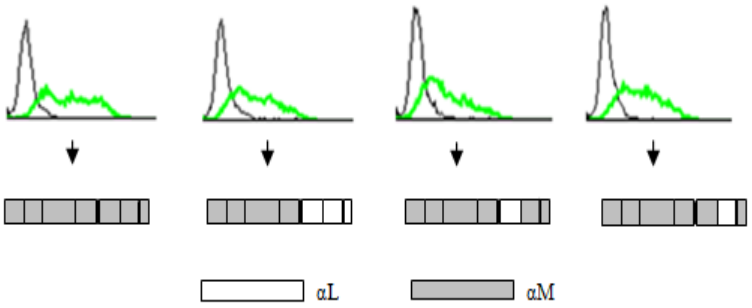

Figure 4.7. ME mediated activation assessed by recombinant αMβ$_2$ transfected cells binding to denatured BSA. Surface expressions analyzed by flow cytometry using mAb MHM23.

4.4 A Putative Ca^{2+} Binding Site at αL Genu and Its Involvement in ME Mediated Activation

Previous structural studies revealed that a well-coordinated Ca^{2+} binding pocket was found in the αV and αIIb genu region (Xiong et al., 2001b; Zhu et al., 2008). However, it was not found in αX due to a different backbone conformation (Xie et al., 2010). There is no evidence of the existence of a Ca^{2+} binding site in αL genu but the possibility of its existence cannot be excluded. The genu Ca^{2+} binding site consists of 2-3 coordinating residues from the genu region and one distal glutamic acid from the calf-1 domain. By aligning the related amino acid sequences of αL, αM, against those of αX, αIIb, αV, we noticed that the distal glutamic acid, E812 of αL is very conserved across these five α subunits (Figure 4.8).

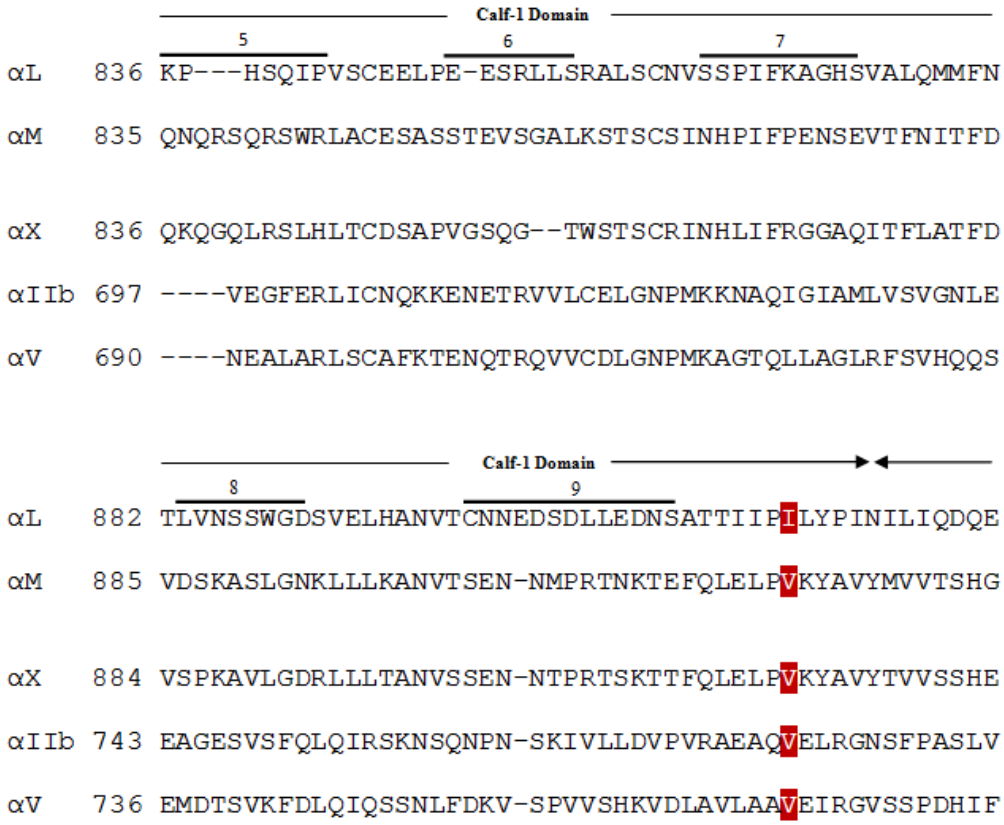

Figure 4.8. Sequence alignment of αL, αM, αX, αIIb and αV genu and calf-1 domains. Domain boundaries are denoted above the sequences by arrow lines. Nine loops in calf-1 are marked above the sequences in bold lines. Ca^{2+} coordinating residues and the conserved glutamic acid are highlighted in red. Genu region is labeled in grey background. The conserved glutamic acid in calf-1is labeled in green background. $\alpha L^{810/811}$ and $\alpha M^{809/810}$ are denoted by yellow dots below the sequence. Unique residues of αL are marked in red background.

To investigate the involvement of the putative αL genu Ca^{2+} binding site in ME mediated activation, the E812 of αL was mutated to the nonpolar residue alanine and uncharged residue glutamine respectively. Shown in Figure 4.9, the expression levels of αL-E812Aβ_2 and αL-E812Qβ_2 are similar to that of wild-type, and both the mutants do not support ICAM-1 binding and only do so in the presence of ME, which is typically wild-type like.

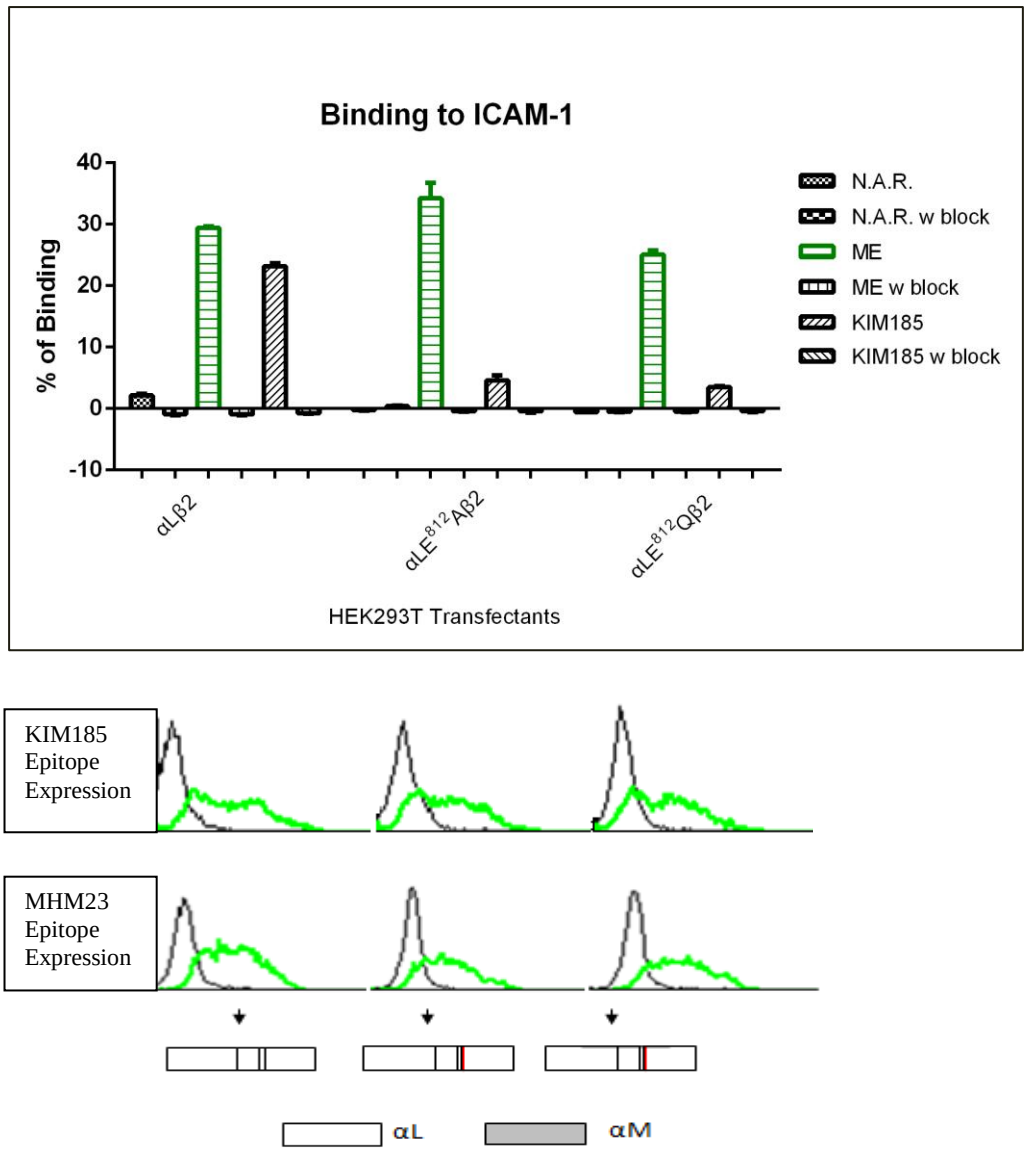

Figure 4.9. $\alpha L\beta_2$ transfected cells binding to immobilized ICAM-1. Upper panel: αL-$E^{812}A\beta_2$ and αL-$E^{812}Q\beta_2$ transfectants adhered to ICAM-1 in the presence of ME and KIM185. Lower panel: KIM185 and MHM23 epitope expressions on αL-$E^{812}A\beta_2$ and αL-$E^{812}Q\beta_2$.

Therefore, we concluded that the Ca^{2+} binding site at genu, if there is any, was not related to ME mediated activation on integrin LFA-1. However, these two mutants are not responsive to KIM185 activation, although the expression of KIM185 epitopes can be well detected by FACS. This observation is unexpected and cannot be explained at this time.

After the elimination of the conserved E812 in ME mediated activation on $\alpha L\beta_2$, we subsequently examined other possible regions in calf-1 which may be responsible for ME induced activation. Since the ME-mediated activation is specific to integrin LFA-1, it is reasonable to investigate the residues which are conserved in αM, αX, αIIb and αV, yet distinct from αL. The alignment shows five possible sites (Figure 4.8): (1) αL-T796 (corresponding residue in other 4 α subunits is glycine), (2) αL-E811 (glycine in other 4 α subunits), (3) αL-I927 (valine in other 4 α subunits). αL-I927 is neglected due to the similarity between them and their corresponding residues in other α subunits. Comparing to Site (1) which both are neutral residues, Site (2) αL-E811 includes a charged residue, we focus on examining the site (2): we found the -1 position to the E811, a non-polar L is found in αL, as opposed to the polar amino acid in αM, αX, αIIb and αV (aspartic acid, glutamic acid and glutamine respectively). These two residues are flanked by an asparagine and an glutamic acid in all given subunits. Due to these unique features, we mutated the αL-L810/E811 double residues into the corresponding ones in αM, which are aspartic acid and glycine respectively (Figure 4.10). The resultant chimeric integrin $\alpha L^{810/811}M\beta_2$ was transfected into HEK293T cells and the adhesion to ICAM-1 was examined. As shown in Figure 4.10, substitution of the two residues significantly reduced the ligand binding induced by ME.

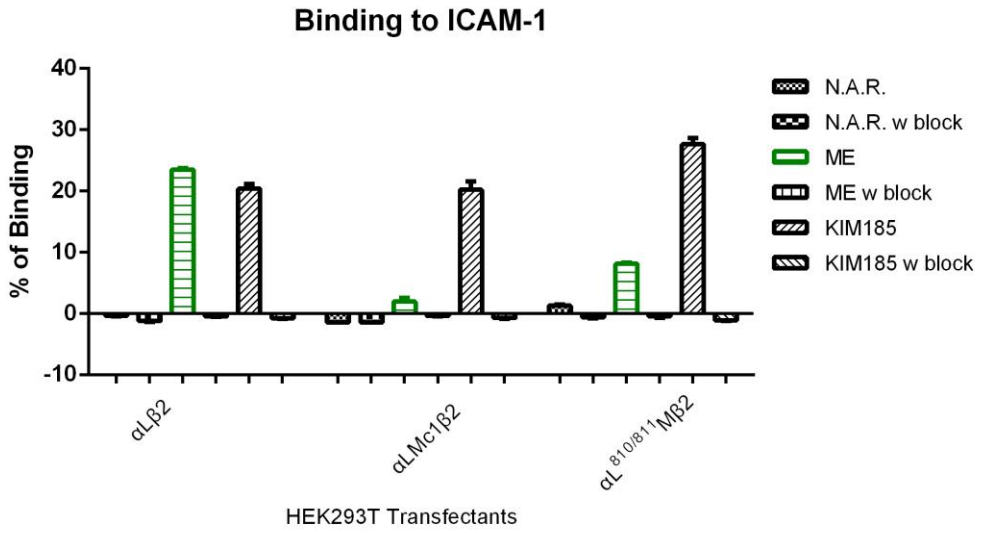

wt	αLMc1β2	αL$^{810/811}$Mβ2	
1.15	0.156	0.261	$R_{Mi/Ki}$
0.080	0.053	0.025	SD(p)
			v.s. ICAM-1 ref.

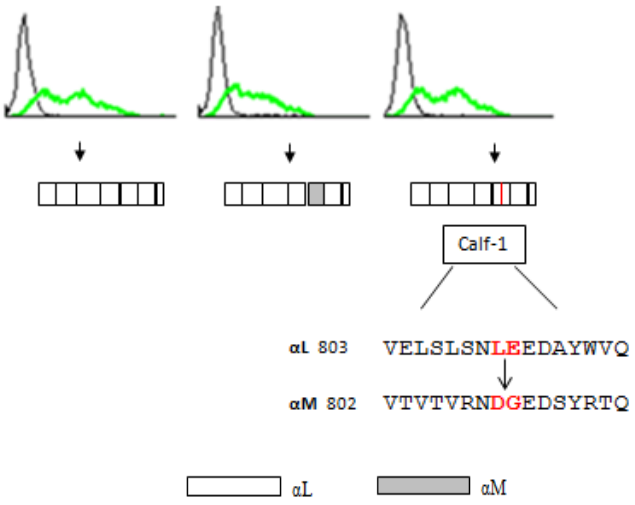

Figure 4.10. ME promoted αLβ$_2$ transfected cells binding to immobilized ICAM-1. Surface expressions detected by mAb MHM23.

4.5 Discussion

Work in this chapter focused on examining the effect of divalent Mg^{2+}/EGTA (5 mM Mg^{2+} and 1.5 mM EGTA) on the integrin αL subunit. The important findings are (1): When replacing αL calf-1 domain with αM calf-1 domain, recombinant integrin LFA-1 cannot respond to Mg^{2+}/EGTA mediated activation; (2) αL lower leg region, calf-1 and calf-2, could restore the Mg^{2+}/EGTA mediated activation on integrin Mac-1, albeit the relative contribution of the two domains are not clear.

In β_2 integrins, the recognized divalent cation binding sites are located at (1), βI domain; (2), αI domain; (3), α subunit β propeller. Among these cation binding sites, (1) and (2) are presumed to be the sites that account for the cation mediated integrin adhesion (Takada et al., 2007).

The divalent cation binding sites on β_2, which are MIDAS, ADMIDAS and SyMBS were demonstrated to play regulatory roles in mediating integrin-ligand adhesion. For example, the LAD-1 mutants β_2-S138P and β_2-D231H, coordinating residue from MIDAS and SyMBS respectively, failed to bind ligand under all conditions tested (Hogg et al., 1999; Mathew et al., 2000). β_2-N229A (SyMBS) resulted in the abolition of ligand binding under divalent cation promoted activation (Chen et al., 2006).

Similar to the βI domain, mutation on αM I domain MIDAS site αM-D140, αM-S142 and αM-S144 abolished the adhesion between Mac-1 mutants to

immobilized iC3b under the activation of divalent cations (McGuire and Bajt, 1995).

Studies on the integrin $\alpha4\beta_1$ calcium binding sites in the β-propeller of the α4 subunit found that mutations on these sites affect both surface expression and ligand binding. The mutation of integrin α4-N283Q abolished the expression of $\alpha4\beta_1$. Other mutations in the α4 subunit, including N283E (located in the blade 5 of the β-propeller), D346E (blade 6) α4-D408E (blade 7) resulted diminished binding of integrin $\alpha4\beta_1$ on CS1-BSA (the alternatively spliced cell attachment domain of fibronectin CS1 conjugated BSA) coated surfaces under the stimulation of mAb TS2/16 or 2 mM Mg^{2+} (Masumoto and Hemler, 1993). In addition, several natural mutations found in Glanzmann thrombasthenia patients, the αIIb-V298F, αIIb-I374T, αIIb-G418D, αIIb-R327H and deletion mutant αIIb-V425/D426 in the αIIb β-propeller calcium binding loops, do not support the normal surface expression of the $\alpha IIb\beta_3$ integrin (Wilcox et al., 1994; Wilcox et al., 1995; Basani et al., 1996; Mitchell et al., 2003).

The calcium binding site on the α genu, the existence of which was shown in αV and αIIb but not the αX structure. By introducing a disulfide bond in the genu of αIIb, the resultant $\alpha IIb\beta_3$ could not bind to the soluble ligand fibrinogen and PAC-1 under the activation of mAb PT25-2, but successful binding could be achieved under the condition of Mn^{2+} treatment (Blue et al., 2010). Whether there is a putative genu calcium binding site on αL is not known. Mutagenesis study on αL genu knee region reported that αL-D749A

(Genu) and αL-E787A (Calf-1) had partially reduced binding to mAb NKI-L16 (Ca^{2+} dependent) and AO3 (both of the antibody could induce the ligand binding of LFA-1) (Xie et al., 2004).

We have established the significant difference of ME promoted ligand binding between LFA-1/ICAM-1and Mac-1/denatured BSA. However, this may not be generalized into other experimental conditions. For example, the activation effect of Mg^{2+}/EGTA were reported in the binding between Jβ2.7 transfected (with CD11b subunit) cells and soluble ICAM-1or ICAM-2 (MacPherson et al., 2011). Nevertheless, many studies used Mn^{2+} as a standard activator for integrin Mac-1 (Ehirchiou, 2004; Cheng et al., 2007; Xie et al., 2010); Mg^{2+}/EGTA as a standard reagent to activate integrin LFA-1 (Tan et al., 2001; Smith et al., 2003; Tng et al., 2004; Cheng et al., 2007; Vararattanavech et al., 2008).

Additionally, we showed that the integrin αLMc1β_2 with the Mac-1 calf-1 domain in a LFA-1 background, the response to Mg^{2+}/EGTA mediated activation is lost. These results lead to the recognition that the αL calf-1 domain has a role in the Mg^{2+}/EGTA regulated adhesion of LFA-1 on ICAM-1. This regulatory effect takes place independent of the cation binding sites in other parts of LFA-1. It should be noted that in the solved integrin structures of α$V\beta_3$, α$IIb\beta_3$ and α$X\beta_2$, no divalent cation binding site was found in the calf-1 domain.

Nevertheless, our results find similarity in another study which focused on examining the distinct regulatory effect of Mn^{2+} on α$IIb\beta_3$ and α$V\beta_3$ adhesions

(Kamata et al., 2005). In their work, $\alpha IIb\beta_3$ could not bind to β_3 integrin ligand fibrinogen under Mn^{2+} activation but $\alpha V\beta_3$ could response to Mn^{2+} mediated adhesion. A series of αIIb/αV chimeras were constructed by domain swapping (including thigh, calf-1, calf-2 and cytoplasmic tail). The $\alpha IIb\beta_3$ bearing with a αV calf-2 domain is the only chimeric integrin that could be activated to bind to fibrinogen in the presence of Mn^{2+}. In the reverse experiment, αIIb with the αV headpiece could not respond to Mn^{2+} mediated adhesion when co-expressed β_3 in CHO cells. The αV genu region coordinating residue αV-D599 (at genu) and αV-D636 (at calf-1) were mutated into alanine, the two mutants did not affect Mn^{2+} mediated adhesion.

It was an intriguing to find the similarity in both Kamata et al's work (2005) and this work, in several aspects. (1) The difference in divalent cation requirement for adhesion was observed in two different integrin families: β_2 in this work and β_3 in Kamata et al's. (2) Different members of each of the two families were found to have different divalent cation requirements for adhesion: $\alpha L\beta_2$ and $\alpha M\beta_2$ in the β_2 family (this work) and $\alpha V\beta_3$ and $\alpha IIb\beta_3$ in the β_3 family (Kamata et al). (3) By domain swapping, it was the leg region, rather than the headpiece, that is responsible for the divalent cation regulated ligand binding in both cases. It is therefore plausible that the mechanisms of the leg region in regulating the divalent cation activation on β_2 family and β_3 family are the same. Given the fact that no divalent cation binding sites were found in the αIIb and αV calf-1 and calf-2 domains, it is reasonable to assume that there is also no divalent cation binding site in αL leg region. The possible explanations for the Mg^{2+}/EGTA regulatory effect on LFA-1 are: (1) The calf-

1 domain of αL serves as a critical remote controller for Mg^{2+} cation occupancy and Ca^{2+} displacement in the headpiece; (2) The αL and αM subunits interact differently with the β_2 subunit. It should be noted that this model is similar to that proposed by Wang et al in their study of the $\alpha IIb\beta_3$ integrin (Wang et al., 2010).

Although we have made progress, the details remain elusive how the divalent cations activate integrins, and the specific regulatory elements in αL that control the Mg^{2+}/EGTA mediated activation. Exploratory experiments by exchanging αL specific residues, in comparison to the αM, αX, αIIb and αV subunits had led to uncertain results. Replacing αL-E812 with alanine or glutamine resulted in the LFA-1 that is not responsive to KIM185 activation. Substitution of the αL-L810/E811 residue with D/G (of αM) results in significant reduction of ME sensitivity. The work will require more systematic approach to identify the amino acids responsible for the ME sensitivity.

Chapter 5: Conclusion

The work in Chapter 3 was the characterization of LAD-1 mutants with emphasis on the missense mutations, as deletions, nonsense mutations, and splice site mutations would invariably lead to proteins of no expression. Nineteen missense mutations were analyzed systematically. We showed that 14 of these mutations were incapable in supporting heterodimer integrin expression on cell surfaces. Nonetheless, all of the mutants can be synthesized intracellularly. This provided us with a novel notion that the non-expressed missense mutations of LAD-1 affect the transportation and heterodimer formation rather than biosynthesis. For the 5 mutants that support the surface expressions, we categorized 3 mutants, β_2-D77N, β_2-S453N and β_2-P648L as polymorphisms. The mutant LFA-1 with β_2-G716A is active to bind ICAM-1, but the reporter KIM127 epitope is masked in the natural form of this mutant suggests the mutant is not extended. It is established that extension is not an absolute conformation for ligand binding. Shi et al (2007) introduced a disulfide bond in the IEGF-2 domain which locks the LFA-1 in a bent configuration but it still can bind ligand. The mutation β_2-G150D is located in the βI domain, with a fair distance away from the βI cation binding sites. This mutation does not affect the heterodimer formation, as illustrated by expression of heterodimer specific mAb MHM23 epitope. The mAb 1B4 epitope was expressed at less than 40% (Supplementary Figure 3), it possible due to that the 1B4 epitope is mapped to the adjacent residues 144-148. It should be noted that in the case of LAD-1 pathogenic mutations β_2-A270V and β_2-A341P, although expressed at low level in COS-7 cells, both mutants

could be stimulated to bind ICAM-1. The glycine is very conserved (see Figure 3.1B), and examination of the $\alpha X\beta_2$ structure did not provide us with any insight in the role of this residue. It is not clear what further experiment would lead to a better understanding of why ligand binding is abolished.

The work in Chapter 4 showed the involvement of integrin α subunit lower leg (Calf-1 and Calf-2 domains) in the difference of the divalent cation dependent activation between LFA-1 and Mac-1. Solving the structure of $\alpha L\beta_2$ lower leg would have helped to understand this phenomenon. Other members in the laboratory and the Protein Expression Facility of the School of Biological Sciences had tried to express the lower leg portion of αL in bacterial, mammalian and insect expression system. All attempts failed. Future studies should aim to refine the location of the α lower leg regions that are specifically responsible for the divalent cation regulation of adhesion. Since this divalent cation regulation appears to affect different members of the same integrin family differently, a coordinated study on the different members is therefore necessary. It is also important to examine the lower leg interface between α and β subunits, and to determine whether the key residues at the interface are responsible for the divalent cation induced activation, as it has been implicated in the β_3 integrins (Kamata et al., 2005).

References

Al-Shamkhani, A., and S.K.A. Law. 1998. Expression of the H52 epitope on the beta 2 subunit is dependent on its interaction with the alpha subunits of the leukocyte integrins LFA-1, Mac-1 and p150,95 and the presence of Ca2+. *Eur J Immunol*. 28:3291-3300.

Altieri, D.C. 1991. Occupancy of Cd11b/Cd18 (Mac-1) Divalent Ion Binding Site(S) Induces Leukocyte Adhesion. *J Immunol*. 147:1891-1898.

Anderson, D.C., and T.A. Springer. 1987. Leukocyte Adhesion Deficiency - an Inherited Defect in the Mac-1, Lfa-1, and P150,95 Glycoproteins. *Annu Rev Med*. 38:175-194.

Arnaout, M.A. 2003. Integrin structure: new twists and turns in dynamic cell adhesion. (vol 186, pg 125, 2002). *Immunol Rev*. 193:146-146.

Arnaout, M.A., N. Dana, S.K. Gupta, D.G. Tenen, and D.M. Fathallah. 1990. Point Mutations Impairing Cell-Surface Expression of the Common Beta-Subunit (Cd-18) in a Patient with Leukocyte Adhesion Molecule (Leu-Cam) Deficiency. *J Clin Invest*. 85:977-981.

Arnaout, M.A., S.L. Goodman, and J.P. Xiong. 2007. Structure and mechanics of integrin-based cell adhesion. *Curr Opin Cell Biol*. 19:495-507.

Arnaout, M.A., J. Pitt, H.J. Cohen, J. Melamed, F.S. Rosen, and H.R. Colten. 1982. Deficiency of a Granulocyte-Membrane Glycoprotein (Gp150) in a Boy with Recurrent Bacterial-Infections. *New Engl J Med*. 306:693-699.

Arnaout, M.A., H. Spits, C. Terhorst, J. Pitt, and R.F. Todd. 1984. Deficiency of a Leukocyte Surface Glycoprotein (Lfa-1) in 2 Patients with Mo1 Deficiency - Effects of Cell Activation on Mo1 Lfa-1 Surface Expression in Normal and Deficient Leukocytes. *J Clin Invest*. 74:1291-1300.

Bachmann, M.F., K. McKall-Faienza, R. Schmits, D. Bouchard, J. Beach, D.E. Speiser, T.W. Mak, and P.S. Ohashi. 1997. Distinct roles for LFA-1 and CD28 during activation of naive T cells: adhesion versus costimulation. *Immunity*. 7:549-557.

Back, A.L., W.W. Kwok, and D.D. Hickstein. 1992. Identification of 2 Molecular Defects in a Child with Leukocyte Adherence Deficiency. *J Biol Chem*. 267:5482-5487.

Bajt, M.L., T. Goodman, and S.L. Mcguire. 1995. Beta(2) (Cd18) Mutations Abolish Ligand Recognition by I-Domain Integrins Lfa-1 (Alpha(L)Beta(2), Cd11a/Cd18) and Mac-1 (Alpha(M)Beta(2), Cd11b/Cd18). *J Biol Chem*. 270:94-98.

Basani, R.B., G. Vilaire, S.J. Shattil, M.A. Kolodziej, J.S. Bennett, and M. Poncz. 1996. Glanzmann thrombasthenia due to a two amino acid deletion in the fourth calcium-binding domain of alpha IIb: demonstration of the importance of calcium-binding domains in the conformation of alpha IIb beta 3. *Blood*. 88:167-173.

Bauer, T.R., and D.D. Hickstein. 2000. Gene therapy for leukocyte adhesion deficiency. *Curr Opin Mol Ther*. 2:383-388.

Bazzoni, G., D.T. Shih, C.A. Buck, and M.E. Hemler. 1995. Monoclonal-Antibody 9eg7 Defines a Novel Beta(1) Integrin Epitope Induced by Soluble Ligand and Manganese, but Inhibited by Calcium. *J Biol Chem*. 270:25570-25577.

Beatty, P.G., H.D. Ochs, J.M. Harlan, T.H. Price, H. Rosen, R.F. Taylor, J.A. Hansen, and S.J. Klebanoff. 1984. Absence of Monoclonal-Antibody-Defined Protein Complex in Boy with Abnormal Leukocyte Function. *Lancet*. 1:535-537.

Becker, D.J., and J.B. Lowe. 1999. Leukocyte adhesion deficiency type II. *Bba-Mol Basis Dis*. 1455:193-204.

Behmanesh, F., and H.R.F. Nezhad. 2009. Leukocyte adhesion deficiency. *Allergy*. 64:262-262.

Berger, B.W., D.W. Kulp, L.M. Span, J.L. DeGrado, P.C. Billings, A. Senes, J.S. Bennett, and W.F. DeGrado. 2010. Consensus motif for integrin transmembrane helix association. *P Natl Acad Sci USA*. 107:703-708.

Bevington, P.R. 1969. Data reduction and error analysis for the physical sciences. New York: McGraw-Hill.

Blue, R., J. Li, J. Steinberger, M. Murcia, M. Filizola, and B.S. Coller. 2010. Effects of limiting extension at the alphaIIb genu on ligand binding to integrin alphaIIbbeta3. *The Journal of biological chemistry*. 285:17604-17613.

Bowen, T.J., H.D. Ochs, L.C. Altman, T.H. Price, D.E. Vanepps, D.L. Brautigan, R.E. Rosin, W.D. Perkins, B.M. Babior, S.J. Klebanoff, and R.J. Wedgwood. 1982. Severe Recurrent Bacterial-Infections Associated with Defective Adherence and Chemotaxis in 2 Patients with Neutrophils Deficient in a Cell-Associated Glycoprotein. *J Pediatr*. 101:932-940.

Boxer, L.A., Hedleywh.T, and T.P. Stossel. 1974. Neutrophil Actin Dysfunction and Abnormal Neutrophil Behavior. *New Engl J Med*. 291:1093-1099.

Busslinger, M., N. Moschonas, and R.A. Flavell. 1981. Beta+ Thalassemia - Aberrant Splicing Results from a Single Point Mutation in an Intron. *Cell*. 27:289-298.

Butta, N., E.G. Arias-Salgado, C. Gonzalez-Manchon, M. Ferrer, S. Larrucea, M.S. Ayuso, and R. Parrilla. 2003. Disruption of the beta3 663-687 disulfide bridge confers constitutive activity to beta3 integrins. *Blood*. 102:2491-2497.

Castriconi, R., A. Dondero, C. Cantoni, M. Della Chiesa, C. Prato, M. Nanni, M. Fiorini, L. Notarangelo, S. Parolini, L. Moretta, L. Notarangelo, A. Moretta, and C. Bottino. 2007. Functional characterization of natural killer cells in type I leukocyte adhesion deficiency. *Blood*. 109:4873-4881.

Chen, J., W. Yang, M. Kim, C.V. Carman, and T.A. Springer. 2006. Regulation of outside-in signaling and affinity by the beta(2) I domain of integrin alpha(L)beta(2). *P Natl Acad Sci USA*. 103:13062-13067.

Cheng, M., S.Y. Foo, M.L. Shi, R.H. Tang, L.S. Kong, S.K.A. Law, and S.M. Tan. 2007. Mutation of a conserved asparagine in the I-like domain promotes constitutively active integrins alpha(L)ss(2) and alpha(IIb)ss(3). *J Biol Chem*. 282:18225-18232.

Cher, T.H.B., H.S. Chan, G.F. Klein, J. Jabkowski, G. Schadenbock-Kranz, O. Zach, X. Roca, and S.K.A. Law. 2011. A novel 3 ' splice-site mutation and a novel gross deletion in leukocyte adhesion deficiency (LAD)-1. *Biochem Bioph Res Co*. 404:1099-1104.

Chng, C.P., and S.M. Tan. 2011. Leukocyte integrin alpha L beta 2 transmembrane association dynamics revealed by coarse-grained molecular dynamics simulations. *Proteins*. 79:2203-2213.

Corbi, A.L., A. Vara, A. Ursa, M.C.G. Rodriguez, G. Fontan, and F. Sanchezmadrid. 1992. Molecular-Basis for a Severe Case of Leukocyte Adhesion Deficiency. *Eur J Immunol*. 22:1877-1881.

Crowley, C.A., J.T. Curnutte, R.E. Rosin, J. Andreschwartz, J.I. Gallin, M. Klempner, R. Snyderman, F.S. Southwick, T.P. Stossel, and B.M. Babior. 1980. An Inherited Abnormality of Neutrophil Adhesion - Its Genetic Transmission and Its Association with a Missing Protein. *New Engl J Med*. 302:1163-1168.

Dana, N., R.F. Todd, J. Pitt, T.A. Springer, and M.A. Arnaout. 1984. Deficiency of a Surface-Membrane Glycoprotein (Mo1) in Man. *J Clin Invest*. 73:153-159.

Dimancheboitrel, M.T., F. Ledeist, A. Quillet, A. Fischer, C. Griscelli, and B. Lisowskagrospierre. 1989. Effects of Interferon-Gamma (Ifn-Gamma) and Tumor Necrosis Factor-Alpha (Tnf-Alpha) on the Expression of Lfa-1 in the Moderate Phenotype of Leukocyte Adhesion Deficiency (Lad). *J Clin Immunol*. 9:200-207.

Dransfield, I., C. Cabanas, A. Craig, and N. Hogg. 1992. Divalent-Cation Regulation of the Function of the Leukocyte Integrin Lfa-1. *J Cell Biol*. 116:219-226.

Ehirchiou, D. 2004. Dual function for a unique site within the beta I-2 domain of integrin alpha(M)beta(2). *Circulation*. 110:312-312.

Etzioni, A., and M. Tonetti. 2001. Leukocyte adhesion deficiency - from A to almost Z (vol 178, pg 138, 2000). *Immunol Rev*. 183:234-234.

Eyerich, K., L. Cifaldi, L.D. Notarangelo, F. Porta, L. Notarangelo, E. Mazzolari, M. Fiorini, A. Paradisi, and A. Cavani. 2009. Chronic eczema in a patient with Leukocyte Adhesion Deficiency (LAD) type I. *Eur J Dermatol*. 19:78-79.

Fagerholm, S.C., M. Varis, M. Stefanidakis, T.J. Hilden, and C.G. Gahmberg. 2006. alpha-Chain phosphorylation of the human leukocyte CD11b/CD18 (Mac-1) integrin is pivotal for integrin activation to bind ICAMs and leukocyte extravasation. *Blood*. 108:3379-3386.

Fathallah, D.M., Jamal, T., Barbouche, M.R., Bejaoui, M., Hariz, M.B., Dellagi, K. 2001. Two novel frame shift, recurrent and de novo mutations in the ITGB2 (CD18) gene causing leukocyte adhesion deficiency in a highly inbred North African population. *J. Biomed. Biotechnol.* 1:114-121.

Faustino, N.A., and T.A. Cooper. 2003. Pre-mRNA splicing and human disease. *Gene Dev*. 17:419-437.

Feng, C., Y.F. Li, Y.H. Yau, H.S. Lee, X.Y. Tang, Z.H. Xue, Y.C. Zhou, W.M. Lim, T.C. Cornvik, C. Ruedl, S.G. Shochat, and S.M. Tan. 2012. Kindlin-3 Mediates Integrin alpha L beta 2 Outside-in Signaling, and It Interacts with Scaffold Protein Receptor for Activated-C Kinase 1 (RACK1). ***J Biol Chem*****. 287:10714-10726.**

Fiorini, M., G. Piovani, R.F. Schumacher, C. Magri, V. Bertini, E. Mazzolari, L. Notarangelo, L.D. Notarangelo, and S. Barlati. 2009. ITGB2 mutation combined with deleted ring 21 chromosome in a child with leukocyte adhesion deficiency. ***J Allergy Clin Immun*****. 124:1356-1358.**

Fiorini, M., W. Vermi, F. Facchetti, D. Moratto, G. Alessandri, L. Notarangelo, A. Caruso, P. Grigolato, A.G. Ugazio, L.D. Notarangelo, and R. Badolato. 2002. Defective migration of monocyte-derived dendritic cells in LAD-1 immunodeficiency. ***J Leukocyte Biol*****. 72:650-656.**

Fischer, A., P. Landais, W. Friedrich, B. Gerritsen, A. Fasth, F. Porta, A. Vellodi, M. Benkerrou, J.P. Jais, M. Cavazzanacalvo, G. Souillet, P. Bordigoni, G. Morgan, P. Vandijken, J. Vossen, F. Locatelli, and P. Dibartolomeo. 1994. Bone-Marrow Transplantation (Bmt) in Europe for Primary Immunodeficiencies Other Than Severe Combined Immunodeficiency - a Report from the European Group for Bmt and the European Group for Immunodeficiency. ***Blood*****. 83:1149-1154.**

Geng, X., R.H. Tang, S.K.A. Law, and S.M. Tan. 2005. Integrin CD11a cytoplasmic tail interacts with the CD45 membrane-proximal protein tyrosine phosphatase domain 1. ***Immunology*****. 115:347-357.**

Gupta, V., A. Gylling, J.L. Alonso, T. Sugimori, P. Ianakiev, J.P. Xiong, and M.A. Arnaout. 2007. The beta-tail domain (beta TD) regulates physiologic ligand binding to integrin CD11b/CD18. ***Blood*****. 109:3513-3520.**

Hamidieh, A.A., Z. Pourpak, M. Hosseinzadeh, M.R. Fazlollahi, K. Alimoghaddam, M. Movahedi, A. Hosseini, Z. Chavoshzadeh, M. Jalili, S. Arshi, M. Moin, and A. Ghavamzadeh. 2012. Reduced-intensity conditioning hematopoietic SCT for pediatric patients with LAD-1: clinical efficacy and importance of chimerism. ***Bone Marrow Transpl*****. 47:646-650.**

Henderson, R.B., L.H. Lim, P.A. Tessier, F.N. Gavins, M. Mathies, M. Perretti, and N. Hogg. 2001. The use of lymphocyte function-associated antigen (LFA)-1-deficient mice to determine the role of LFA-1, Mac-1, and alpha4 integrin in the inflammatory response of neutrophils. ***The Journal of experimental medicine*****. 194:219-226.**

Hidalgo, A., S.H. Ma, A.J. Peired, L.A. Weiss, C. Cunningham-Rundles, and P.S. Frenette. 2003. Insights into leukocyte adhesion deficiency type 2 from a novel mutation in the GDP-fucose transporter gene. ***Blood*****. 101:1705-1712.**

Hildreth, J.E.K., and J.T. August. 1985. The Human-Lymphocyte Function-Associated (Hlfa) Antigen and a Related Macrophage Differentiation Antigen (Hmac-1) - Functional-Effects of Subunit-Specific Monoclonal-Antibodies. ***J Immunol*****. 134:3272-3280.**

Hildreth, J.E.K., F.M. Gotch, P.D.K. Hildreth, and A.J. Mcmichael. 1983. A Human Lymphocyte-Associated Antigen Involved in Cell-Mediated Lympholysis. *Eur J Immunol*. 13:202-208.

Hinze, C.H., A.W. Lucky, K.E. Bove, R.A. Marsh, J.H. Bleesing, and M.H. Passo. 2010. Leukocyte Adhesion Deficiency Type 1 Presenting with Recurrent Pyoderma Gangrenosum and Flaccid Scarring. *Pediatr Dermatol*. 27:500-503.

Hixson, P., C.W. Smith, S.B. Shurin, and M.F. Tosi. 2004. Unique CD18 mutations involving a deletion in the extracellular stalk region and a major truncation of the cytoplasmic domain in a patient with leukocyte adhesion deficiency type 1. *Blood*. 103:1105-1113.

Hogervorst, F., I. Kuikman, A.E.G.K. Vondemborne, and A. Sonnenberg. 1990. Cloning and Sequence-Analysis of Beta-4 Cdna - an Integrin Subunit That Contains a Unique 118 Kd Cytoplasmic Domain. *Embo J*. 9:765-770.

Hogg, N., M.P. Stewart, S.L. Scarth, R. Newton, J.M. Shaw, S.K.A. Law, and N. Klein. 1999. A novel leukocyte adhesion deficiency caused by expressed but nonfunctional beta 2 integrins Mac-1 and LFA-1. *J Clin Invest*. 103:97-106.

Hughes, P.E., F. DiazGonzalez, L. Leong, C.Y. Wu, J.A. McDonald, S.J. Shattil, and M.H. Ginsberg. 1996. Breaking the integrin hinge - A defined structural constraint regulates integrin signaling. *J Biol Chem*. 271:6571-6574.

Hynes, R. 2002. Integrins bidirectional, allosteric signaling machines. *Cell*. 110:673-687.

Hyun, Y.M., C.T. Lefort, and M. Kim. 2009. Leukocyte integrins and their ligand interactions. *Immunol Res*. 45:195-208.

Iwasaki, K., K. Mitsuoka, Y. Fujiyoshi, Y. Fujisawa, M. Kikuchi, K. Sekiguchi, and T. Yamada. 2005. Electron tomography reveals diverse conformations of integrin alpha IIb beta 3 in the active state. *J Struct Biol*. 150:259-267.

Kamata, T., M. Handa, Y. Sato, Y. Ikeda, and S. Aiso. 2005. Membrane-proximal {alpha}/{beta} stalk interactions differentially regulate integrin activation. *The Journal of biological chemistry*. 280:24775-24783.

Kijas, J.M.H., T.R. Bauer, S. Gafvert, S. Marklund, G. Trowald-Wigh, A. Johannisson, A. Hedhammar, M. Binns, R.K. Juneja, D.D. Hickstein, and L. Andersson. 1999. A missense mutation in the beta-2 integrin gene (ITGB2) causes canine leukocyte adhesion deficiency. *Genomics*. 61:101-107.

Kim, C., F. Ye, and M.H. Ginsberg. 2011. Regulation of Integrin Activation. *Annu Rev Cell Dev Bi*. 27:321-345.

Kishimoto, T.K., K. Oconnor, A. Lee, T.M. Roberts, and T.A. Springer. 1987. Cloning of the Beta-Subunit of the Leukocyte Adhesion Proteins - Homology to an Extracellular-Matrix Receptor Defines a Novel Supergene Family. *Cell*. 48:681-690.

Kishimoto, T.K., K. Oconnor, and T.A. Springer. 1989. Leukocyte Adhesion Deficiency - Aberrant Splicing of a Conserved Integrin Sequence Causes a Moderate Deficiency Phenotype. *J Biol Chem*. 264:3588-3595.

Kulkarni, R.D., M.R. Thon, H.Q. Pan, and R.A. Dean. 2005. Novel G-protein-coupled receptor-like proteins in the plant pathogenic fungus Magnaporthe grisea. *Genome Biol*. 6.

Laemmli, U.K. 1970. Cleavage of Structural Proteins during Assembly of Head of Bacteriophage-T4. *Nature*. 227:680-&.

Lau, T.L., C. Kim, M.H. Ginsberg, and T.S. Ulmer. 2009. The structure of the integrin alpha IIb beta 3 transmembrane complex explains integrin transmembrane signalling. *Embo J*. 28:1351-1361.

Law, S.K.A., J. Gagnon, J.E.K. Hildreth, C.E. Wells, A.C. Willis, and A.J. Wong. 1987. The Primary Structure of the Beta-Subunit of the Cell-Surface Adhesion Glycoproteins Lfa-1, Cr3 and P150,95 and Its Relationship to the Fibronectin Receptor. *Embo J*. 6:915-919.

Li, L., Y.Y. Jin, R.M. Cao, and T.X. Chen. 2010. A novel point mutation in CD18 causing leukocyte adhesion deficiency in a Chinese patient. *Chinese Med J-Peking*. 123:1278-1282.

Li, R.H., N. Mitra, H. Gratkowski, G. Vilaire, R. Litvinov, C. Nagasami, J.W. Weisel, J.D. Lear, W.F. DeGrado, and J.S. Bennett. 2003. Activation of integrin alpha IIb beta 3 by modulation of transmembrane helix associations. *Science*. 300:795-798.

Li, W., D.G. Metcalf, R. Gorelik, R.H. Li, N. Mitra, V. Nanda, P.B. Law, J.D. Lear, W.F. DeGrado, and J.S. Bennett. 2005. A push-pull mechanism for regulating integrin function. *P Natl Acad Sci USA*. 102:1424-1429.

Liu, S.C., D.A. Calderwood, and M.H. Ginsberg. 2000. Integrin cytoplasmic domain-binding proteins. *J Cell Sci*. 113:3563-3571.

López Rodríguez C, N.A., Grospierre B, Sánchez-Madrid F, Fischer A, Springer TA, Corbí AL. 1993. Characterization of two new CD18 alleles causing severe leukocyte adhesion deficiency. *Eur J Immunol*. 23:2792-2798.

Lorusso, F., D. Kong, A.K. Abdul Jalil, C. Sylvestre, S.L. Tan, and S. Ao. 2006. Preimplantation genetic diagnosis of leukocyte adhesion deficiency type I. *Fertil Steril*. 85.

Lu, C.F., M. Ferzly, J. Takagi, and T.A. Springer. 2001. Epitope mapping of antibodies to the C-terminal region of the integrin beta(2) subunit reveals regions that become exposed upon receptor activation. *J Immunol*. 166:5629-5637.

Luo, B.H., C.V. Carman, and T.A. Springer. 2007. Structural basis of integrin regulation and signaling. *Annu Rev Immunol*. 25:619-647.

Luo, B.H., C.V. Carman, J. Takagi, and T.A. Springer. 2005. Disrupting integrin transmembrane domain heterodimerization increases ligand binding affinity, not valency or clustering. *P Natl Acad Sci USA*. 102:3679-3684.

Luo, B.H., T.A. Springer, and J. Takagi. 2004. A specific interface between integrin transmembrane helices and affinity for ligand. *Plos Biol*. 2:776-786.

MacPherson, M., H.S. Lek, A. Prescott, and S.C. Fagerholm. 2011. A Systemic Lupus Erythematosus-associated R77H Substitution in the CD11b Chain of the Mac-1 Integrin Compromises Leukocyte Adhesion and Phagocytosis. *J Biol Chem*. 286:17303-17310.

Malawista, S.E., A.D. Chevance, E.J. Brown, L.A. Boxer, and S.K.A. Law. 2003. Chemotaxis of non-compressed blood polymorphonuclear leukocytes from an adolescent with severe leukocyte adhesion deficiency. *Am J Hematol*. 73:115-120.

Masumoto, A., and M.E. Hemler. 1993. Mutation of putative divalent cation sites in the alpha 4 subunit of the integrin VLA-4: distinct effects on adhesion to CS1/fibronectin, VCAM-1, and invasin. *The Journal of cell biology*. 123:245-253.

Mathew, E.C., J.M. Shaw, F.A. Bonilla, S.K.A. Law, and D.A. Wright. 2000. A novel point mutation in CD18 causing the expression of dysfunctional CD11/CD18 leucocyte integrins in a patient with leucocyte adhesion deficiency (LAD). *Clin Exp Immunol*. 121:133-138.

Matsuura, S., F. Kishi, M. Tsukahara, H. Nunoi, I. Matsuda, K. Kobayashi, and T. Kajii. 1992. Leukocyte Adhesion Deficiency - Identification of Novel Mutations in 2 Japanese Patients with a Severe Form. *Biochem Bioph Res Co*. 184:1460-1467.

McGuire, S.L., and M.L. Bajt. 1995. Distinct ligand binding sites in the I domain of integrin alpha M beta 2 that differentially affect a divalent cation-dependent conformation. *The Journal of biological chemistry*. 270:25866-25871.

Mevorach, D., J.O. Mascarenhas, D. Gershov, and K.B. Elkon. 1998. Complement-dependent clearance of apoptotic cells by human macrophages. *J Exp Med*. 188:2313-2320.

Miedema, F., P.A.T. Tetteroo, F.G. Terpstra, G. Keizer, M. Roos, R.S. Weening, C.M.R. Weemaes, D. Roos, and C.J.M. Melief. 1985. Immunological Studies with Lfa-1-Deficient and Mo1-Deficient Lymphocytes from a Patient with Recurrent Bacterial-Infections. *J Immunol*. 134:3075-3081.

Mitchell, W.B., J.H. Li, F. Singh, A.D. Michelson, J. Bussel, B.S. Coller, and D.L. French. 2003. Two novel mutations in the alpha IIb calcium-binding domains identify hydrophobic regions essential for alpha IIbbeta 3 biogenesis. *Blood*. 101:2268-2276.

Moore, S.W., D. Sidler, and M.G. Zaahl. 2008. The ITGB2 immunomodulatory gene (CD18), enterocolitis, and Hirschsprung's disease. *J Pediatr Surg*. 43:1439-1444.

Moser, M., M. Bauer, S. Schmid, R. Ruppert, S. Schmidt, M. Sixt, H.V. Wang, M. Sperandio, and R. Fassler. 2009. Kindlin-3 is required for beta(2) integrin-mediated leukocyte adhesion to endothelial cells. *Nat Med*. 15:300-305.

Mould, A.P., S.J. Barton, J.A. Askari, P.A. McEwan, P.A. Buckley, S.E. Craig, and M.J. Humphries. 2003. Conformational changes in the integrin beta A domain provide a mechanism for signal transduction via hybrid domain movement. *J Biol Chem*. 278:17028-17035.

Nelson, C., H. Rabb, and M.A. Arnaout. 1992. Genetic Cause of Leukocyte Adhesion Molecule Deficiency - Abnormal Splicing and a Missense Mutation in a Conserved Region of Cd18 Impair Cell-Surface Expression of Beta-2 Integrins. *J Biol Chem*. 267:3351-3357.

Nishida, N., C. Xie, M. Shimaoka, Y.F. Cheng, T. Walz, and T.A. Springer. 2006. Activation of leukocyte beta(2) integrins by conversion from bent to extended conformations. *Immunity*. 25:583-594.

Nolan, S.M., E.C. Mathew, S.L. Scarth, A. Al-Shamkhani, and S.K.A. Law. 2000. The effects of cysteine to alanine mutations of CD18 on the expression and adhesion of the CD11/CD18 integrins. *Febs Lett*. 486:89-92.

Ohashi, Y., T. Yambe, S. Tsuchiya, H. Kikuchi, and T. Konno. 1993. Familial Genetic-Defect in a Case of Leukocyte Adhesion Deficiency. *Hum Mutat*. 2:458-467.

Oxvig, C., and T.A. Springer. 1998. Experimental support for a beta-propeller domain in integrin alpha-subunits and a calcium binding site on its lower surface. *P Natl Acad Sci USA*. 95:4870-4875.

Partridge, A.W., S.C. Liu, S. Kim, J.U. Bowie, and M.H. Ginsberg. 2005. Transmembrane domain helix packing stabilizes integrin aIIb beta 3 in the low affinity state. *J Biol Chem*. 280:7294-7300.

Parvaneh, N., S. Mamishi, A. Rezaei, N. Rezaei, B. Tamizifar, L. Parvaneh, R. Sherkat, B. Ghalehbaghi, S. Kashef, Z. Chavoshzadeh, A. Isaeian, F. Ashrafi, and A. Aghamohammadi. 2010. Characterization of 11 New Cases of Leukocyte Adhesion Deficiency Type 1 with Seven Novel Mutations in the ITGB2 Gene. *J Clin Immunol*. 30:756-760.

Perez, O.D., D. Mitchell, G.C. Jager, S. South, C. Murriel, J. McBride, L.A. Herzenberg, S. Kinoshita, and G.P. Nolan. 2003. Leukocyte functional antigen 1 lowers T cell activation thresholds and signaling through cytohesin-1 and Jun-activating binding protein 1. *Nat Immunol*. 4:1083-1092.

Plow, E.F., T.K. Haas, L. Zhang, J. Loftus, and J.W. Smith. 2000. Ligand binding to integrins. *J Biol Chem*. 275:21785-21788.

Pluskota, E., D.A. Soloviev, D. Szpak, C. Weber, and E.F. Plow. 2008. Neutrophil apoptosis: Selective regulation by different ligands of integrin alpha(M)beta(2). *J Immunol*. 181:3609-3619.

Poloni, F., P. Puddu, F. Moretti, M. Flego, G. Romagnoli, M. Tombesi, I. Capone, A. Chersi, F. Feleci, and M. Cianfriglia. 2001. Identification of a LFA-1 region involved in the HIV-1-induced syncytia formation through phage-display technology. *Eur J Immunol*. 31:57-63.

Qasim, W., M. Cavazzana-Calvo, and E.G. Davies. 2009. Allogeneic Hematopoietic Stem-Cell Transplantation for Leukocyte Adhesion Deficiency (vol 123, pg 836, 2009). *Pediatrics*. 123:1436-1436.

Riveramatos, I.R., R.M. Rakita, M.M. Mariscalco, F.F.B. Elder, S.A. Dreyer, and T.G. Cleary. 1995. Leukocyte Adhesion Deficiency Mimicking Hirschsprung Disease. *J Pediatr*. 127:755-757.

Robinson, M.K., D. Andrew, H. Rosen, D. Brown, S. Ortlepp, P. Stephens, and E.C. Butcher. 1992. Antibody against the Leu-Cam Beta-Chain (Cd18) Promotes Both Lfa-1-Dependent and Cr3-Dependent Adhesion Events. *J Immunol*. 148:1080-1085.

Roos, D., and S.K.A. Law. 2001. Hematologically important mutations: Leukocyte adhesion deficiency. *Blood Cell Mol Dis*. 27:1000-1004.

Roos, D., C. Meischl, M. de Boer, S. Simsek, R.S. Weening, O. Sanal, I. Tezcan, T. Gungor, and S.K.A. Law. 2002. Genetic analysis of patients with leukocyte adhesion deficiency: Genomic sequencing reveals otherwise undetectable mutations. *Exp Hematol*. 30:252-261.

Ross, G.D., R.A. Thompson, M.J. Walport, T.A. Springer, J.V. Watson, R.H.R. Ward, J. Lida, S.L. Newman, R.A. Harrison, and P.J. Lachmann. 1985. Characterization of Patients with an Increased Susceptibility to Bacterial-Infections and a Genetic Deficiency of Leukocyte Membrane Complement Receptor Type-3 and the Related Membrane Antigen Lfa-1. *Blood*. 66:882-890.

San Sebastian, E., J.M. Mercero, R.H. Stote, A. Dejaegere, F.P. Cossio, and X. Lopez. 2006. On the affinity regulation of the metal-ion-dependent adhesion sites in integrins. *J Am Chem Soc*. 128:3554-3563.

Schleiffenbaum, B., R. Moser, M. Patarroyo, and J. Fehr. 1989. The Cell-Surface Glycoprotein Mac-1 (Cd11b/Cd18) Mediates Neutrophil Adhesion and Modulates De-Granulation Independently of Its Quantitative Cell-Surface Expression. *J Immunol*. 142:3537-3545.

Schurpf, T., and T.A. Springer. 2011. Regulation of integrin affinity on cell surfaces. *Embo J*. 30:4712-4727.

Shaw, J.M., A. Al-Shamkhani, L.A. Boxer, C.D. Buckley, A.W. Dodds, N. Klein, S.M. Nolan, I. Roberts, D. Roos, S.L. Scarth, D.L. Simmons, S.M. Tan, and S.K.A. Law. 2001. Characterization of four CD18 mutants in leucocyte adhesion deficient (LAD) patients with differential capacities to support expression and function of the CD11/CD18 integrins LFA-1, Mac-1 and p150,95. *Clin Exp Immunol*. 126:311-318.

Shi, M.L., S.Y. Foo, S.M. Tan, E.P. Mitchell, S.K.A. Law, and J. Lescar. 2007. A structural hypothesis for the transition between bent and extended conformations of the leukocyte beta 2 integrins. *J Biol Chem*. 282:30198-30206.

Shi, M.L., K. Sundramurthy, B. Liu, S.M. Tan, S.K.A. Law, and J. Lescar. 2005. The crystal structure of the plexin-semaphorin-integrin domain/hybrid domain/I-EGF1 segment from the human integrin beta(2) subunit at 1.8-angstrom resolution. *J Biol Chem*. 280:30586-30593.

Sligh JE Jr, H.M., Zhu CM, Anderson DC, Beaudet AL. 1992. An initiation codon mutation in CD18 in association with the moderate phenotype of leukocyte adhesion deficiency. *J Biol Chem*. 267:714-718.

Smith, A., M. Bracke, B. Leitinger, J.C. Porter, and N. Hogg. 2003. LFA-1-induced T cell migration on ICAM-1 involves regulation of MLCK-mediated attachment and ROCK-dependent detachment. *J Cell Sci*. 116:3123-3133.

Southwick, F.S., T. Holbrook, T. Howard, T. Springer, T.P. Stossel, and M.A. Arnaout. 1986. Neutrophil Actin Dysfunction Is Associated with a Deficiency of Mol. *Clin Res*. 34:A533-A533.

Springer, T.A., and M.L. Dustin. 2012. Integrin inside-out signaling and the immunological synapse. *Curr Opin Cell Biol*. 24:107-115.

Stephens, P., J.T. Romer, M. Spitali, A. Shock, S. Ortlepp, C.G. Figdor, and M.K. Robinson. 1995. KIM127, an antibody that promotes adhesion, maps to a region of CD18 that includes cysteine-rich repeats. *Cell Adhes Commun*. 3:375-384.

Takada, Y., X.J. Ye, and S. Simon. 2007. The integrins. *Genome Biol*. 8.

Takagi, J., B.M. Petre, T. Walz, and T.A. Springer. 2002. Global conformational rearrangements in integrin extracellular domains in outside-in and inside-out signaling. *Cell*. 110:599-611.

Takagi, J., and T.A. Springer. 2002. Integrin activation and structural rearrangement. *Immunol Rev*. 186:141-163.

Takagi, J., K. Strokovich, T.A. Springer, and T. Walz. 2003. Structure of integrin alpha(5)beta(1) in complex with fibronectin. *Embo J*. 22:4607-4615.

Tamkun, J.W., D.W. Desimone, D. Fonda, R.S. Patel, C. Buck, A.F. Horwitz, and R.O. Hynes. 1986. Structure of Integrin, a Glycoprotein Involved in the Transmembrane Linkage between Fibronectin and Actin. *Cell*. 46:271-282.

Tan, S.M. 2012. The leucocyte beta 2 (CD18) integrins: the structure, functional regulation and signalling properties. *Bioscience Rep*. 32:241-269.

Tan, S.M., R.H. Hyland, A. Al-Shamkhani, W.A. Douglass, J.M. Shaw, and S.K.A. Law. 2000. Effect of integrin beta(2) subunit truncations on LFA-1 (CD11a/CD18) and Mac-1 (CD11b/CD18) assembly, surface expression, and function. *J Immunol*. 165:2574-2581.

Tan, S.M., M.K. Robinson, K. Drbal, Y. van Kooyk, J.M. Shaw, and S.K.A. Law. 2001. The N-terminal region and the mid-region complex of the integrin beta(2) subunit. *J Biol Chem*. 276:36370-36376.

Tang, R.H., E. Tng, S.K.A. Law, and S.M. Tan. 2005. Epitope mapping of monoclonal antibody to integrin alpha(L)beta(2) hybrid domain suggests different requirements of affinity states for intercellular adhesion molecules (ICAM)-1 and ICAM-3 binding. *J Biol Chem*. 280:29208-29216.

Tang, X.Y., Y.F. Li, and S.M. Tan. 2008. Intercellular adhesion molecule-3 binding of integrin alpha(L)beta(2) requires both extension and opening of the integrin headpiece. *J Immunol*. 180:4793-4804.

Tng, E., S.M. Tan, S. Ranganathan, M. Cheng, and S.K.A. Law. 2004. The integrin alpha(L)beta(2) hybrid domain serves as a link for the propagation of activation signal from its stalk regions to the I-like domain. *J Biol Chem*. 279:54334-54339.

Tone, Y., T. Wada, F. Shibata, T. Toma, Y. Hashida, Y. Kasahara, S. Koizumi, and A. Yachie. 2007. Somatic revertant mosaicism in a patient with leukocyte adhesion deficiency type 1. *Blood*. 109:1182-1184.

Uciechowski, P., and R.E. Schmidt. 1989. NK and non-lineage antigens cluster report: CD11. . *In Leukocyte Typing IV: White Cell Differentiation Antigens.* . W. Knapp, editor . Oxford University Press, Oxford .543-551.

Ulmer, T.S., B. Yaspan, M.H. Ginsberg, and I.D. Campbell. 2001. NMR analysis of structure and dynamics of the cytosolic tails of integrin alpha IIb beta 3 in aqueous solution. *Biochemistry-Us*. 40:7498-7508.

Uzel, G., D. Kuhns, A. Hussey, C. Spalding, J. Stoddard, A. Hsu, and S. Holland. 2010. The new face of leukocyte adhesion deficiency type 1 (LAD-1). *XIVth Meeting of the European Society for Immunodeficiencies*:132 (Abstr. P256).

Uzel, G., E. Tng, S.D. Rosenzweig, A.P. Hsu, J.M. Shaw, M.E. Horwitz, G.F. Linton, S.M. Anderson, M.R. Kirby, J.B. Oliveira, M.R. Brown, T.A. Fleisher, S.K.A. Law, and S.M. Holland. 2008. Reversion mutations in patients with leukocyte adhesion deficiency type-1 (LAD-1). *Blood*. 111:209-218.

van de Vijver, E., A. Maddalena, O. Sanal, S.M. Holland, G. Uzel, M. Madkaikar, M. de Boer, K. van Leeuwen, M.Y. Koker, N. Parvaneh, A. Fischer, S.K.A. Law, N. Klein, F.I. Tezcan, E. Unal, T. Patiroglu, B.H. Belohradsky, K. Schwartz, R. Somech, T.W. Kuijpers, and D. Roos. 2012. Hematologically important mutations: Leukocyte adhesion deficiency (first update). *Blood Cell Mol Dis*. 48:53-61.

Vararattanavech, A., C.P. Chng, K. Parthasarathy, X.Y. Tang, J. Torres, and S.M. Tan. 2010. A Transmembrane Polar Interaction Is Involved in the Functional Regulation of Integrin alpha L beta 2. *J Mol Biol*. 398:569-583.

Vararattanavech, A., M.L. Tang, H.Y. Li, C.H. Wong, S.K.A. Law, J. Torres, and S.M. Tan. 2008. Permissive transmembrane helix heterodimerization is required for the expression of a functional integrin. *Biochem J*. 410:495-502.

Vinogradova, O., A. Velyvis, A. Velyviene, B. Hu, T.A. Haas, E.F. Plow, and J. Qin. 2002. A structural mechanism of integrin alpha(IIb)beta(3) "inside-out" activation as regulated by its cytoplasmic face. *Cell*. 110:587-597.

Wang, W., G.Y. Fu, and B.H. Luo. 2010. Dissociation of the alpha-Subunit Calf-2 Domain and the beta-Subunit I-EGF4 Domain in Integrin Activation and Signaling. *Biochemistry-Us*. 49:10158-10165.

Wardlaw, A.J., M.L. Hibbs, S.A. Stacker, and T.A. Springer. 1990. Distinct Mutations in 2 Patients with Leukocyte Adhesion Deficiency and Their Functional Correlates. *J Exp Med*. 172:335-345.

Watts, C., and A. Lanzavecchia. 1993. Suppressive Effect of Antibody on Processing of T-Cell Epitopes. *J Exp Med*. 178:1459-1463.

Weitzman, J.B., C.E. Wells, A.H. Wright, P.A. Clark, and S.K.A. Law. 1991. The Gene Organization of the Human Beta-2 Integrin Subunit (Cd18). *Febs Lett*. 294:97-103.

Wilcox, D.A., C.M. Paddock, S. Lyman, J.C. Gill, and P.J. Newman. 1995. Glanzmann thrombasthenia resulting from a single amino acid substitution between the second and third calcium-binding domains of GPIIb. Role of the GPIIb amino terminus in integrin

subunit association. *The Journal of clinical investigation*. 95:1553-1560.

Wilcox, D.A., J.L. Wautier, D. Pidard, and P.J. Newman. 1994. A single amino acid substitution flanking the fourth calcium binding domain of alpha IIb prevents maturation of the alpha IIb beta 3 integrin complex. *The Journal of biological chemistry*. 269:4450-4457.

Wright, A.H., W.A. Douglass, G.M. Taylor, Y.L. Lau, D. Higgins, K.A. Davies, and S.K.A. Law. 1995. Molecular Characterization of Leukocyte Adhesion Deficiency in 6 Patients. *Eur J Immunol*. 25:717-722.

Wright, S.D., and S.C. Silverstein. 1982. Tumor-Promoting Phorbol Esters Stimulate C3b and C3b' Receptor-Mediated Phagocytosis in Cultured Human-Monocytes. *J Exp Med*. 156:1149-1164.

Wright, S.D., W.C. Vanvoorhis, and S.C. Silverstein. 1983. Identification of the C3b'-Receptor on Human-Leukocytes Using a Monoclonal-Antibody. *Fed Proc*. 42:1079-1079.

Xiao, T., J. Takagi, B.S. Coller, J.H. Wang, and T.A. Springer. 2004. Structural basis for allostery in integrins and binding to fibrinogen-mimetic therapeutics. *Nature*. 432:59-67.

Xie, C., M. Shimaoka, T. Xiao, P. Schwab, L.B. Klickstein, and T.A. Springer. 2004. The integrin alpha-subunit leg extends at a Ca2+-dependent epitope in the thigh/genu interface upon activation. *P Natl Acad Sci USA*. 101:15422-15427.

Xie, C., J. Zhu, X. Chen, L. Mi, N. Nishida, and T.A. Springer. 2009. Structure of an integrin with an alphaI domain, complement receptor type 4. *EMBO J*.

Xie, C., J.H. Zhu, X. Chen, L.Z. Mi, N. Nishida, and T.A. Springer. 2010. Structure of an integrin with an alpha I domain, complement receptor type 4. *Embo J*. 29:666-679.

Xiong, J.P., T. Stehle, B. Diefenbach, R. Zhang, R. Dunker, D.L. Scott, A. Joachimiak, S.L. Goodman, and M.A. Arnaout. 2001a. Crystal structure of the extracellular segment of integrin alpha Vbeta3. *Science*. 294:339-345.

Xiong, J.P., T. Stehle, B. Diefenbach, R.G. Zhang, R. Dunker, D.L. Scott, A. Joachimiak, S.L. Goodman, and M.A. Arnaout. 2001b. Crystal structure of the extracellular segment of integrin alpha V beta 3. *Science*. 294:339-345.

Xiong, J.P., T. Stehle, S.L. Goodman, and M.A. Arnaout. 2003. Integrins, cations and ligands: making the connection. *Journal of Thrombosis and Haemostasis*. 1:1642-1654.

Xiong, J.P., T. Stehle, S.L. Goodman, and M.A. Arnaout. 2004. A novel adaptation of the integrin PSI domain revealed from its crystal structure. *J Biol Chem*. 279:40252-40254.

Xiong, J.P., T. Stehle, R. Zhang, A. Joachimiak, M. Frech, S.L. Goodman, and M.A. Arnaout. 2002. Crystal structure of the extracellular segment of integrin alpha Vbeta3 in complex with an Arg-Gly-Asp ligand. *Science*. 296:151-155.

Xiong, Y.M., and L. Zhang. 2001. Structure-function of the putative I-domain within the integrin beta(2) subunit. *J Biol Chem*. 276:19340-19349.

Yakubenko, V.P., N. Beleuych, D. Mishchuk, A. Schurin, S.C.T. Lam, and T.P. Uyarova. 2008. The role of integrin alpha(D)beta(2) (CD11d/CD18) in monocyte/macrophage migration. *Exp Cell Res*. 314:2569-2578.

Yakubenko, V.P., S.P. Yadav, and T.P. Ugarova. 2006. Integrin alpha(D)beta(2), an adhesion receptor up-regulated on macrophage foam cells, exhibits multiligand-binding properties. *Blood*. 107:1643-1650.

Zhang, K., and J.F. Chen. 2012. The regulation of integrin function by divalent cations. *Cell Adhes Migr*. 6:20-29.

Zhu, J.H., B.H. Luo, T. Xiao, C.Z. Zhang, N. Nishida, and T.A. Springer. 2008. Structure of a Complete Integrin Ectodomain in a Physiologic Resting State and Activation and Deactivation by Applied Forces. *Mol Cell*. 32:849-861.

Zhu, J.Q., B. Boylan, B.H. Luo, P.J. Newman, and T.A. Springer. 2007. Tests of the extension and deadbolt models of integrin activation. *J Biol Chem*. 282:11914-11920.

Appendix I: Supplementary Results

A: MHM23

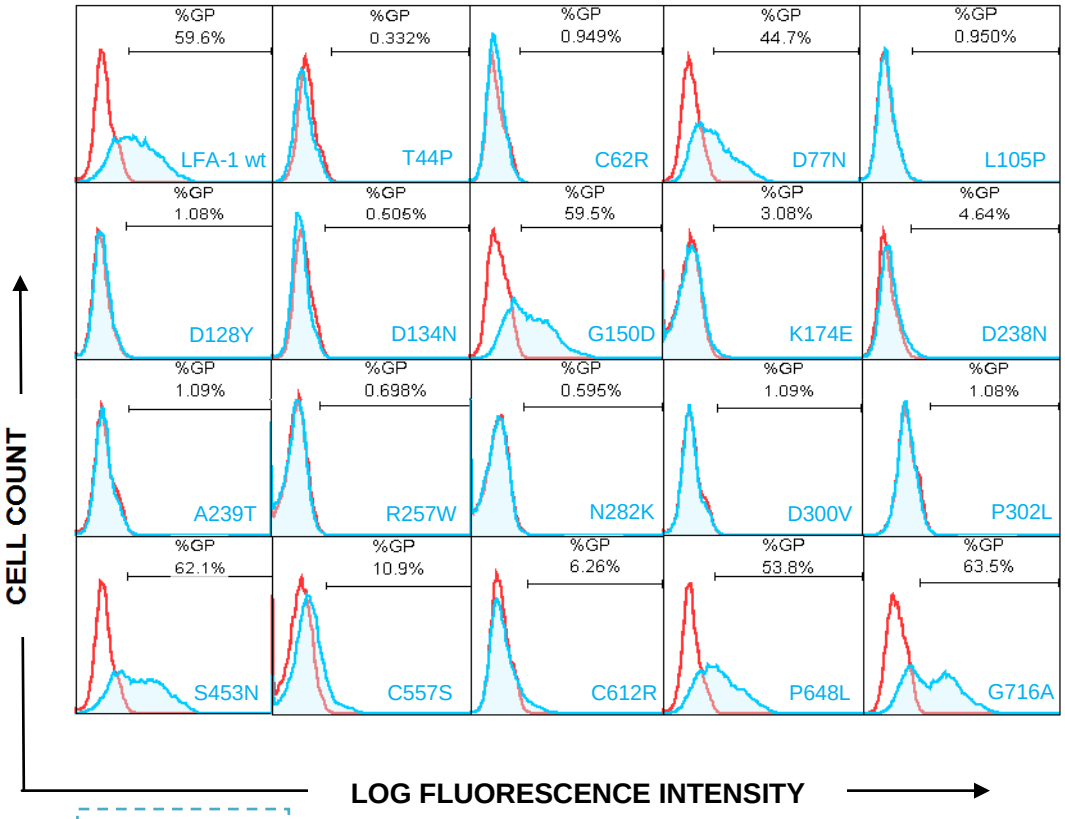

B: MHM24

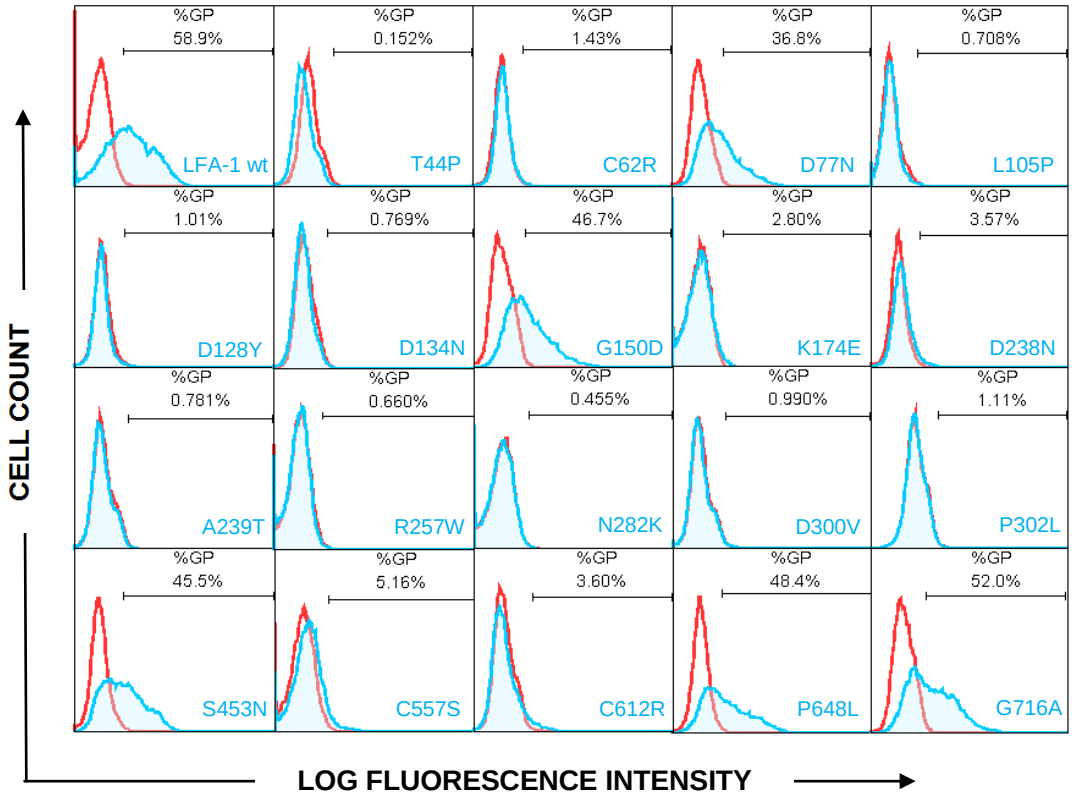

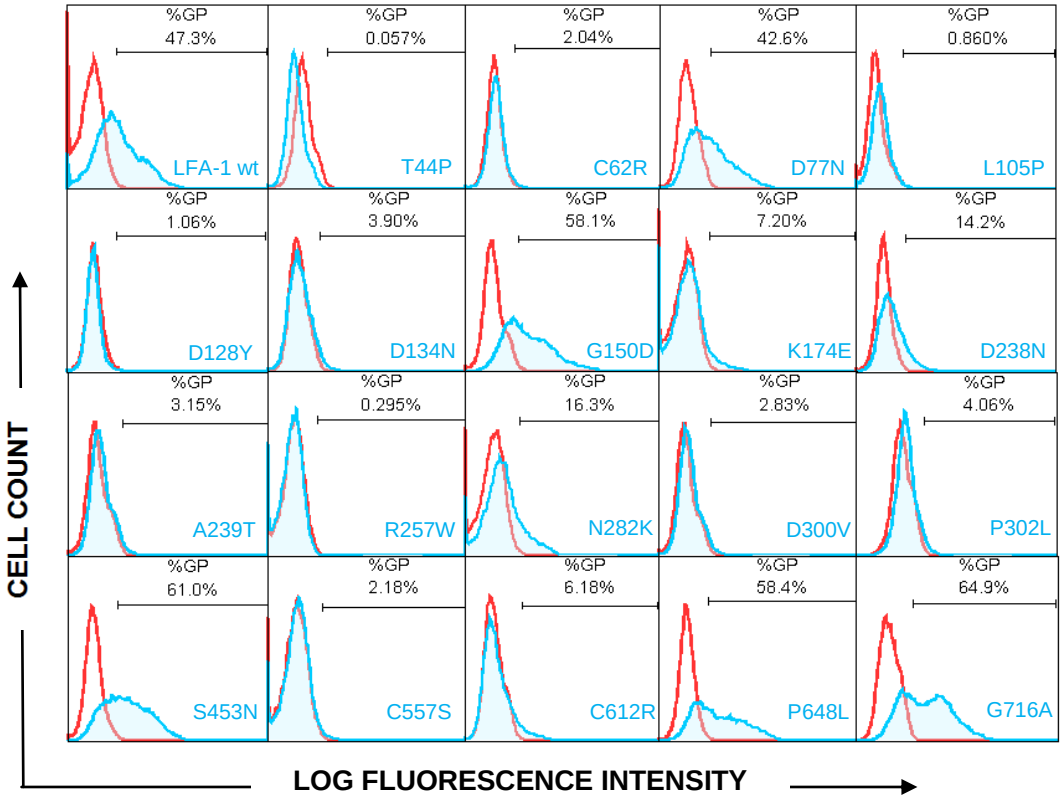

Supplementary Figure 1. Surface expressions of 19 LAD-1 mutants in supporting integrin LFA-1. (A) Expression detected by the heterodimer specific mAb MHM23; (B) by the αL I domain specific mAb MHM24; (C) by the anti-β_2 subunit mAb H52. In all cases, unstained cells were used as background control, %GP stands for "percentage of gated positive". Background gating was controlled at a range from 0.6%-0.8%.

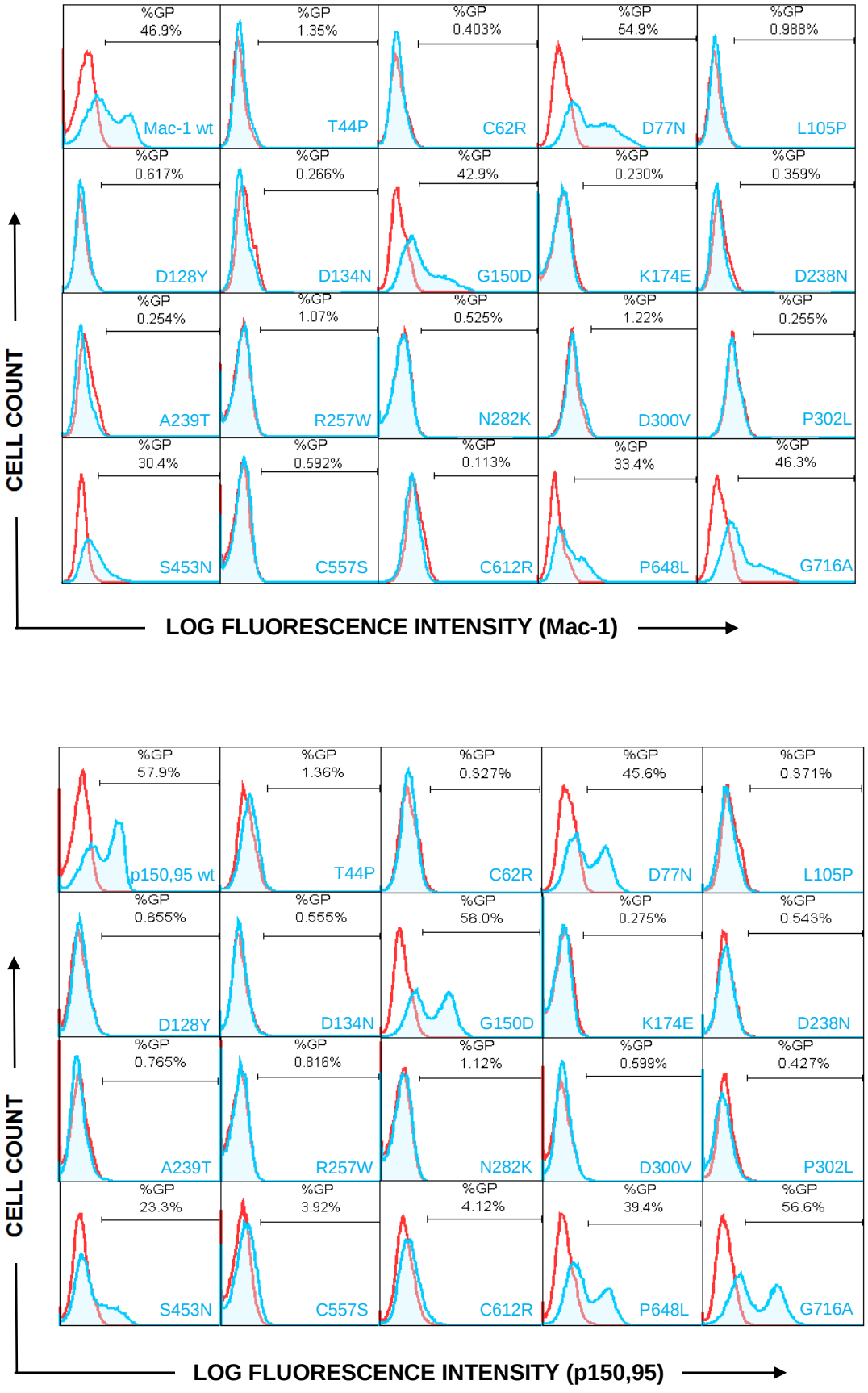

Supplementary Figure 2. Surface expression of integrin Mac-1 and p150,95 bearing LAD-1 mutation (19) analyzed using mAb MHM23.

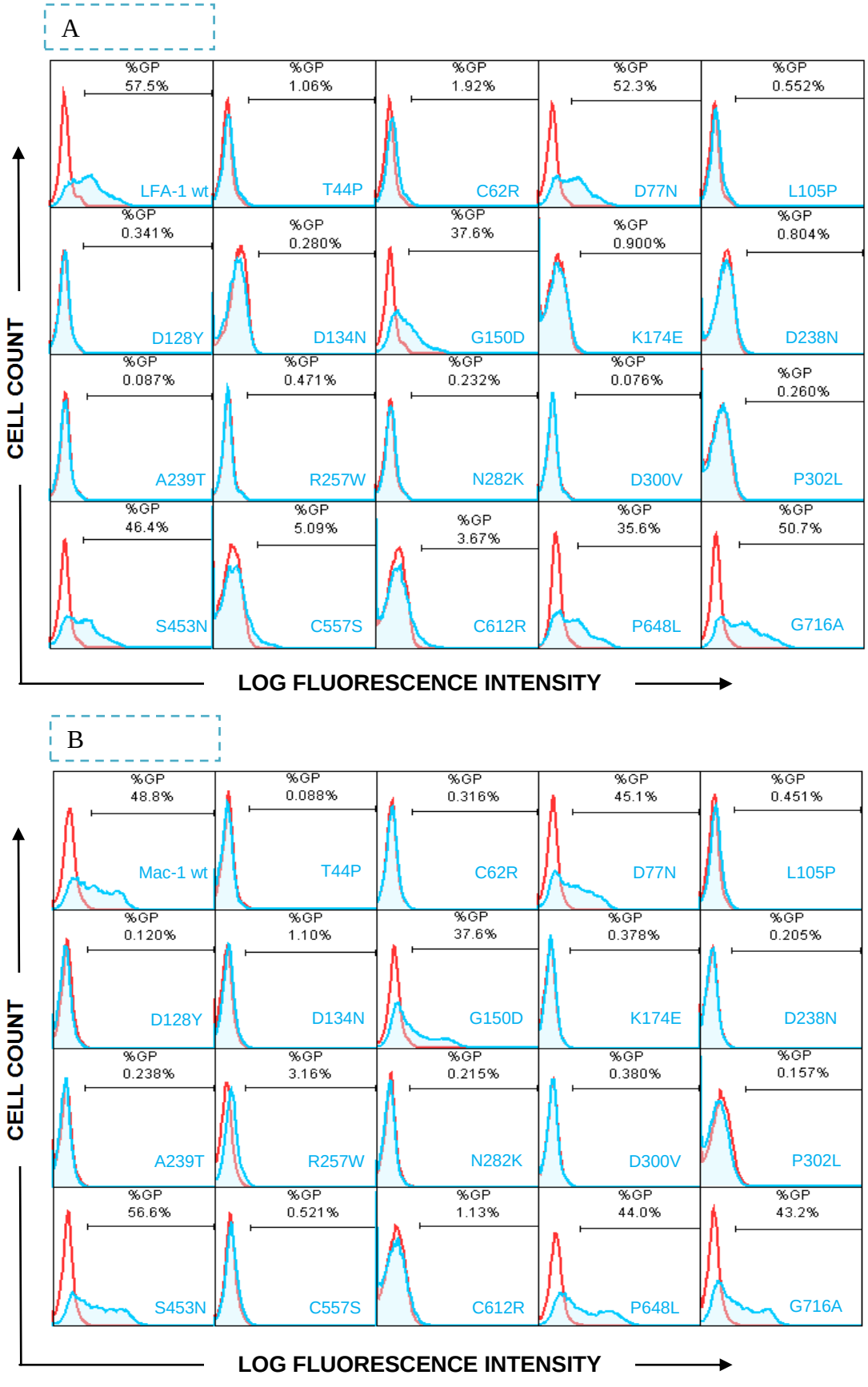
A
%GP 57.5%
LFA-1 wt
%GP 1.06%
T44P
%GP 1.92%
C62R
%GP 52.3%
D77N
%GP 0.552%
L105P
%GP 0.341%
D128Y
%GP 0.280%
D134N
%GP 37.6%
G150D
%GP 0.900%
K174E
%GP 0.804%
D238N
%GP 0.087%
A239T
%GP 0.471%
R257W
%GP 0.232%
N282K
%GP 0.076%
D300V
%GP 0.260%
P302L
%GP 46.4%
S453N
%GP 5.09%
C557S
%GP 3.67%
C612R
%GP 35.6%
P648L
%GP 50.7%
G716A
CELL COUNT
LOG FLUORESCENCE INTENSITY
B
%GP 48.8%
Mac-1 wt
%GP 0.088%
T44P
%GP 0.316%
C62R
%GP 45.1%
D77N
%GP 0.451%
L105P
%GP 0.120%
D128Y
%GP 1.10%
D134N
%GP 37.6%
G150D
%GP 0.378%
K174E
%GP 0.205%
D238N
%GP 0.238%
A239T
%GP 3.16%
R257W
%GP 0.215%
N282K
%GP 0.380%
D300V
%GP 0.157%
P302L
%GP 56.6%
S453N
%GP 0.521%
C557S
%GP 1.13%
C612R
%GP 44.0%
P648L
%GP 43.2%
G716A
CELL COUNT
LOG FLUORESCENCE INTENSITY

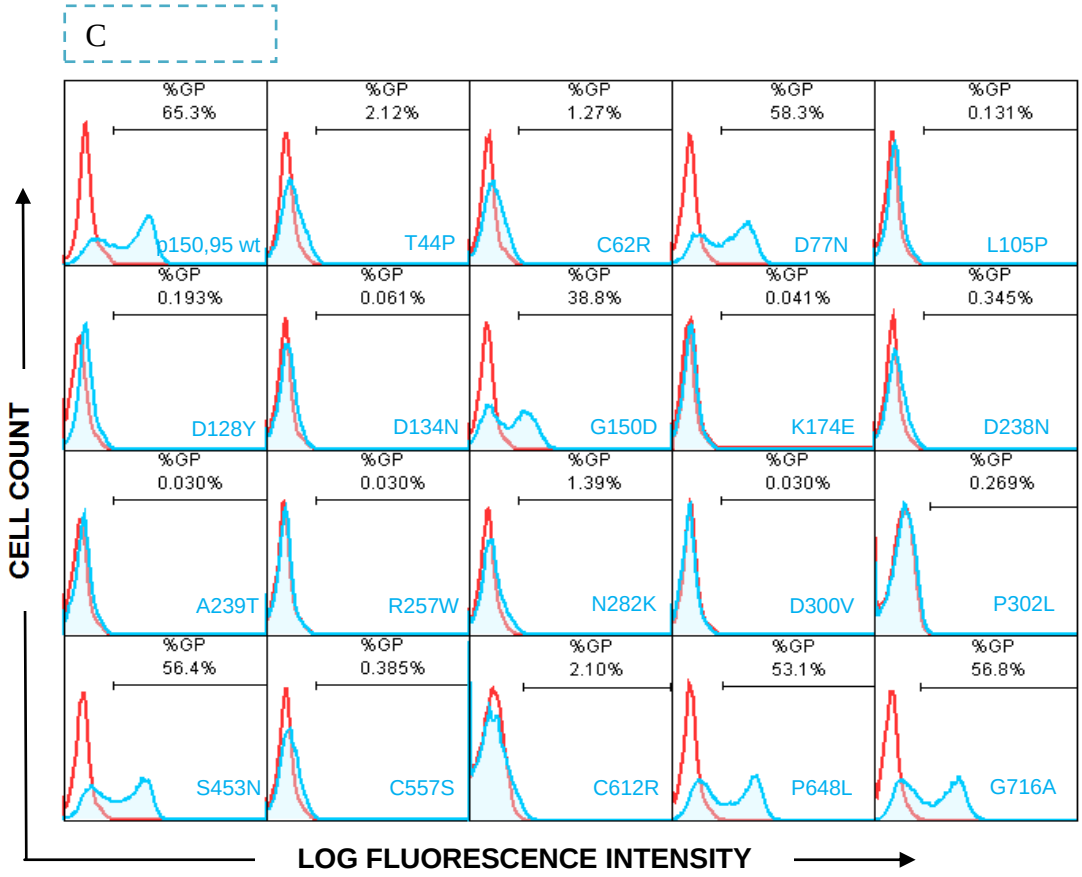

Supplementary Figure 3. Surface expression of integrin LFA-1 (A) Mac-1(B) and p150,95 (C) bearing LAD-1 mutation (19) analyzed using mAb 1B4. (A) LPM19C was used for background. (B-C): MHM24 was used for background control.